12-19-2008

Preparation, Characterization, And Application of Liposomes in the Study of Lipid Oxidation Targeting Hydroxyl Radicals

Chanel Fortier
University of New Orleans

Preparation, Characterization, And Application of Liposomes in the Study of Lipid Oxidation Targeting Hydroxyl Radicals

A Dissertation

Submitted to the Graduate Faculty of the
University of New Orleans
in partial fulfillment of the
requirements for the degree of

Doctor of Philosophy
in
The Department of Chemistry

by

Chanel Angelique Fortier

B.S. Chemistry, Louisiana State University, Baton Rouge, 2000

December 2008

ACKNOWLEDGEMENTS

I would first, like to thank God for his many blessings and giving me the preparation I needed to complete this degree.

This dissertation is dedicated to my mother, Lorraine K. Fortier and my late father, Alfred J. Fortier, Jr., who sacrificed so much and gave me the foundation I needed to complete this degree. I share this milestone in my life with my sisters Doretha Williams, Sharon Barnes, and my brothers Alfred Fortier III, Dwayne Fortier, and Jason Fortier and my extended family that always encouraged me to complete this degree even when times were challenging.

I would like to thank Dr. Matthew Tarr, in a special way for his unconditional support, guidance and mentoring of me during my acquisition of this degree. I would also like to thank my committee members, Drs. Matthew Tarr, Guijun Wang, Yang Cai, and Edwin Stevens for assistance and helpful discussions. I am forever indebted to Drs. Richard Cole and Bing Guan for their partnership in the success of the MALDI-MS studies.

I would like to thank Drs. Gabriela Blagoi and Thuvan Piehler for teaching me how to prepare liposomes and characterize them with Digital Fluorescence Microscopy and use the Fluorescence spectroscopy instrumentation, their help was invaluable. Thanks to my group members past and present, Sourav Chakraborty, Anindya Pradhan, Sarah King, Gayatri Sahu, Curt Jarand, Weixi Zheng, and Guoxiang Xi, and Bo Wei for their support and helpful discussions. I would also like to thank Harry Rees whose

ingenious knowledge of instrumentation allowed me to get back up and running as soon as possible.

In addition, to my friends who traveled this road with me Jeanelle Jenkins, Zakhia Moore, Kelly Morten, Kimari Slaughter, April Noble, Elisha Josepha, Arriel Wicks Bryant Jones, and Drs. Leyte Winfield, Brandi Darensbourg, Crystal Benjamin and Florastina Payton when one of us succeeds all of us succeed. Also, to my mentor Dr. Isiah Warner, who always believed that I could earn a PhD. in chemistry no matter what, I share this achievement with you.

With deepest gratitude, I thankfully acknowledge Dr. Vicki Colvin and her group at Rice University for welcoming me and the Tarr group following Hurricane Katrina so that we could continue our research.

Finally, I thank the Board of Regents, Health Excellence Grant, and the National Science Foundation for funding this research.

TABLE OF CONTENTS

List of Tables and Figures

List of Tables and Figures cont'd.

List of Tables and Figures cont'd.

ABSTRACT

In the onset of many chronic illnesses including Parkinson's, Alzheimer's, and cardiovascular diseases, there is evidence to support the delicate balance between pro-oxidant and antioxidant species is shifted in favor of the former. Under these conditions, many reactive oxygen species (ROS) including hydroxyl radicals, are generated. Hydroxyl radicals formed in close proximity to DNA, nucleotides, proteins, and lipids rapidly oxidize these biological molecules in a nonspecific way. However, their toxicity is limited by their short lifetimes.

Currently, the mechanism by which hydroxyl radicals are involved in the onset of many illnesses, particularly with regard to lipid peroxidation, has yielded some controversy in the literature. Conventional studies which generate hydroxyl radicals with Fenton chemistry through bolus additions of iron and hydrogen peroxide do not mimic conditions found physiologically because there is a steady-state concentration of hydrogen peroxide concentration found in normal cellular systems. Also, former reports that used fluorescent fatty acids or free probes intercalated within liposomal membranes did not have the probes covalently attached to the phospholipids making up the liposomes. Thus, the actual placement of the probes over the analysis time may vary with experimental conditions.

The objective of this research project was to prepare, characterize, and employ liposomes as models for cell membranes during free radical oxidation.

Also, compared to the popularly-used technique of electron spin resonance, (ESR), our aim was to use a fluorescence-based approach which yielded the advantages of high sensitivity, fast analysis time, and less expensive equipment requirements.

Degradation of fluorescently-tagged liposomes with probes covalently bound to the phospholipids was correlated with the ability of hydroxyl radicals and other possible reactive oxygen species to penetrate into the liposomes to deeper into the lipophilic layer. However, alone this experimental setup may not fully define the mechanistic role of hydroxyl radicals in lipid oxidation. Thus, a complementary approach embracing the use of MALDI-TOF mass spectrometry, lipophilic scavenger studies, and the effects of cholesterol and temperature allow a deeper understanding of the radically-driven oxidation of lipids. It was determined that hydroxyl radicals were generated and reacted with three fluorescent probes.

Keywords: liposomes, free radical reactions, Fenton chemistry

Chapter 1. INTRODUCTION

Section 1.1. Reactive Oxygen Species

A free radical is defined as any species that has one or more unpaired electrons. This definition includes the hydrogen atom, some transition elements and oxygen, which itself is a biradical.[1] If molecular oxygen is reduced by a single electron it generates superoxide. The formation of superoxide is very favorable owing to the biradical formation of molecular oxygen. Once molecular oxygen abstracts an electron during the aerobic events constantly occurring in the human body, it can go on to help generate hydrogen peroxide through the Haber-Weiss reaction.[2] If superoxide picks up another electron, it generates the peroxide ion which is not a radical. This peroxide ion quickly gets protonated to generate hydrogen peroxide. In the course of these serial reactions, hydrogen peroxide can undergo dismutation generating superoxide and water or it can react with available iron(II) to generate the toxic hydroxyl radical through Fenton chemistry.[3]

Hydroxyl radicals are characterized as being a type of reactive oxygen species (ROS). Other reactive oxygen species include singlet oxygen and peroxynitrite. The resulting hydroxyl radical has been reported to initiate lipid peroxidation through reactions beginning with abstraction of an allylic hydrogen from a polyunsaturated fatty acid generating a lipid radical. Subsequent addition of oxygen to the carbon-centered radical can generate a peroxyl radical which can generate further lipid peroxidation through additional reactions.[4]

Section 1.2 Fenton Chemistry

The discovery of Fenton chemistry, involving the generation of hydroxyl radicals through the oxidation of iron (II) by hydrogen peroxide and a host of other related reactions have been credited to Henry J. Fenton [5, 6] with further definition of this chemistry being investigated by Haber and Weiss.[2] The Fenton reaction,

$$Fe^{+2} + H_2O_2 \longrightarrow Fe^{+3} + OH\bullet + OH^- \qquad \text{Equation 1.1}$$

given by Equation 1.1 has been used to describe the generation of hydroxyl radicals, but the Fenton process is actually a set of reactions that occur together. Some of the additional reactions that occur include:[7]

$$Fe^{+3} + H_2O_2 \longrightarrow Fe^{+2} + H^+ + HO_2\bullet \qquad \text{Equation 1.2}$$

$$Fe^{+3} + HO_2\bullet \longrightarrow Fe^{+2} + H^+ + O_2 \qquad \text{Equation 1.3}$$

$$Fe^{+2} + HO_2\bullet \longrightarrow Fe^{3+} + HO_2^- \qquad \text{Equation 1.4}$$

$$Fe^{+2} + OH\bullet \longrightarrow Fe^{+3} + OH^- \qquad \text{Equation 1.5}$$

$$H_2O_2 + OH\bullet \longrightarrow H_2O + HO_2\bullet \qquad \text{Equation 1.6}$$

Equations 1.2 and 1.3 show how iron is catalytically regenerated. Equations 1.5 and 1.6 show what happens at high concentrations of iron (II) and H_2O_2 where both effectively scavenge the hydroxyl radical. Hydroxyl radical scavengers can also affect the rates of the above reactions by changing the concentration of reactants. Some of these reactions occur with the formation of a second radical and thus may continue to propagate free radical reactions until two radicals react with each other to form non-radical products. [7]

Section 1.3. Fenton Chemistry in Biological Systems

Reactive oxygen species can be formed at various places in the human body, but the mitochondria are the primary source of superoxide and hydrogen peroxide in cells. Superoxide in the mitochondria will generally undergo superoxide dismutation due to action of the enzyme superoxide dismutase. The two main factors controlling oxygen radical production is oxygen tension and concentration of partially reduced mitochondrial components. Oxidative stress occurs when electrons "leak" outside of the mitochondrial membrane.[4, 8] Physiologically much of the iron required to catalyze Fenton-generated hydroxyl radicals are bound to storage proteins such as transferrin, ferritin or hemoglobin and do not exist "freely" [8]. However, "free" iron also referred to as non-transferrin bound iron (NTBI) may exist. Chelation of this "free" iron by citrate or albumin usually stabilizes the iron, and the concentration is usually 1-10μM. [9 10, 11]

Recent reports have shown that under oxidative stress "bound" iron can be released from these storage proteins and even at low concentrations, less than 10μM iron can act as the catalyst needed to generate hydroxyl radicals in the presence of a steady-state concentration of hydrogen peroxide, which itself has been shown to penetrate cell membranes freely due to its uncharged state and can participate in cell apoptosis at 0.3μM.[10]

Section 1.4. Techniques to measure hydroxyl radicals and other reactive oxygen species

Hydroxyl radicals have been measured in lipid phases using a variety of techniques. Measuring hydroxyl radicals directly has proved to be challenging because of their short lifetimes. Electron paramagnetic resonance has been touted as one of the most direct methods to measure hydroxyl radicals. [12] Hydroxyl radical formation has previously been measured with the spin trap 5,5-dimethyl-1-pyrroline-N-oxide (DMPO) while observing the ability of iron chelates to penetrate into bulk lipid phases. Although they were certain that hydroxyl radicals were formed in oleic acid, in lipid esters the formation of hydroxyl radical adducts was uncertain. It was also shown that due to the short lifetimes of hydroxyl radicals that they were most likely to exist within lipid phases if they were formed there instead of the exterior environment. Hay and co-workers designed new spin traps that would be anchored at specific depths within the membrane of large unilamellar vesicles.[13] The spin traps were highly lipophilic and were used to position the nitrone trap deep within the lipid bilayer. However, the spin traps were not covalently attached to the phospholipids so some "wagging and bobbing" of the spin traps were detected.

Braughler and co-workers[14] studied whether ferrous iron was oxidized in the presence of various medium compositions and in the presence of lipid. Their results revealed that ferrous iron oxidation was significant in the presence of phosphate or ethylenediaminetetraacetic acid (EDTA). The products of ferrous iron and ferric iron, was reported to be recoverable in the presence of the reducing agent ascorbic acid.

However, it was shown that in the presence of liposomes, membranes, micelles and fatty acids, the recoverable efficiency of ferrous iron was reduced to less than 50%. It is interesting to note the result that commercial lipids are unavoidably contaminated with lipid hydroperoxides on the order of 0.02 to 0.1%. Moreover, the authors suggested that oxidation of ferrous iron by lipid hydroperoxide and also hydrogen peroxide is more complex than simple ferric iron which can not be easily reduced.[14]

Section 1.5 Lipids, Micelles, and Liposomes

Lipids are separated into three general classes, free fatty acids, triacylglycerols and phospholipids. The free fatty acids are long chain aliphatic carboxylic acids which can be saturated or unsaturated. The common types of saturated fatty acids contain an even number of carbon atoms ranging from 12 to 22 [15]. Phospholipids are the primary components of cell membranes. They are composed of a dialkyl-, diacyl-, or acylalkyl-glycerol esterified to phosphate which in turn is bonded to a variety of polar groups, such as choline[16].Their structures include variations in the nature of the polar head group and acyl chains. Myristic, palmitic and stearic acids are three common saturated free fatty acids that are denoted 14:0, 16:0, and 18:0 because they contain 14, 16 and 18 carbon atoms with no double bonds.[16] Some common unsaturated free fatty acid which contain double bonds are oleic acid denoted (18:1) because it has 18 carbon atoms and one double bond, linoleic acid (18:2), linolenic acid (18:3), arachidonic acid (20:4), eicosapentaienoic acid (20:5) and docosahexaenoic acid (22:6).

Figure 1.1 Example of fatty acid, triacylglycerol, and phospholipids, respectively

a.) palmitic acid (fatty acid)

CH_3-$(CH_2)_{14}$-COOH

b.) triacylglycerol

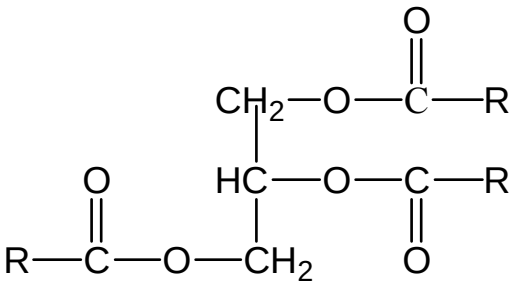

c.) phospholipid, dimyristoylphosphatidylcholine

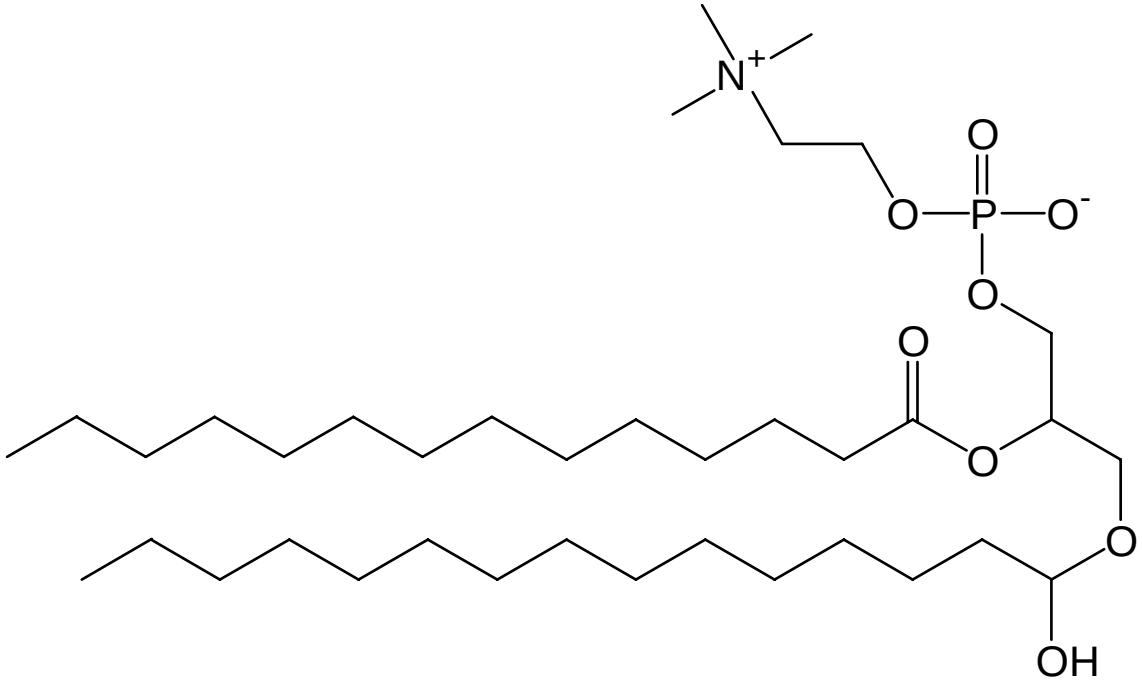

The unsaturated free fatty acids commonly occur in the cis formation separated by a single methylene group. However, some trans unsaturated fatty acids do occur to a small extent such as elaidic acid which has the same denotation as oleic acid except that it occurs in the trans rather than cis formation. Some of the unsaturated free fatty acids, such as linoleic and linolenic acids, are noted as being essential nutrients because they are not synthesized in the body. Moreover, docosahexaenoic acid from fish and algae has been included in infant formula to improve visual and brain functions [17].

Triacylglycerols are composed of fatty acids esterified to glycerol. They are the main constituent of vegetable oils and food lipids and are important storage lipids. In contrast, phospholipids are fatty acids esterified to glycerol which contain phosphoric acid and organic bases. Phospholipids constitute the major component of cell membranes and liposomes[15].

Micelles are composed of an aggregate of surfactant molecules where the surfactant is composed of a single polar headgroup and a single fatty acid chain. Micelles were used as a substrate to study the oxidation of methyl linoleate in tetradecyltrimethylammonium bromide (TTAB) and sodium dodecyl sulfate (SDS) solutions. Results were measured using UV spectroscopy and electrospray mass spectroscopy. [18]

Interestingly enough, Fe(II) was able to catalyze oxidation of methyl linoleate in the acidic TTAB media but not the basic SDS media. Moreover, Fe(II)/H_2O_2 was able to catalyze oxidation of methyl linoleate in TTAB but not in SDS micelles.

In addition, Fe(II)/ascorbic acid was able to catalyze methyl linoleate in SDS but not in TTAB micellar solutions. In summary, the Fe(II)/Fe(III) couple was necessary to oxidize the methyl linoleate at the acidic pH of the TTAB micellar solutions. Also, ascorbic acid can behave as an antioxidant and pro-oxidant and the formation of an iron/ascorbate complex was suggested.[18]

In a related study[19], the oxidation of methyl linolenate based on its physical state in octadecane oil-in-water emulsions was investigated. Also, the effect of pH, iron concentration, emulsifier type and cooling rate on the oxidation of methyl linolenate was determined. The results revealed that oxidation rates were higher with solid octadecane compared to the liquid emulsions, In addition, higher iron concentrations and lower pH were more favorable for oxidation rates of octadecane. The authors attributed the behavior to the migration of methyl linolenate to the surface of the oil in water crystalline octadecane where it could interact with the iron in the aqueous media to a greater extent.[19]

Section 1.6. Liposomes as models for cell membranes

Liposomes were first introduced by A.D. Bangham and co-workers in 1965 and have been used frequently in experimental studies to garner a deeper understanding into the mechanisms governing lipid peroxidation [20]

The suitability of using liposomes as models for cell membranes is proven by their composition of one or more phospholipids which is found to constitute the bulk of cell membranes and their heterogeneous nature, with both hydrophobic and hydrophilic components. [21-25]

Liposome systems are convenient to use because the effect of pH and temperature can easily be monitored [26] In addition, incorporating hydrophobic and hydrophilic probes within the hydrophobic bilayer or encapsulated aqueous interior is straight-forward. The advantages of a liposomal model also include a simplified construct without the complexity of authentic cell membranes which also contain proteins, DNA, and other important biomolecules which could make interpretation of experimental findings complicated by their interferences. Obviously the simplified model is limited in that it may not represent a typical cellular membrane in all respects and the liposomes should always be prepared fresh to avoid autoxidation of the lipids. However, liposomal systems can be used to give introductory insight towards and explanation of the complex mechanisms that govern lipid oxidation and may also be used to create benchmarks for experimentation involving complex cellular systems[27].

Many synthetic methods are currently available to generate liposomes.[28, 29] In a method first introduced by Bangham,[20] liposomes are formed spontaneously when the acyl chains of a lipid film, created by evaporation of the solvent by a gentle stream of nitrogen or rotoevaporation, interact through hydrophobic interactions forming a bilayer which encapsulates an aqueous interior.

One set of polar headgroups are simultaneously directed toward the aqueous interior while the other set is directed toward the outer aqueous medium. One advantage of this method is the absence of any alcohols which could affect the permeability of the generated liposomes [30, 31].

Initially, multilammelar vesicles (MLVs) are formed which are characterized by multiple concentric bilayers with each bilayer encapsulating aqueous interiors at increasing diameters, though liposomes have also been shown to adopt tubular shapes as well. The spacing between each bilayer is established by a balance of the Van der Waals, electrostatic and hydration forces between adjacent bilayers.[20] However in most applications employing lipsomes these MLVs are subjected to an extrusion process to generate unilamellar liposomes which have a single bilayer [29]. During the extrusion process, the MLVs are taken up by a gas-tight syringe (in many cases having a volume of 1mL) and this suspension is passed back and forth through a filter housing containing a polycarbonate membrane which is size exclusive (in many cases having a diameter of equal or lesser value than 100nm) to a second gas-tight syringe of the same volume as the first syringe. Multiple odd passes are performed to ensure unilamellarity without contamination from larger vesicles on even passes [27]. These unilamellar liposomes are labeled small (diameter of 0.02-0.05μm) or large (diameter of 0.06μm or greater.

Liposomes, also known as vesicles, have been previously used as models for cell membranes due to their similarity in composition and behavior to cells. Liposomes are generated spontaneously when phospholipids are added to an aqueous environment with agitation.

Entropically driven forces cause the phospholipids to line up tail-to-tail generating a spherical hydrophobic bilayer structure which encapsulates water where one set of the hydrophilic polar head groups are directed to the center and the other polar head groups are directed to the outer aqueous medium. The hydrophobic bilayer of the liposome, in addition to phospholipids, may contain cholesterol, proteins or other additives to mimic conditions commonly found in cells. Both the lipid bilayer and the aqueous interior have been previously labeled with fluorescent probes in drug-delivery, and biosensor studies.[27]

Figure 1.2 Phospholipid, lipid bilayer, and unilamellar and multilamellar liposomes.

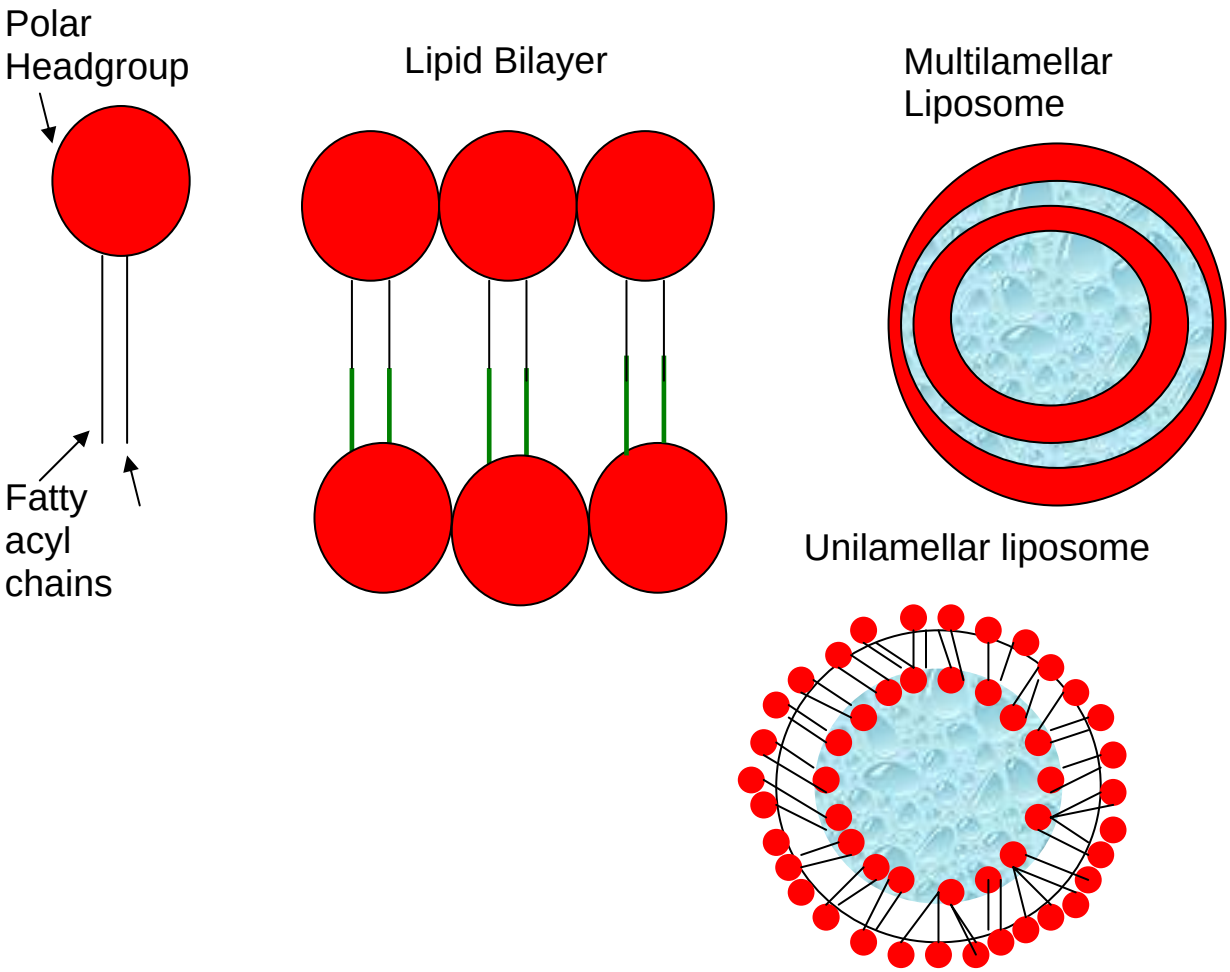

Section 1.7. Characterization of Liposomes

Typical characterization methods used to evaluate lamellarity of liposomes include electron microscopy, ^{1}H, ^{13}C and ^{31}P NMR, dyanamic light scattering, and digital fluorescence microscopy.

Electron microscopy can be used to yield information on the size, size distribution, volume distribution and the lamellarity of the liposomes by bombarding the sample with electrons[26, 29]. In NMR studies information on the orientation of the fatty acids and the polar headgroups, packing density, and distribution of lipids in the inner and outer layers can be obtained.[32, 33]. In dynamic light scattering[34], also known as photo-correlation spectroscopy, a laser source is used to measure the scattering of a dilute suspension of liposomes in which the particles are assumed to be moving but are independent entities which do not interact with each other. Upon taking a series of measurements, a histogram can be generated showing the size distribution of the liposomes. A unimodal histogram suggest unilamellar liposomes are present, with the average hydrodynamic radius (R_H) calculated over a series of measurements signifying the average radius of the particles and the polydispersity term (polyd) giving a measure of the standard deviation in the size distribution. In digital fluorescence microscopy, whether or not the liposomes are aggregated is assessed.Images can be taken of the fluorescent liposome at their excitation and emission wavelengths.

Section 1.8. Liposomes: Phase Transition Temperature

The phase behavior of liposomes is regulated by the same properties of the phospholipids constituting them[35].

Specifically, a phase transition temperature (T_m) exists separating a more-ordered solid-gel phase below T_m from a more fluid liquid-crystalline temperature above T_m.

In the solid-gel phase, the head groups are closely packed with very little spacing between the acyl chains which are positioned in a tilted position. In contrast, the liquid-crystalline phase is characterized by more spacing between the polar head groups and acyl chains.

At the phase transition temperature, a combination of the solid-gel and liquid-crystalline phases exist with large mass defects within the bilayer. It was previously reported by Kraske and co-workers[36] that an uncharged molecule, glucose, was able to penetrate dimyristoylphosphatidylcholine liposomes to the greatest extent at the phase transition temperature rather than at the maximum temperature examined.

Figure 1.3 The Phase Transition of Phosphatidylcholine

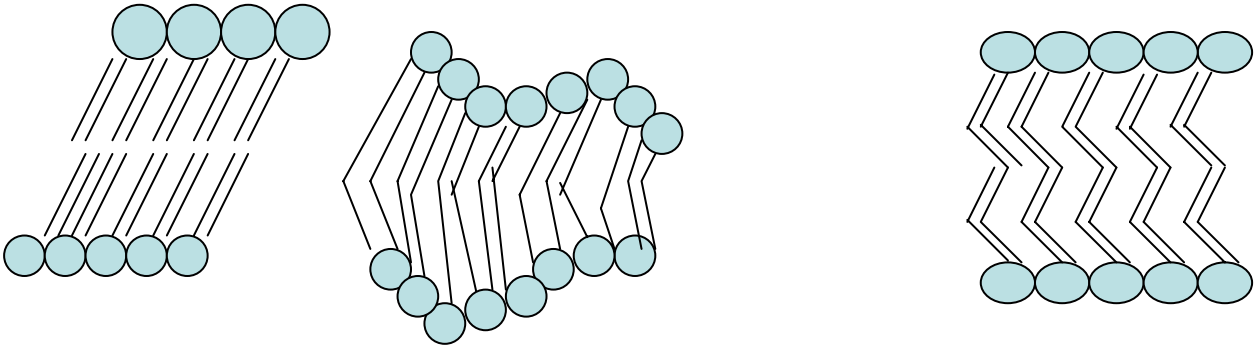

Below T_m At T_m Above T_m

Solid-Gel Phase Liquid-Crystalline Phase

Section 1.9. Lipid Oxidation

Lipid Oxidation is a topic that spans many fields including biology, free radical chemistry, nutrition, and biochemistry. It has been studied for over sixty years and yet many problems still remain unresolved. In vivo mechanisms of lipid peroxidation, the effects of antioxidants including phytochemicals, and the mechanisms of polyunsaturated lipid nutrition still remain a mystery. Lipid oxidation refers to the oxidation of unsaturated fatty acids and their derivatives. These oxidation reactions generally occur when the lipids are exposed to air and there is an imbalance between pro-oxidant species such as hydroxyl radicals, superoxide, hypochlorous acid, hydrogen peroxide, and singlet oxygen compared to antioxidant species such as vitamins A, D, E, and K.

In biological systems, only hydroxyl radicals,[37-39] and high oxidation states of iron such as the ferryl iron, [40] peroxynitrite,[3] and nitrogen dioxide[41] have been shown to initiate lipid oxidation. Superoxide and hydrogen peroxide have not been shown to initiate lipid oxidation unless through the Haber-Weiss mechanism which includes formation of hydroxyl radical.

Section 1.10. Free Radical Reactions

The free radical reactions that lipids engage in are largely due to the pi electrons of unsaturated lipids.[15] This reactivity is due to the pi electrons being of lower energy compared to sigma electrons. The chain reaction mechanism of free radical reactions occurs in three steps: initiation, propagation, and termination.

The lower energy of pi electrons makes them accessible for hydrogen abstraction, addition and elimination reactions, fragmentation reactions, rearrangement reactions, disproportionation reactions, and oxidation-reduction reactions, all of which can be the initiating start of free radical reactions. Propagation reactions occur when free radicals react to form new free radicals. The free radical reactions are ended when two radicals combine to form non-radical products.[15]

Taking a look at these reactions more closely, initiators (I) such as singlet oxygen, superoxide, and hydroxyl radicals can abstract a hydrogen from unsaturated lipids (LH) generating a lipid free radical (L•).

$$LH + I \longrightarrow IH + L\bullet \qquad \text{Equation 1.7}$$

The propagation reaction where oxygen (O_2) reacts with the lipid free radical is very fast which generates a lipid peroxyl radical (LOO•).

$$L\bullet + O_2 \longrightarrow LOO\bullet \qquad \text{Equation 1.8}$$

Then this peroxyl radical can react to form hydroperoxides (LOOH) and another lipid radical (L•).

$$LOO\bullet + LH \longrightarrow LOOH + L\bullet \qquad \text{Equation 1.9}$$

The termination reaction occurs when two free radicals react to form non-radical products such as two lipid peroxyl radicals reacting together.

$$LOO\bullet + LOO\bullet \longrightarrow \text{non-radical products} \qquad \text{Equation 1.10}$$

A termination reaction can also occur when a radical reacts with an antioxidant which donates an electron or hydrogen atom.

$$LOO\bullet + A \longrightarrow LOOH + A\bullet \quad \text{Equation 1.11}$$

Antioxidants are defined as substances which can attenuate or prevent the oxidation of a substrate when it is present in small amounts relative to the amount of the substrate. There are numerous ways an antioxidant can affect lipid peroxidation including having a decrease in oxygen concentration, scavenging initial radicals, chelating metal catalysts, decomposing radical products and breaking the chain reactions that abstract hydrogens or electrons.[10, 42] These former reactions are by no means all of the chain reactions because alkoxyl radicals, alkyl radicals and other radicals and products can be generated during this free radical process.

The kinetics of the above reaction scheme are complicated in the presence of trace metals such as copper or iron because metals can catalyze the decomposition of unsaturated lipids by electron transfer,

$$M^{(n+1)} + LH \longrightarrow M^{n+} + L\bullet + H^{+} \quad \text{Equation 1.12}$$

or by one-electron redox reactions,

$$M^{n} + ROOH \longrightarrow M^{n+1} + RO\bullet + OH^{-} \quad \text{Equation 1.13}$$

$$M^{n+1} + ROOH \longrightarrow M^{n} + ROO\bullet + H^{+} \quad \text{Equation 1.14}$$

Another complicating factor exists in heterogeneous systems where metals and lipid components exists in different phases.

SECTION 1.11. Antioxidants: Endogenous and Exogenous

In the human body there are endogenous enzymes and water and lipid soluble antioxidants which maintain the delicate balance between pro-oxidant and antioxidant species. Peroxisomes are endogenous enzymes located in the mitochondria which convert oxygen radicals into non-deleterious species.

Superoxide dismutase, which is in the intracellular and extracellular media, controls the amount of superoxide in the body converting it into hydrogen peroxide. In addition, catalase and glutathione decompose hydrogen peroxide and hydroperoxides, respectively. [43]

Some non-enzymatic antioxidants also exist and are classified as being water-soluble and lipid-soluble. Some water-soluble antioxidants include ascorbic acid, uric acid, or glutathione. Some lipid-soluble antioxidants include vitamin E and beta-carotene. Both the water and lipid-soluble antioxidants' main role is to scavenge free radicals[43]. Vitamin E is composed of different tocopherols and tocotrienols which have been shown to behave as an antioxidant and scavenge two molecules of peroxyl radicals. However, there is also evidence to support the pro-oxidant activity of Vitamin E under certain reaction conditions. [44] Moreover, though Vitamin C is a poor antioxidant alone, in the presence of Vitamin E, a synergistic affect occurs where the tocopheroxyl radicals formed during radical scavenging is reduced. This allows for propagation of chain reactions to be reduced.

Exogenous antioxidants made available through a diet high in fruits and vegetables have been reported to reduce disease risk.[45]

Flavonoids, another type of exogenous antioxidants, usually react by free radical scavenging. However, flavonoids can also become pro-oxidants under certain experimental conditions by greatly accelerating the production of hydroxyl radicals from H_2O_2 in the presence of Fe^{+3}-EDTA at physiological pH.

Fukuzawa et al.[46] investigated the oxidation of alpha-tocopherol in micelles and liposomes by the hydroxyl, peroxyl, and superoxide free radicals. . In this study, samples underwent radiolysis of the aqueous solutions with gamma rays. Micelles and liposomes were both charged and uncharged. Hydroxyl radicals were effective oxidants of both the micelles and the liposomes.The perhydroxyl ion was also effective as an oxidant of as long as the pH was acidic. The alpha tocopherol, due to its low water solubility was found in the micelles and the liposomes. The alpha tocopherol in the positively charged micelles and liposomes were oxidized as a higher rate by superoxide than in uncharged or negative liposomes or micelles.

Alessi and co-workers[47] investigated the similarities and differences between the kinetics of peroxidation of vitamin E-containing liposomes and human low-density lipoprotein. Interestingly enough, it was found that for tocopherol-mediated peroxidation (TMP) to occur, the liposomes must exists as isolated systems to protect the tocopherol radical. This premise was supported by the highly lipophilic character of the vitamin E, where it will prefer to stay inside the liposome it was generated in.

Section 1.12. Cholesterol and its oxidation

Cholesterol has been widely studied due to its oxidation products that have been implicated in adverse health effects. Cholesterol is an apolar lipid constituent of cell membranes. It is present in large amounts in the lipoproteins of blood and is the precursor for the generation of glucocorticoids, sexual hormones, and vitamin D[48]. The oxidation products of cholesterol are commonly called oxysterols or cholesterol oxides. The oxidation products can be generated enzymatically or non-enzymatically in biological systems.

The allylic 7-position carbon is susceptible to oxygen attack to produce its hydroperoxides. These oxides have been observed in low-density lipoprotein (LDL), oxidized in vitro, rat skin, marine animals and plant tissues. Cholesterol oxidation in solution or in aqueous media is initiated by hydrogen abstraction to produce a delocalized three carbon allylic radical followed by oxygen attack mainly at carbon 7 to produce the epimeric hydroperoxy products at 7-alpha and 7-beta, with the 7-beta-hydroperoxide dominating.

It is interesting to note that oxygen attack at carbon position 4 is not favored due to steric hindrance by the trialkyl-substituted carbon-5 and the neighboring effect of the OH group on carbon-3.

Cholesterol oxidation can also occur in the solid or crystalline phase generating the 25-hydroperoxycholesterol product through a side chain oxidation scheme involving the tertiary carbon-25 position. [15]This 25-hydroperoxycholesterol product can be thermally decomposed to generate 25-hydroxycholesterol.

Moreover, two dihydroperoxides, 3-beta-hydroxy-20R- and 20S-cholesterol, have been isolated in autooxidized bulk cholesterol as well. The monohydroxides of cholesterol also decompose into complex mixtures of hydroxyl, keto, epoxyene and ketodiene secondary products that have received considerable attention because of their biological significance.[15]

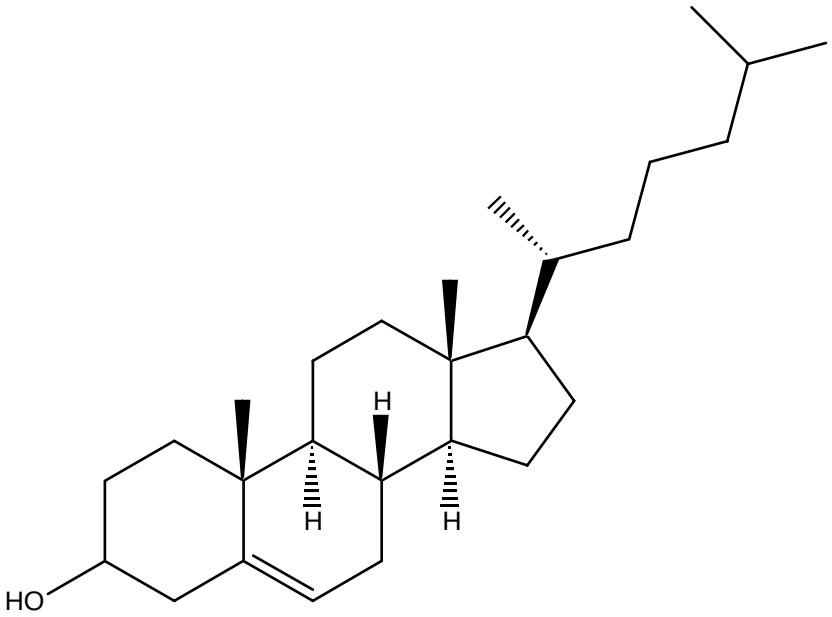

Figure 1.5 Structure of Cholesterol

Section 1.13. Methods to Determine Amount of Lipid Oxidation

Section 1.13A. Peroxide Value

The peroxide value, or the amount of peroxides in a sample, can be determined empirically using an iodometric titration, colorimetrically or electrometrically. This method requires typically a gram or more of potassium iodide to perform the titration. Its results are affected by light, air, and iodine reaction with double bonds. In addition there is a ferric thiocyanate method to determine oxidation which only requires 0.1g sample sizes. This method typically yields higher values than the iodometric technique on the order of 1.5 to 2 times the relative peroxide value. The peroxide value technique is very sensitive to the sample history with the peroxide value reaching a maximum with degree of oxidation according to temperature, degree of polyunsaturation, exposure to light and metals.[15]

Section 1.13B. Conjugated Dienes

The conjugated diene method of measuring lipid oxidation relies on the strong absorption of conjugated dienes at a maximum of 234nm. It offers the advantage of being a direct, sensitive method to follow lipid oxidation, and is suitable for monitoring early stages of lipid oxidation. However, it is of limited utility at high stages of lipid oxidation due to secondary products absorbing in the ultraviolet range, such as carbonyls and conjugated trienes.

In addition, high temperatures, metals and light can yield low values due to decomposition of the conjugated dienes. Moreover, interferences such as partially hydrogenated fats are a limitation of this method. [15]

Section 1.13C. Carbonyl Compounds

The amount of total carbonyls in a sample can be determined by its reaction with 2,4-dinitrophenylhydrazine (2,4-DNPH), which yields colored hydrazone derivatives that are measured by an absorbance of 430-460nm, and expressed as nmol hexanal/kg sample.[15]

Section 1.13D. 2-Thiobarbituric acid (TBA) value

The 2-thiobarbituric acid value test is an older, more widely used test than some of the other techniques. This test is a colorimetric assay to measure oxidation products in biological systems. To perform this test, it is necessary to observe the pink product that absorbs in the range of 532-535 nm. This signal is due to the product formed upon reaction of TBA with oxidation products of polyunsaturated lipids. One limitation of this method is that it is not specific, meaning a positive signal is produced by a large number of secondary oxidation products, these products are referred to as TBA-reactive substances or TBARS. The test is standardized by malondialdehyde. [15]

A variety of factors affect the production of the pink color in the TBA test including temperature and heating time, pH, metal ions, and antioxidants. The selectivity of the method has been enhanced by adding a high-performance liquid chromatography step.

Section 1.14A. Fluorescence and Fluorescence-Based Methods

Fluorescence is a luminescent analytical technique which involves analytes absorbing a photon of light followed by emission of a photon of light at a longer wavelength.[49] Molecules which undergo fluorescence are called fluorophores. Fluorescence usually occurs within aromatic and heterocyclic compounds.

The three luminescent techniques include fluorescence, phosphorescence and chemiluminescence all of which are characterized by the excited state. Fluorescence involves molecules absorbing energy from a ground state to an excited singlet state, partially relaxation, and then emission of a photon to return the molecules back to the ground electronic state. In phosphorescence, the molecule returns to the ground state following emission of a photon from the spin-forbidden triplet excited state, which involves a change in spin. In chemiluminescence, a chemical reaction generates an electronic excited state which subsequently emits a photon to return to the ground state [49]Fluorescence is short-lived with a lifetime existing at less than 10^{-5} seconds. In the case of phosphorescence the change of spin leads to longer lifetimes at several seconds or longer. An advantage of fluorescence is the high sensitivity with detection limits one to three orders of magnitude lower than absorption spectroscopy. Moreover, fluorescence has long linear concentration ranges compared to absorption spectroscopy. In addition, fluorescence also has greater selectivity than absorbance.

The Jablowski diagram outlines the possible pathways a molecule can take to return to the ground state following absorption of electromagnetic radiation. Absorption of light is signified by **A** from a ground singlet state to an excited singlet state signified by $\mathbf{S_1}$ **or** $\mathbf{S_2}$**.**. Each of the singlet excited states is composed of a number of vibrational energy levels. When a molecule returns to a lower excited state of the same spin such as $\mathbf{S_1}$ from $\mathbf{S_2}$**,** without emitting a photon the process is called internal conversion, signified by **IC**. Fluorescence emission signified by **F** occurs when light is emitted as a molecule returns to the ground state from a singlet state of the same spin, $\mathbf{S_o}$, the singlet ground state. The light is emitted at a longer wavelength due to energy loss during the excited state lifetime. This process is known as the Stokes shift.

Phosphoresence signified by **P** involves a molecule returning to a singlet ground state, $\mathbf{S_o}$ from a spin forbidden excited triplet electronic state signified by $\mathbf{T_1}$. Since fluorescence is spin favored over phosphorescence, it takes place over a shorter time interval (1E-5 to 1E-8 seconds) compared to (1E-4 seconds to hours). Vibrational relaxation is another radiationless phenomenon which occurs when excited molecules transfer energy to other molecules through collisions over a short time scale (<1E-12 seconds).

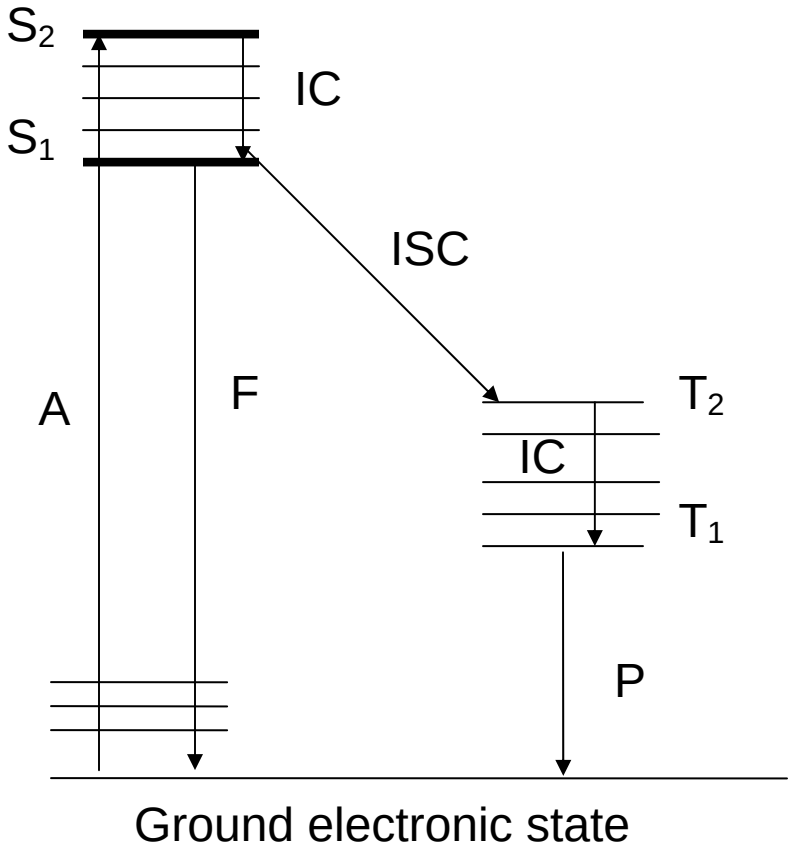

Figure 1.6 Jablowski Diagram

Section1.14B. Fluorescence Spectra

A fluorescence emission spectrum is taken when the excitation wavelength is held constant (often at the absorbance maximum), and the emission wavelength is scanned. The excitation spectrum is taken when the emission wavelength is held constant (often at its maximum), and the excitation wavelengths is scanned. The Stokes shift is the peak-to-peak distance of the maxima of the excitation and emission spectra.

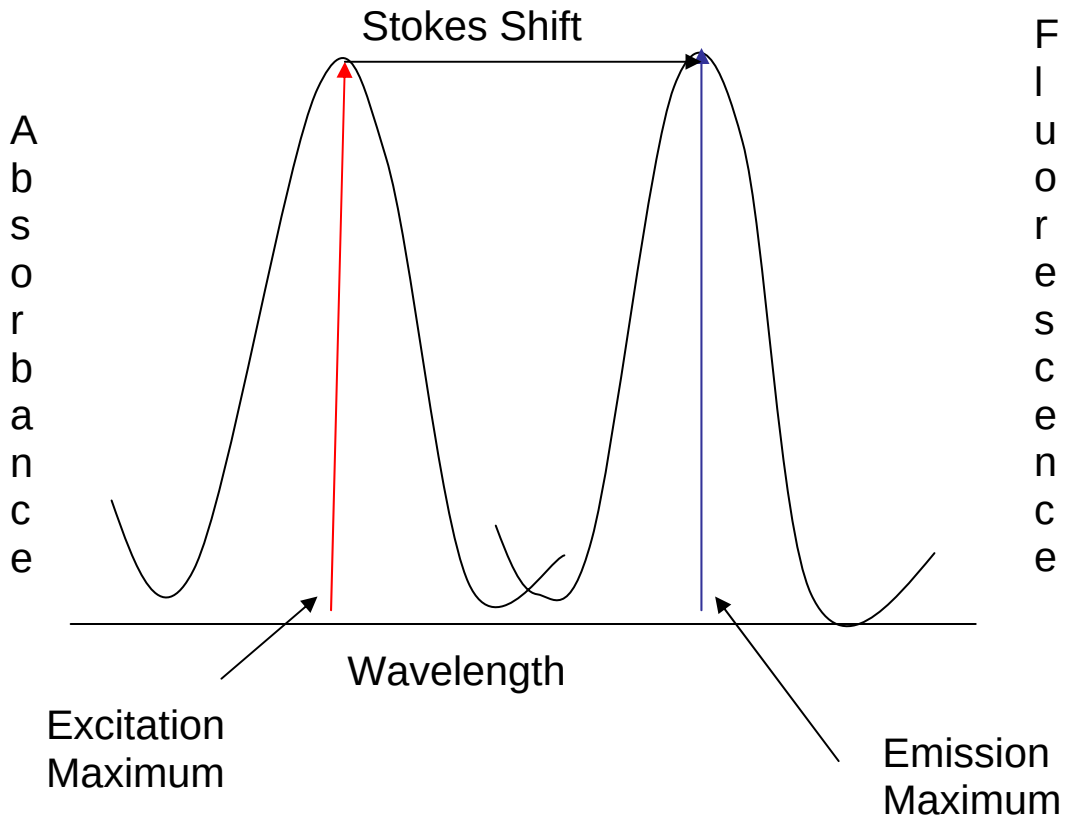

Figure 1.6 Absorbance, Fluorescence emission and the Stokes shift

There is an inherent benefit of fluorescence over absorbance because the fluorescence method is based on a dark background, whereas in absorbance, the background is the highest observed light intensity. In a typical fluorescence spectrometer, the detector is positioned at a 90 degree angle relative to the light source. This configuration minimizes transmitted and reflected light reaching the detector. The signal to noise enhancement is significant and the detection limit is lowered by a factor of 10000 compared to the 180 degree setup. The excitation and emission monochromators are wavelength filters which allowed specific wavelengths to be selected before and after fluorescence events[50]. In addition, the sensitivity of the fluorescence instrument is high because the process of fluorescence is cyclical, with the same fluorophore being excited and detected. In fact, a single fluorophore can yield thousands of detectable photons. The cycling does not help the absorbance technique because the detector is in line with the light source.

The excitation and emission spectra are sensitive to the type of solvent, microenvironment and chemical structure of the fluorophore.[49]

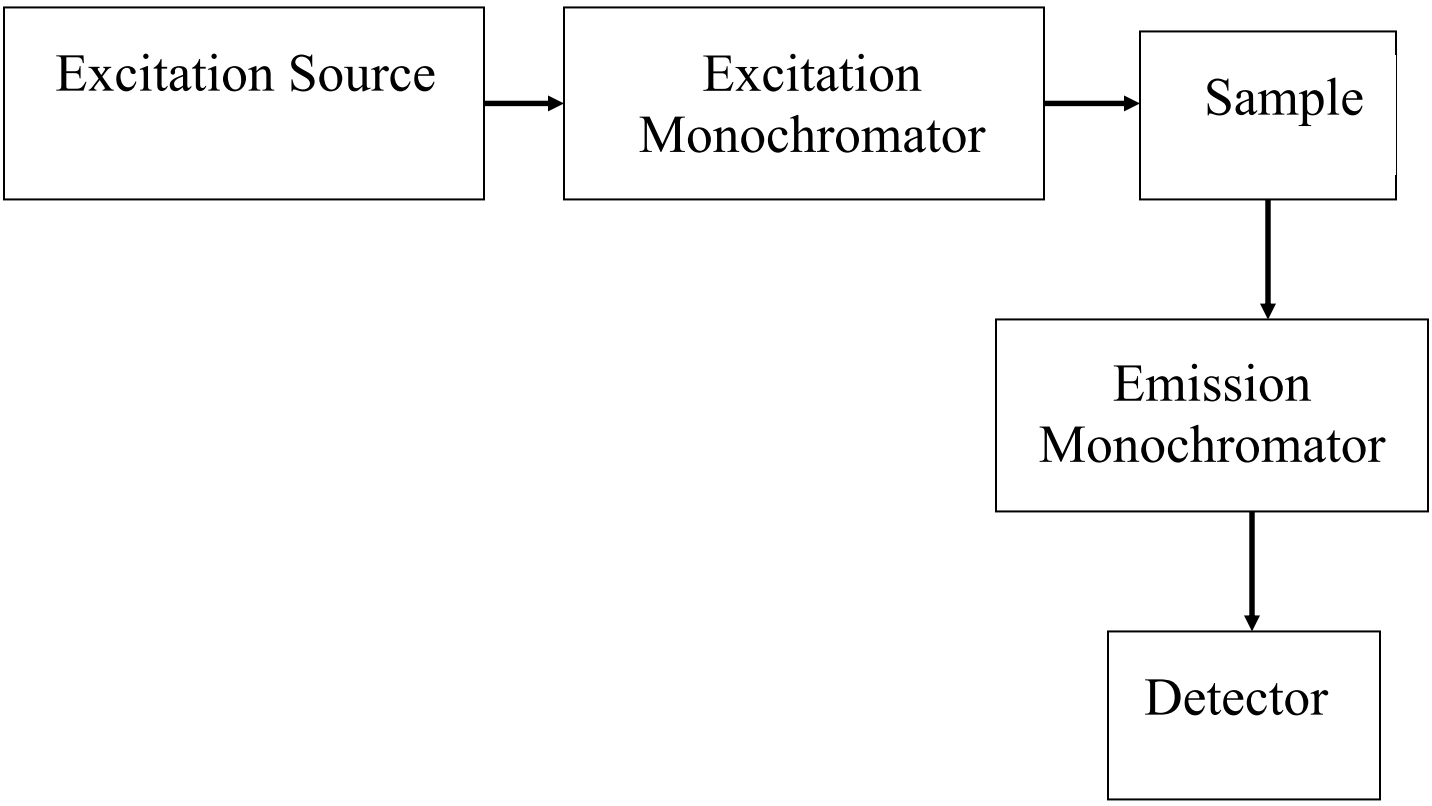

Figure 1.7. General schematic of a fluorimeter with 90º setup.

Section 1.15. Effect of Chelator on Fenton Chemistry

One of the most commonly used chelators with Fenton chemistry is ethylenediaminetetraacetate or (EDTA). Like many other chelators, the reactivity of EDTA is strongly dependent upon the chelator-to-metal ion ratio. Thus, it can inhibit or enhance the lipid oxidation of detergents and liposomes. The chelation of iron can alter its redox potential, solubility, and reactivity in reactions leading to the initiation of lipid peroxidation[51]. It was determined that chelation of iron (II) by EDTA led to a rapid autoxidation of iron (II). The rate of autoxidation increased up to equimolar concentrations of EDTA-to-iron (II).However, when iron (II) was chelated by (Adenosine diphosphate) ADP it did not result in a rapid oxidation of iron (II).

Section 1.16. MALDI-TOF Mass Spectrometry of Phospholipids

GC/MS methods have been used to study phospholipids but often require time-consuming, labor-intensive derivitization methods which do not maintain the structural integrity of the phospholipids. With the introduction of soft ionization methods, phospholipids can now be studied without prior chemical alteration of the analyte. Phospholipids have been previously studied using matrix-assisted laser desorption ionization-time of flight mass spectrometry (MALDI-TOF MS) and electrospray ionization (ESI MS). The advantages afforded by using MALDI-TOF MS compared to electrospray ionization MS are fast sample preparation and analysis time, ease of use, simpler spectral interpretation, and insensitivity to impurities. MALDI-TOF MS also offers high sensitivity and mass accuracy.

A note of interest is that the ion yield from MALDI-TOF studies are not highly dependent on the degree of saturation of the phospholipids as opposed to ESI. Also, compounds with a lower molecular weight are more sensitively detected with MALDI. With ESI the interpretation of the low mass region is not complicated by matrix peaks and it is easily coupled to chromatographic columns. However, quantitative studies with MALDI-MS are sensitive to the homogeneity of the matrix-analyte co-crystallization. Thus, statistical studies are essential to determine the reproducibility of the method.[48]Moreover, when using MALDI-TOF MS, it was found that the signals were highly dependent on the nature of the matrix, and whether or not water was a part of the matrix. Some of the best matrices to use include alpha-cyano-4-hydroxycinnamic acid, esculetin, and 2,5-dihydroxybenzoic acid.

It was determined that the negative ion mode yielded mainly (M-H)- ions and were more simpler to interpret compared to the positive ion mode which led to the formation of the protonated, sodiated, and potassiated adducts.[16]

Post-source decay MS by Al-Saad in the positive ion mode [52]of phospholipids showed that the nature of the cation coordinated at the negatively charged oxygen position of the choline headgroup had a dramatic effect on the subsequent products formed. The sodiated ion produced many fragment ions while the protonated ion contained only one fragment corresponding to the headgroup at m/z 184.

This difference in fragmentation is thought to stem from the binding of the proton only to the negatively charged oxygen while the sodium was found to associate with several regions of the phosphatidylcholine molecule. In addition, phosphatidylcholines were not detected in the negative ion mode.

MALDI-TOF MS has been previously used to study lipid oxidation. Oborina and Yappert[53] compared the oxidation of stearoyl-arachidonyl phosphatidylcholine in sphingomyelin (SM) versus dipalmitoylphosphatidylcholine (DPPC). The results revealed that oxidation was faster with the DPPC compared to the SM. The data was explained by the fact that SM had the slower oxidation by the hydrophobic tails of SM being more disordered and the SM vesicles had a tight network of H-bonds that bridge neighboring SM molecules and poses a stronger interfacial barrier to the passage of oxidants.

Shadyro and co-workers[54] coupled radiation, thin layer chromatography and MALDI-TOF MS to study the fragmentation of cardioplin in model membranes. Cardioplin is found in the inner mitochondrial membrane and is a proton trap which is a mitochondrial enzyme involved in oxidative phosphorylation.

When cardioplin levels decrease it can lead to programmed cell death. A mechanism was determined in this study from gamma-radiation on a model membrane. Two fragmentation products were isolated from this free radical mechanism, phosphatidic acid and phospatidylhydroxyacetone. This work was followed up by the iron-mediated free radical formation of signaling lipids in a liposome system. [55]

The free radical mechanism involved hydroxyl radical attack on the polar headgroup of two starting substrates, cardioplin and galactocerebroside to generate phosphatidic acid and ceramide.

Using ^{31}P-NMR and MALDI-TOF MS a study was done to compare the analysis of high-density and low-density lipoprotein. The motivation behind the study was to further the understanding of atherosclerosis. It was determined that lysophosphatidylcholine could be monitored by both techniques but only 31P-NMR could be used to detect chlorohydrines. The limitations of ^{31}P-NMR was that it had low sensitivity and provided only a small amount of information on fatty acid composition. [56]

MALDI-TOF MS was also used to study phosphorylated lipids in biological fluids using immobilized metal affinity chromatography with a solid ionic crystal matrix.[57] This study employed a novel ionic crystal matrix composed of p-nitroaniline with butyric acid. Moreover, a new extraction, isolated and cleanup procedure was developed using ZipTip which had an immobilized metal ion affinity stationary phase.

Section 1.17. Initial Rates

When complicated kinetic profiles are observed in reactive oxygen species studies, calculating the initial rates is often a straight-forward way to analyze the data. The initial rate is calculated by taking a measurement over the beginning of the data where the data can be analyzed with linear regression since all data is relatively linear over a small enough time scale[58].

Fluorescent Probes as Reporters for Hydroxyl Radical Penetration into Liposomal Membranes and Lipid Oxidation

Abstract

The ability of hydroxyl radicals to penetrate into liposomal model membranes (dimyristoylphosphatidylcholine, DMPC) has been demonstrated. Liposomes were prepared then characterized with digital fluorescence microscopy and dynamic light scattering following extrusion to determine liposomal lamellarity, size, and shape. Hydroxyl radicals were generated in the surrounding aqueous media using modified-Fenton reagent (hydrogen peroxide and Fe^{2+}) with the water-soluble iron-chelator, ethylenediaminetetraacetic acid (EDTA). High and low doses of radical were used, and the low dose was achieved with physiologically relevant iron and peroxide concentrations. Fluorescent probes covalently bound to the membrane phospholipid were used, including two lipophilic pyrenyl probes within the membrane bilayer and one polar NBD probe at the water-membrane interface. Radical reactions with the probes were monitored by following loss of fluorescence and by observing oxidation products via matrix-assisted laser desorption ionization-time of flight mass spectrometry (MALDI-TOF MS). Differences in the probe position within the membrane were correlated with the reactivity of the probe in order to assess radical access to the site of the probe. For all probes, reaction rates increased with increasing temperature. Within the membrane bilayer, reaction rates were greater for the probe closest to the membrane-water interface. Cholesterol protected these probes from oxidation.

Kinetic models, scavenger studies, and product identification studies indicated that hydroxyl radical reacted directly with the in-membrane probes without the mediation of a secondary radical.

Introduction

Hydroxyl radicals are a class of reactive oxygen species (ROS) which have been implicated in the onset of many illnesses including Parkinson's[1] and Alzheimer's[2] diseases, cancer[3] and atherosclerosis.[4] Their toxicity is manifested physiologically through attack on biomolecules[5, 6] in close proximity to the site of their formation. A recent review by Pignatello[7] and co-workers outline the typical reaction scheme of hydroxyl radicals with organic compounds. The first step of hydroxyl radical attack on organic molecules typically involves either hydrogen atom abstraction or addition to double bonds. After initial attack by one of these mechanisms, additional reactions occur, often involving molecular oxygen. However, the role of hydroxyl radicals in lipid oxidation of cells and liposomes has yielded some controversy.[8] Previous reports have suggested that the high reactivity and short lifetime of hydroxyl radicals generated in the exterior aqueous phase of liposomes or cells exclude these radicals from being the direct initiators of lipid peroxidation[9] and that hydroxyl radicals instead create secondary radicals, including peroxyl radicals, which subsequently oxidize cells.[10, 11] In contrast, other authors have proposed that Fenton-generated hydroxyl radicals can occur in lipid phases, and that hydroxyl radicals can, in fact, directly initiate oxidation of lipids.[12-15]

These potential pathways for hydroxyl radical oxidation of lipids are of interest since the impact of hydroxyl radicals formed in various cellular regions depends on the mechanisms by which these radicals react with cellular material.

The ability of hydroxyl radicals to penetrate into lecithin liposomal membranes intercalated with pyrene has been previously studied.[16] It has been shown that hydroxyl radicals created in the surrounding aqueous media with pulse radiolysis can in fact penetrate into the liposomal membranes and react with the pyrene and lecithin in the hydrophobic membranes in a competitive manner. In addition, it was shown that hydroxyl radicals react near the phospholipid headgroup. However, these experiments employed pyrene as a free probe within the liposomal membrane, and therefore the pyrene could diffuse readily within the lipid layer. Consequently, the specific site of pyrene-hydroxyl radical reaction within the membrane was not known. In addition, varying the concentration of pyrene within the membrane in the millimolar range could have lead to the formation of pyrenyl dimmers within the membrane.[17]

Lipid peroxidation has been formerly investigated using fluorescent pyrenyl probes in the presence of liposomes and lipoproteins.[18, 19] A pyrenyl fatty acid and pyrenyl sphingosine were both shown to degrade by observing loss of fluorescence when incubated with iron (II) sulfate and ascorbic acid or copper (II) sulfate only. In addition, the thiobarbituric acid approach was used to measure lipid oxidation. Though this approach is commonly used, it can be complicated by the presence of other species in the matrix giving rise to a false positive response for lipid oxidation. Thus, this method is limited by its poor selectivity.[19]

In addition, one of these investigations also added 0.1 mol% hydroperoxides (relative to the phospholipids) to the experimental system. The presence of these hydroperoxides complicated the interpretation of hydroxyl radical impact in these systems.

Phospholipids covalently labeled with N-(7-nitrobenz-2-oxa-1,3-diazol-4-yl) (NBD) have been widely used to study biochemical and biophysical lipid phenomena including membrane organization and dynamic properties.[20] Moreover, the NBD probe has been shown to be highly polar. Thus, this probe was used in our study for probing the reactivity of hydroxyl radicals at the aqueous interface of the phospholipid.[21]

The fluidity of the membrane may also affect the ability of hydroxyl radicals to penetrate into the liposomal membrane. Kraske previously reported that DMPC liposomes have maximum permeability to small molecules at the phase transition temperature (T_m)[22] compared to above and below this temperature. Thus, the effect of temperature on this system was also investigated in the current study.

In this study, we utilized small, unilammellar liposomes as models for cell membranes due to their similar composition and structure compared to cellular membranes.[23] The work reported here differs from previous research in that we used fluorophores that were covalently bound to the phospholipids. This approach allowed for monitoring the probe reaction with hydroxyl radical as a function of probe position within the membrane. In addition, our system used a Fenton approach to generate hydroxyl radicals in the aqueous environment exterior to the liposomes with chelated iron-II, since most iron present in the human body is present in a chelated form.[24]

Aqueous hydrogen peroxide was continuously added at low flow rates to liposome suspensions in order to generate a steady-state concentration of hydroxyl radicals, as similarly performed previously.[25] [26, 27]

In comparison to the popularly-used ESR technique,[28, 29] the fluorescence approach used in our study has the advantages of high sensitivity, fast analysis time, ease of use, and less expensive equipment requirements. A multi-faceted approach embracing the enhanced specificity of MALDI-TOF-MS[30, 31] and scavenger studies[32] coupled to the high sensitivity of the fluorescence studies was used to provide a deeper understanding of the in-membrane oxidation by hydroxyl radicals. A better understanding of hydroxyl radical attack on membranes can help elucidate the mechanistic role this radical plays in the development of some diseases.

Experimental Methods

Materials

Three separate fluorescent probes, each purchased from Invitrogen, were used in this study: N-(7-nitrobenz-2-oxa-1,3-diazol-4-yl)-1,2-dihexadecanoyl-*sn*-glycero-3-phosphoethanolamine (NBD-PE), 1-hexadecanoyl-2-(1-pyrenehexanoyl)-sn-glycero-3-phosphocholine (C6-PYR-PC), and 1-hexadecanoyl-2-(1-pyrenedecanoyl)-sn-glycero-3-phosphocholine (C10-PYR-PC). Each of these probes has a fluorescent label covalently attached to the phospholipid molecule. For NBD-PE, the probe is attached to the headgroup, while C6-PYR-PC and C10-PYR-PC have the fluorophore attached to the tail group. These probes are depicted in Figure 1.

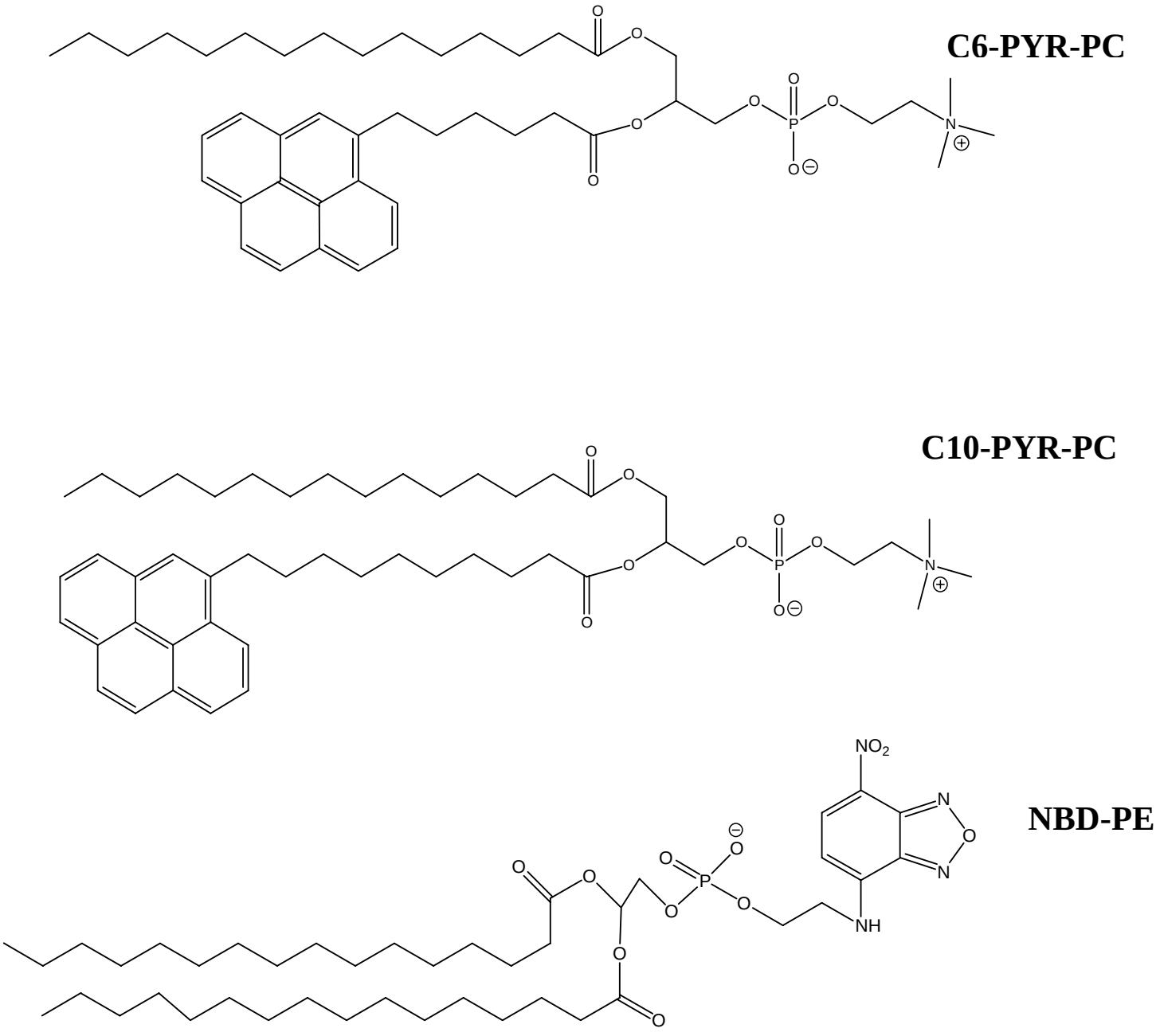

Figure 2.1. Structure of Fluorescent Phospholipids

Ferrous sulfate heptahydrate and phosphate-buffered saline (PBS, 0.9% NaCl) were obtained from Sigma. Hydrogen peroxide (30% aqueous) was purchased from Fisher and its concentration was measured iodometrically.[33] Cholesterol was purchased from Aldrich. Chloroform and EDTA were purchased from EM Science. All aqueous solutions were prepared using Nanopure UV (Barnstead/Thermolyne, Dubuque, IA) deionized water with a distilled water feed to the water purifier. All reagents were used as received without further purification.

Preparation of Liposomes

Our pyrenyl-labeled liposomes characterized the penetration depth of hydroxyl radicals into the hydrophobic membrane. The NBD-labeled probe [34] was chosen to characterize its reaction with hydroxyl radical at the aqueous interface due to its high hydrophilicity. NBD-PE or pyrenyl-labeled DMPC liposomes were prepared using a modified version of the procedure reported by McNamara and Rosenzweig.[35] A 40 µL aliquot of a 50 mM lipid cocktail composed of a 1:1 molar ratio of DMPC:cholesterol was placed under a stream of nitrogen overnight. To incorporate the fluorescent label, one of the fluorescent probes was included in the mixture prior to drying at 1 mol% relative to the unlabelled lipid content. Next, the film was hydrated while vigorously vortexing with 1 mL of 1 mM PBS. The final lipid concentration was 2 mM. The liposomes were extruded 9 times using an Avanti Mini-extruder with a 100 nm polycarbonate filter in order to remove any multilammelar liposomes present. Liposomes were used within one week, with storage at 4ºC.

Dynamic Light Scattering

All dynamic light scattering experiments were carried out with a Protein Solution Dynamic Light scattering instrument and analyzed using Dynamics Software. Settings on the instrument were for aqueous buffer conditions. For each sample, 40 measurements were taken at a total lipid concentration of 0.2 mM.

Digital Fluorescence Microscopy

All digital fluorescence images of pyrenyl and NBD-labeled liposomes were obtained using an Olympus IX71 inverted fluorescence microscope as described previously.[35] A 5 µL sample of labeled liposomes with a total lipid concentration of 3.3 µM was pipetted onto a glass coverslip and then covered with a second coverslip. The filter cube for imaging the C6-PYR-PC liposomes consisted of an excitation bandpass filter at 330-385 nm with dichroic mirror at 400 nm and emission wavelength at 429 nm. The filter cube for imaging the NBD liposomes consisted of excitation at 460 nm with a 50 nm bandpass, dichroic mirror set at 500 nm, with emission wavelength at 515 nm. The liposome images were collected using a 10X objective with a neutral density filter (0.55 o.d.). A CCD camera (Olympus DP70) was employed for digital imaging of the liposomes. The liposome sample was vortexed before imaging with five, 5 second pulses to disperse the sample. An exposure time of 0.3 s was used to acquire the images. ImagePro software was used for image collection. Adobe Photoshop v7.0 was used for manipulation of the presented images.

Fluorescence Studies

The fluorescence experiments were carried out on a Perkin Elmer LS 55 Luminescence Spectrometer equipped with a magnetic stirrer set on low. The quartz cuvette path length was 10 mm (Starna Cells, Atascadero, CA). Degradation of the fluorescent probes was followed by monitoring fluorescence emission at fixed excitation and emission wavelengths as a function of time. For pyrene, the excitation and emission wavelengths were set at 345 and 377 nm, respectively. For NBD, the excitation and emission wavelengths were set at 463 and 536 nm, respectively. For these time-based emission studies, two separate reaction protocols were used.

For degradation studies using high iron and peroxide loadings, a 3 mL aqueous solution of 0.2 mM Fe^{+2} and 0.2 mM EDTA was added to the cuvette. After 300 seconds of stirring, 1.5 M H_2O_2 (aq) was added continuously at 0.8 mL/hr with a syringe pump (kd Scientific Model 100). The total volume of H_2O_2 delivered during a 16 minute experiment was 0.23 mL. This volume was sufficiently small to not cause substantial changes in solution concentrations due to increased volume. Addition of peroxide was continued for 300 s, then a bolus addition of 300 µL of liposomes was added to the cuvette so that a final lipid concentration of 0.2 mM was achieved in the cuvette. All figures for these experiments are presented so that time zero corresponds to the time of addition of liposomes.

Additional experiments were conducted with iron and peroxide concentrations near physiological conditions. For these studies, 3 mL of a buffered solution of liposomes (3.3 μM lipid) was added to the cuvette.

To the cuvette were then added Fe^{+2} and EDTA to achieve a concentration of 0.3 μM for each. The solution was stirred for 600 s, then a 3 μM solution of H_2O_2 (aq) was continuously added at 0.8 mL/hr until the final volume of 0.23 mL was delivered. For these experiments, all figures are labeled time zero when H_2O_2 addition began.

For all experiments, the temperature of the cuvette and its contents were controlled by a thermostated cuvette holder. Temperatures used in this study include 15, 23, and 35ºC.

Biphenyl Scavenger Studies

Pyrenyl-labeled liposomes with varying concentrations of biphenyl were prepared in order to assess the effect of biphenyl as a scavenger in the lipid layer. A 40 μL aliquot of a 50 mM lipid cocktail consisting of a molar ratio of 1:1 DMPC/cholesterol with 0-3 mol% biphenyl per mol of the lipid was added to a test tube and the pyrenyl probe (either C6-PYR-PC or C10-PYR-PC) was added at 1 mol% of the total lipid content. The solution was allowed to evaporate under a stream of nitrogen. The liposomes were reconstituted in 1 mL of 1 mM PBS buffer and extruded as described above in order to remove multilamellar vesicles.

MALDI-TOF MS Studies

Matrix assisted laser desorption-time of flight mass spectrometry (MALDI-TOF MS) was used to identify lipid and cholesterol oxidation products that were formed after treatment with hydroxyl radical. Aqueous lipid extracts were prepared by using a modified scheme from Schiller *et al.*.[36] Stock solutions of 1:1 DMPC /cholesterol were prepared in chloroform.

A 300 µL aliquot of each solution was placed in a round bottom flask and rotovaped for 2 hours at room temperature and protected from light. Next, the flask was placed under a gentle stream of nitrogen overnight to remove any remaining chloroform. Lipid films were then reconstituted in 6 mL of 1 mM PBS buffer to give a lipid concentration of 1 mM while vortexing to spontaneously generate multilammelar liposomes. Liposomes in this study were shown to aggregate following extrusion at this high lipid concentration as evidenced by dynamic light scattering results (data not shown). The high lipid loading was utilized in order to improve the ability to detect analytes in the mass spectral analysis. A 1 mL aliquot of the liposome solution was placed in a quartz container and Fe^{+2} and EDTA were added to yield a concentration of 5 mM for each. After stirring for 300 s, 1.5 M hydrogen peroxide was added continuously at a rate of 0.8 mL/hr. The total volume of H_2O_2 delivered was 0.23 mL. The sample was thermostatted at 15, 23, or 35C using a circulating water bath. Following Fenton degradation, lipids were extracted with a twofold excess of $CHCl_3$:MeOH (2:1) as previously reported by Bligh and Dyer.[37] Samples were then centrifuged for 20 min and the aqueous layer was separated.

Aqueous lipid extracts were then mixed with 0.5 M 2,5-dihydroxybenzoic acid (DHB) in MeOH with 0.5% trifluoroacetic acid (TFA) at a ratio of 1:1 and spotted on a gold-coated MALDI plate as previously reported by Zschornig and co-workers.[38] The spots were allowed to air dry before MALDI analysis. Mass spectra were obtained using an Applied Biosystems 4700 Proteomics Analyzer 171 MALDI-TOF mass spectrometer fitted with a N_2 laser (337nm). Spectra were internally calibrated using DMPC and DHB standards.

Spectra were analyzed using Data Explorer software v4.8. A blank consisting of DMPC and cholesterol only without Fenton reagent, an control with H_2O_2 added to liposomes but with no Fe^{+2}-EDTA added, and the Fenton degraded lipid extracts were each analyzed separately.

Quantitation of Hydroxyl Radical

Hydroxyl radical concentrations were determined in the absence of liposomes. Phenol degradation in aqueous PBS was followed using high performance liquid chromatography (HPLC). The initial concentration of phenol was 500μM in 1mM PBS buffer. An aliquot of aqueous Fe^{+2}-EDTA was added to the sample to yield a final concentration of 10 mM. Hydrogen peroxide was added at a rate of 1 mL/hr using a syringe pump with an initial concentration of 2.0 M. The total volume of peroxide added was 0.2 mL. The amount of phenol degradation was determined from the peak area at the appropriate retention time in the chromatogram. The experiment was run at three temperatures 15, 23, and 35C. Pseudo first order rate constants were calculated from linear regressions of ln[phenol] versus time.

An Alltech C_{18} column (250 x 4.6mm, 5µm particle size) was used with a 40/60 acetonitrile/water mobile phase adjusted to pH 3 with dilute acid. The HPLC flow rate was 0.5 mL/min, and UV absorbance was measured at 254 nm.

Results and Discussion

Dynamic Light Scattering and Digital Fluorescence Microscopy

The extruded liposomes were diluted to a lipid concentration of 0.2 mM with 1 mM PBS buffer and analyzed using dynamic light scattering to determine the hydrodynamic radius as well as the lamellarity. For all liposomes, a monomodal distribution of particle sizes was observed, indicating that only unilammelar liposomes were present. If multilamellar liposomes had been present as well, a bimodal distribution would have been observed. Liposomes prepared without fluorescent labels showed a hydrodynamic radius of 62 ± 4 nm (uncertainty is confidence interval at 95% confidence, N = 40). For the fluorescently labeled liposomes, the measured hydrodynamic radii were 67 ± 5 nm, 69 ± 6 nm, and 73 ± 6 nm for NBD-PE, C6-PYR-PC, and C10-PYR-PC, liposomes, respectively. Based on a t-test at 95% confidence, only the C10-PYR-PC labeled liposomes were statistically larger than the unlabeled liposomes.

Fluorescence microscope images of the extruded liposomes showed no evidence of aggregation for liposomes prepared at a 0.2 mM total lipid concentration (see Figure 2). These data are consistent with the results from dynamic light scattering.

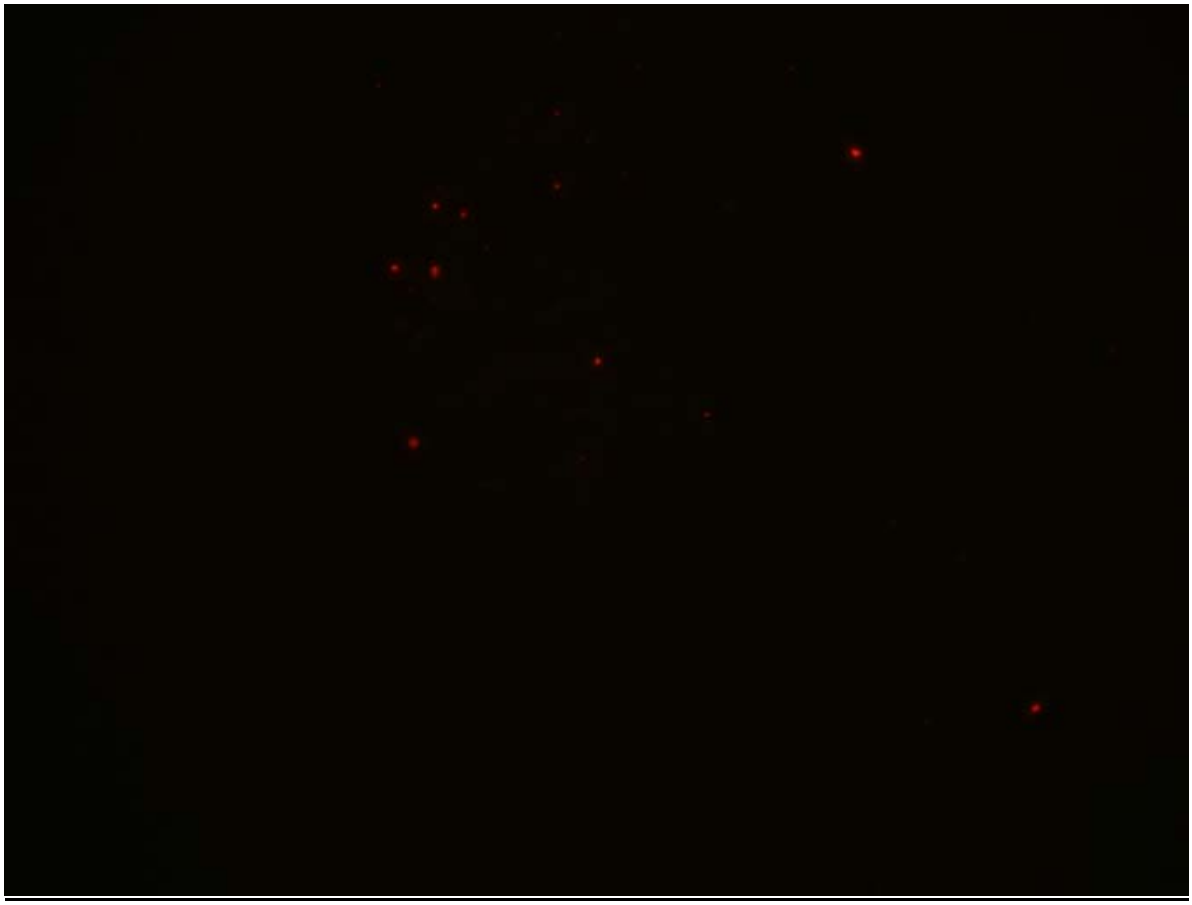

Figure 2.2.Digital Fluorescence Microscopy Image of C6-PYR-PC Liposomes

Fluorescence Studies

Figure 3a shows the loss in fluorescence upon degradation of NBD-PE liposomes with Fenton reagent at three different temperatures. In these experiments, labeled liposomes were added at t = 0 to preformed Fenton reagent as discussed in the experimental section. The data reveals an enhancement in the rate of degradation of the NBD-PE probe as the temperature increased. Initial rates were approximated from the slope of fluorescence vs time plots during the time period of 30-230 s (Table 1). Very good linearity was observed in all traces during this time period ($R^2 > 0.995$, N = 100). The first 30 seconds was not used in order to allow the system to stabilize after addition of the liposomes. For these experiments, the data is truncated around 800 s due to interference from increasing background chemiluminescence.[39] This background emission was observed in the absence of fluorescent probes (see Figure 4) when high concentrations of iron and peroxide were used, and the background emission was more severe at higher temperature. The decrease in the slope of the 35ºC trace at longer times in Fig. 3a is at least partly due to interference from this background signal. Nevertheless, the data in Fig. 3a clearly indicate a substantial increase in NBD oxidation by hydroxyl radical with increasing temperature. Comparing the slopes of these data from 30-230 s, a 42% increase in NBD reaction rate was observed upon increasing from 15 to 23ºC. This change was statistically significant based on a t-test at 95% confidence. Although the slope for the 35ºC experiment is less certain, the observed rate increased by 113% compared to the 15ºC experiment (statistically significant based on a t-test at 98% confidence).

Table 2.1. Approximate initial rates of fluorescence loss for fluorescent membrane probes degraded with high dose of hydroxyl radical generated with 0.2 mM Fe^{+2}-EDTA and 1.5 M H_2O_2 (aq) added at 0.8 mL/hr. The unit is arbitrary fluorescence units per second. Reported error is one standard deviation for replicate experiments (N = 3).

	15 °C	23 °C	35 °C
NBD	$(1.60 \pm 0.09) \times 10^{-4}$	$(2.3 \pm 0.2) \times 10^{-4}$	$(3.4 \pm 0.4) \times 10^{-4}$
C6-PYR	$(10.7 \pm 0.5) \times 10^{-4}$	$(16.5 \pm 0.7) \times 10^{-4}$	$(23.0 \pm 0.3) \times 10^{-4}$
C10-PYR	$(6.1 \pm 0.4) \times 10^{-4}$	$(10.5 \pm 0.9) \times 10^{-4}$	$(21 \pm 1) \times 10^{-4}$

Possible explanations for these results include: 1) the concentration of hydroxyl radical increased with temperature, 2) the rate constant for reaction of NBD with hydroxyl radical increased with temperature, or 3) accessibility of the radical to the surface of the membrane increased with temperature. In order to test the first explanation, we studied the reaction of hydroxyl radical with phenol in aqueous solution at varying temperatures. These experiments were conducted with no lipids present since the aim was only to assess the temperature dependence of the reactions. As can be seen from the data presented in Table 2, observed pseudo first order kinetics for phenol degradation only changed slightly over the temperature range studied. On increasing from 15 to 25ºC, an increase in the pseudo first order rate constant of about 9% was observed. Based on a t-test, this difference was statistically significant at the 99.5% confidence level. The values at 25 and 35ºC were not statistically different even when tested at the 90% confidence level. These data indicate that in the absence of a membrane interface, a slight increase (~10%) in hydroxyl radical mediated degradation rate is expected upon increasing the temperature from 15 to 35ºC. Consequently, it is unlikely that the hydroxyl radical concentration changed by more than 10% upon increasing the temperature from 15 to 35ºC. For the NBD labeled liposomes, the increase in reactivity with temperature exceeded that expected based on the phenol studies.

Table 2.2. Observed pseudo first order rate constants for aqueous phenol degradation with Fenton reagent under steady state hydroxyl radical concentration. Reported error is one standard deviation for replicate experiments (N = 3).

T (°C)	k′ (s^{-1})
15	0.594 ± 0.004
25	0.65 ± 0.01
35	0.635 ± 0.004

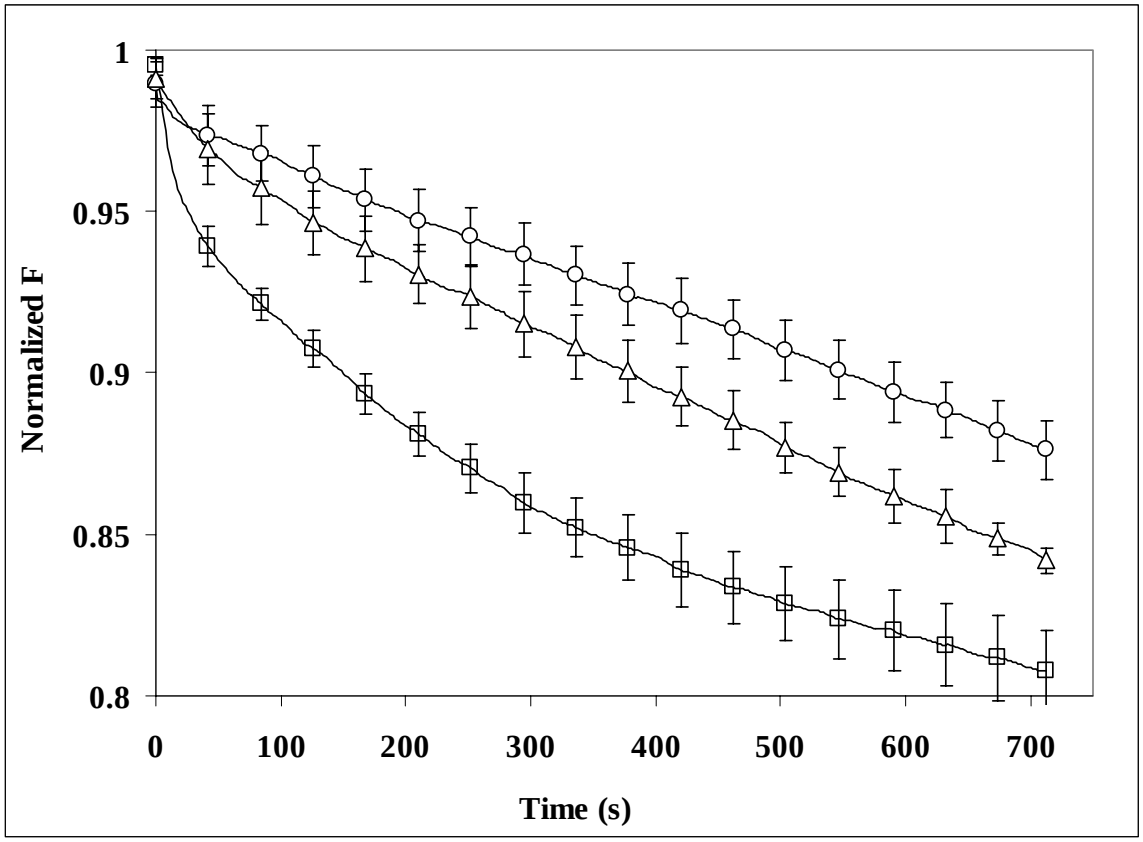

Figure 2.3a.1% NBD-PE liposomes with 0.2mM Fe^{+2}-EDTA and H_2O_2 addition at 0.8mL/hr with initial concentration at 1.5M. Curves were normalized to 1 where liposomes were added. Each curve represents triplicate runs at each temperature.
O-15ºC Δ-23ºC □-35ºC

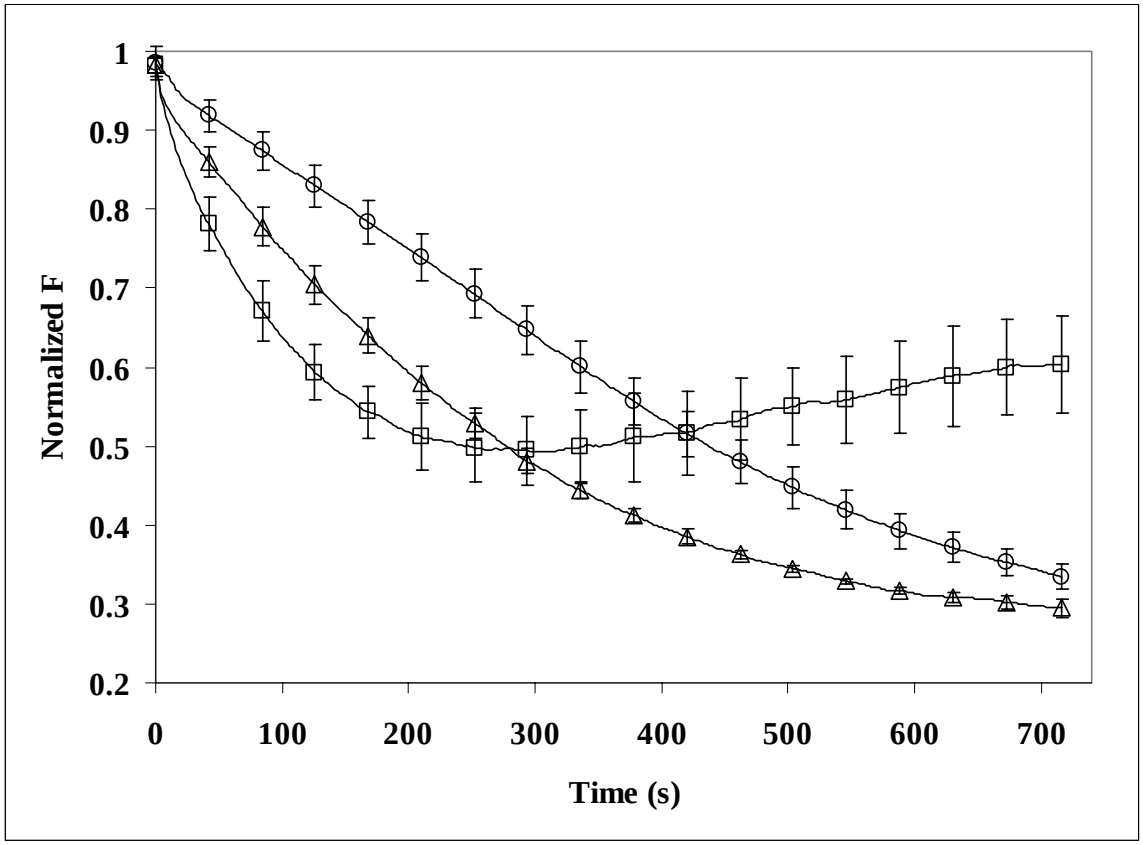

Figure 2.3b. 1% C6-PYR-PC Liposomes with 0.2mM Fe^{+2}-EDTA and H_2O_2 addition 0.8mL/hr with an initial concentration of 1.5M. Curves were normalized to 1, where liposomes were added. Each curve represents triplicate runs at each temperature.
O= 15ºC, Δ= 23ºC, □=35ºC

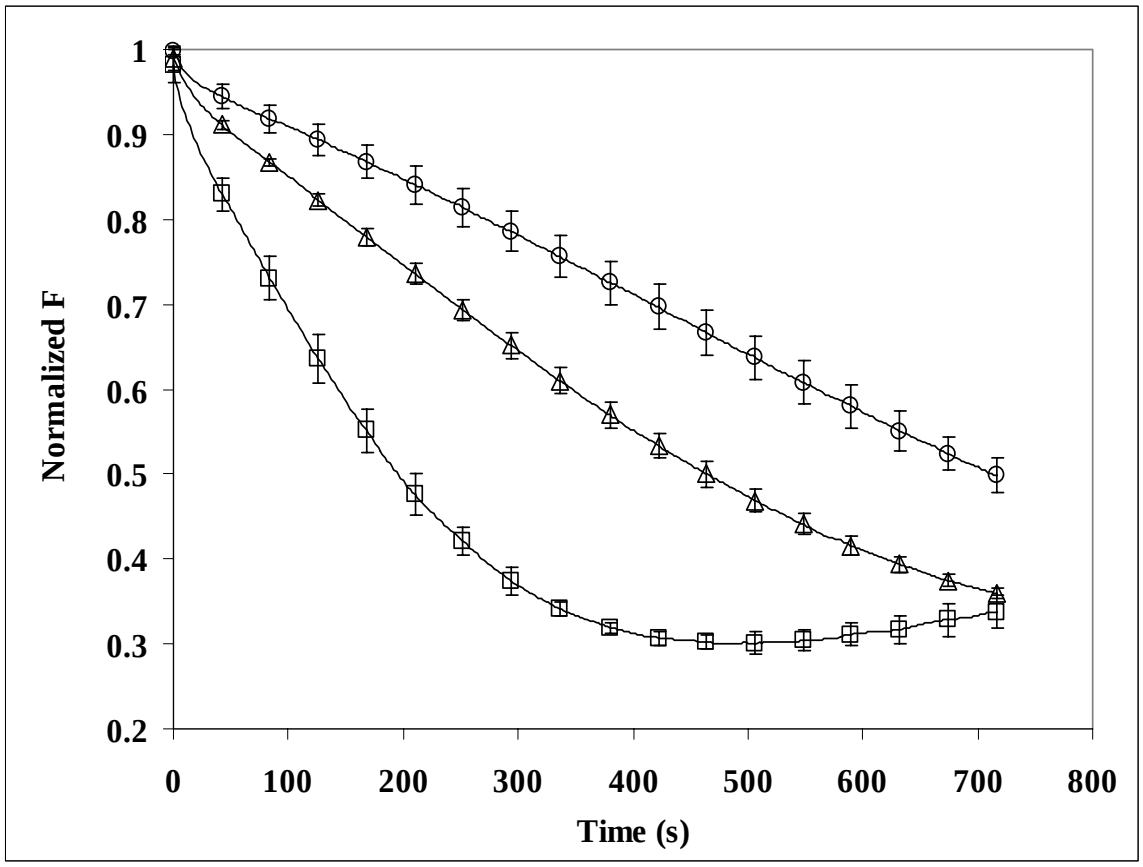

Figure 2.3c. 1% C10-PYR-PC liposomes with 0.2mM Fe^{+2}-EDTA and H_2O_2 addition at 0.8mL/hr with initial concentration at 1.5M. Curves were normalized to 1 where liposomes were added. Each curve represents triplicate runs at each temperature.
O= 15ºC, Δ= 23ºC, □=35ºC

Therefore, the changes in observed reaction rate at the membrane interface are likely due to changes in surface accessibility of the radical, possibly due to a change in the orientation of the NBD probe caused by changes in membrane structure.

Figures 3b and 3c show the loss in fluorescence during degradation of C6 and C10-PYR-PC probes with 0.2 mM Fe-EDTA present while adding 1.5 M H_2O_2 at 0.8 mL/hr. Addition of peroxide to the iron-EDTA solution began prior to liposome addition, which occurred at t = 0. These experiments were conducted at three temperatures: 15, 23, and 35ºC. The intitial rates of fluorescence loss were determined as described above for the NBD probe. These data, determined from the slope during the period 50-250 s, are presented in Table 1. At all three temperatures, the C6 probe, located closer to the water interface, degraded more rapidly than the deeper C10 probe. These data indicate that the hydroxyl radical was able to penetrate to both positions within the membrane, but the radical was less likely to reach regions of the membrane that were farther from the aqueous media in which the radical was generated. For both the C6 and C10 systems, probe degradation was fastest at 35ºC and slowest at 15ºC. Near the phase transition temperature of the membrane (23ºC), an intermediate degradation rate was observed. These results suggest that membrane disorder at the phase transition temperature is not a major factor in controlling radical permeation into and reaction within the membrane. Furthermore, for the in-membrane probes, the increase in degradation rate with increasing temperature was much greater than for that observed using a liposome free system (see discussion above for phenol degradation).

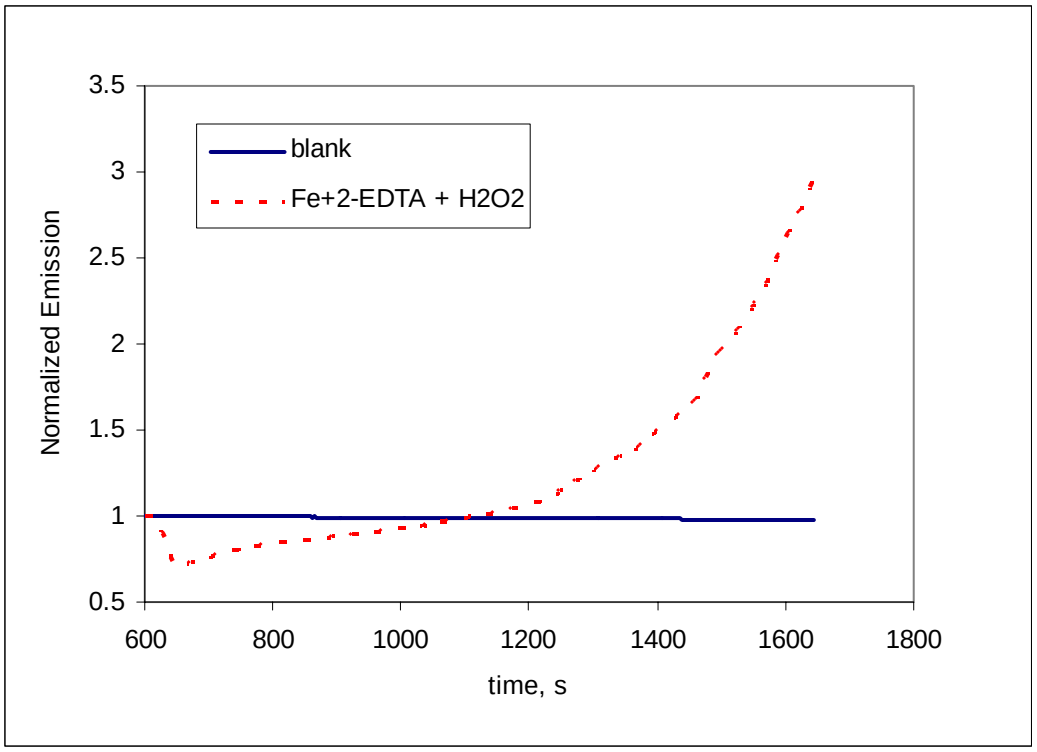

Figure 2.4. Chemiluminescence Background Signal from Unlabelled liposomes at 37ºC

The C6-PYR-PC system showed a 1.5 fold increase in degradation rate upon increasing the temperature from 15 to 23 °C. Increasing the temperature to 35 °C resulted in a 2.1 fold increase in reaction rate compared to 15 °C. The C10-PYR-PC system showed increases of 1.7 and 3.4 fold upon increasing from 15 to 23 or 35 °C, respectively.

Comparing the pyrene probes, the C6-PYR-PC probe contained a fluorophore that was tethered to a six carbon chain, resulting in positioning of the probe within the interior of the lipid bilayer. In comparison, the C10-PYR-PC probe had pyrene tethered to a 10 carbon chain, resulting in a deeper average position of the pyrene within the lipid bilayer. The C6-PYR-PC probe showed greater reactivity than the C10-PYR-PC probe. This greater reactivity is expected since it lies closer to the aqueous interface and is more accessible to radicals generated in the aqueous phase. Direct comparison with the NBD probe is not possible since NBD and pyrene have different rate constants for reaction with hydroxyl radical.

As discussed above, the shape of the fluorescence vs. time plots did not follow simple kinetic models. In order to verify that fluorescent products were not formed upon reaction of the pyrene probes, we completed additional investigations of the emission spectra. We examined the fluorescence emission spectra of the pyrene probes before and after degradation with hydroxyl radical. These data are presented in Figure 3 in which each spectrum is normalized to its maximum value. Comparing the spectra before and after degradation, only slight differences in the spectral shape were noticeable, and no new emission peaks were observed.

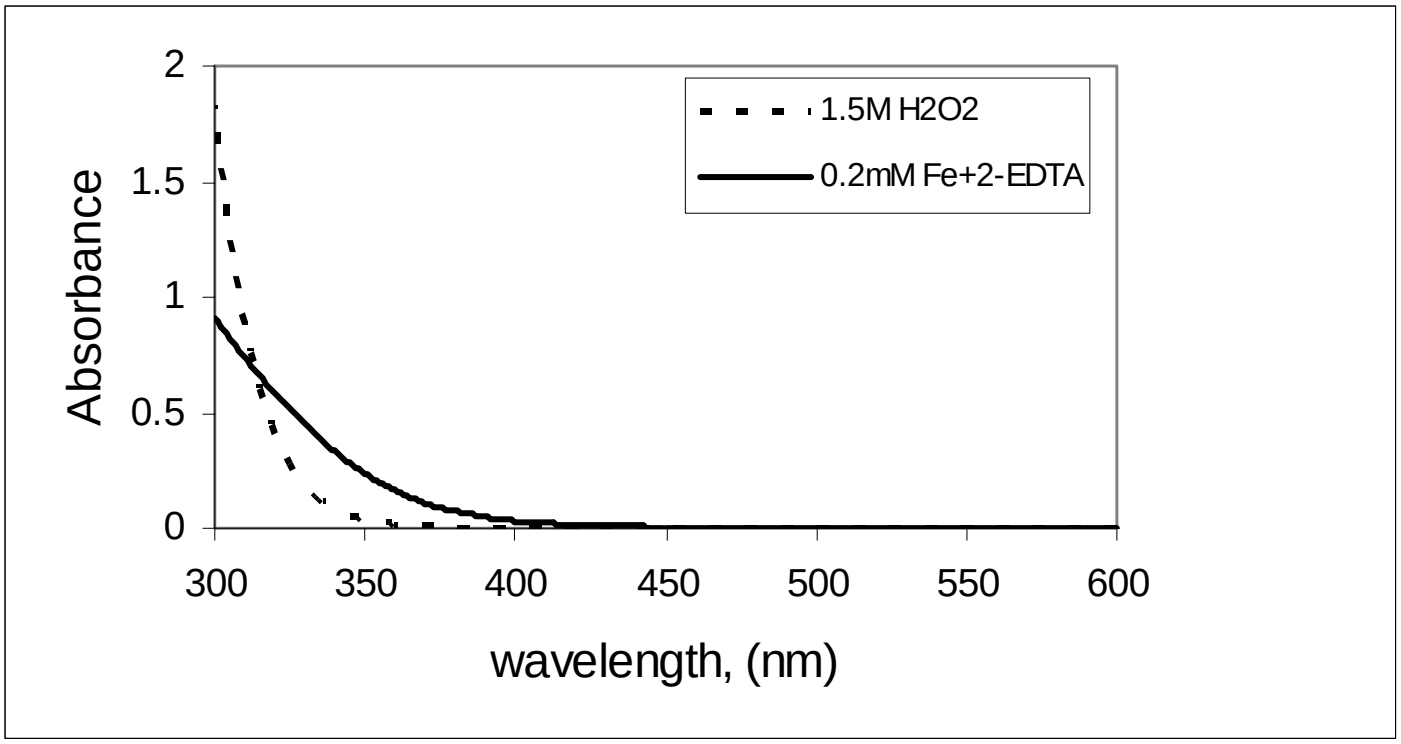

Figure 2.5. Absorbance spectra of 0.2mM Fe^{+2}-EDTA and 1.5M H_2O_2.

The small differences between the two spectra are likely due to inner filter effects caused by iron and peroxide absorbance. The before degradation spectrum had no iron or peroxide, while the post degradation spectrum contained both. Since the iron and peroxide absorbances decrease substantially with increasing wavelength (see Figure 5), the fluorescence at short wavelengths was partially absorbed by these species before exiting the cuvette, causing a shift in the relative intensity of observed fluorescence at short and long wavelengths.

The III/I vibronic band ratio of pyrene emission is an excellent tool for measuring the hydrophobicity of the pyrene microenvironment.[40-42] Band III has a maximum at 396 nm and band I has a maximum at 381 nm. Clearly visible in Figure 5 is a small change in the III/I vibronic band ratio between the before and after degradation spectra. This change is predominantly due to the inner filter effect described above, and therefore little if any change was caused by the degradation. Since little or no change in the III/I ratio was observed, the microenvironment of the pyrene did not change before and after degradation. Pyrene probe molecules that were degraded showed the same microenvironment as that observed prior to degradation, suggesting that the membrane integrity is sufficient to maintain this environment. The III/I ratio observed for pyrene in the membrane used in this study was around 1.04. Based on this observation, the pyrene microenvironment is comparable in hydrophobicity to bulk acetone which has a reported III/I ratio of 1.02[40]. The fluorescence data presented in Figure 3 also indicate that no pyrene excimers were present in the system either before or after degradation.

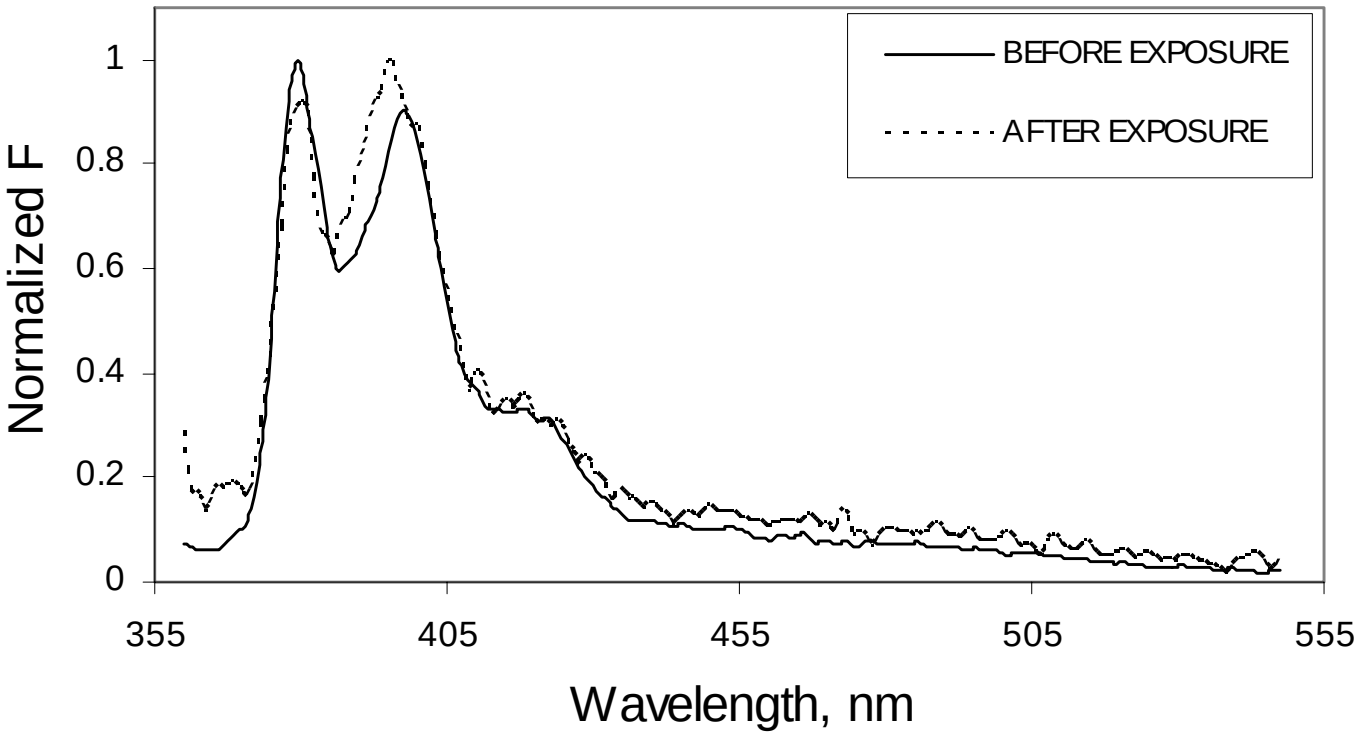

Figure 2.6. III/I ratio of C6-PYR-PC before and after Fenton degradation.

Excimers form when pyrene molecules aggregate to form dimer pairs.[43-45] Such pairing usually occurs when pyrene is at high concentration in a hydrophobic medium. The lack of excimer emission around 480 nm shows that the pyrene probes did not aggregate substantially in the liposomal membranes, either before or after degradation, indicating that the pyrene probes in the membrane were sufficiently isolated from each other to prevent excimer formation. Both the III/I vibronic band ratios and the lack of excimer emission provide evidence that the pyrene probes were dispersed uniformly within the lipid region of the liposomes and that intact pyrene probes experienced little if any change in microenvironment during the degradation experiments.

As can be seen for degradation of the membrane-bound pyrenyl probes presented in Figures 3b and 3c, it is clear that the kinetic regime is complex over the reaction time studied. In order to simplify the kinetic regime, and to operate under conditions closer to that of physiological systems, we completed additional studies with low iron and low peroxide loading. For these studies, pyrene labeled liposomes were first equilibrated with 0.3 μM Fe-EDTA for 300 s with stirring. At that point, 3 μM H_2O_2 (aq) was added at a rate of 0.8 mL/hr for an additional 300 s before fluorescence data acquisition began. These equilibration steps allowed the Fenton system to come to steady state prior to monitoring pyrene degradation. Under these conditions near linear decreases in fluorescence were observed (see Figures 7a, 7b, 8a, and 8b). Linear regressions were used to calculate the rate of probe degradation. Each experiment was completed in triplicate, and the average rate was calculated from the triplicate measurements. The results are shown in Table 3.

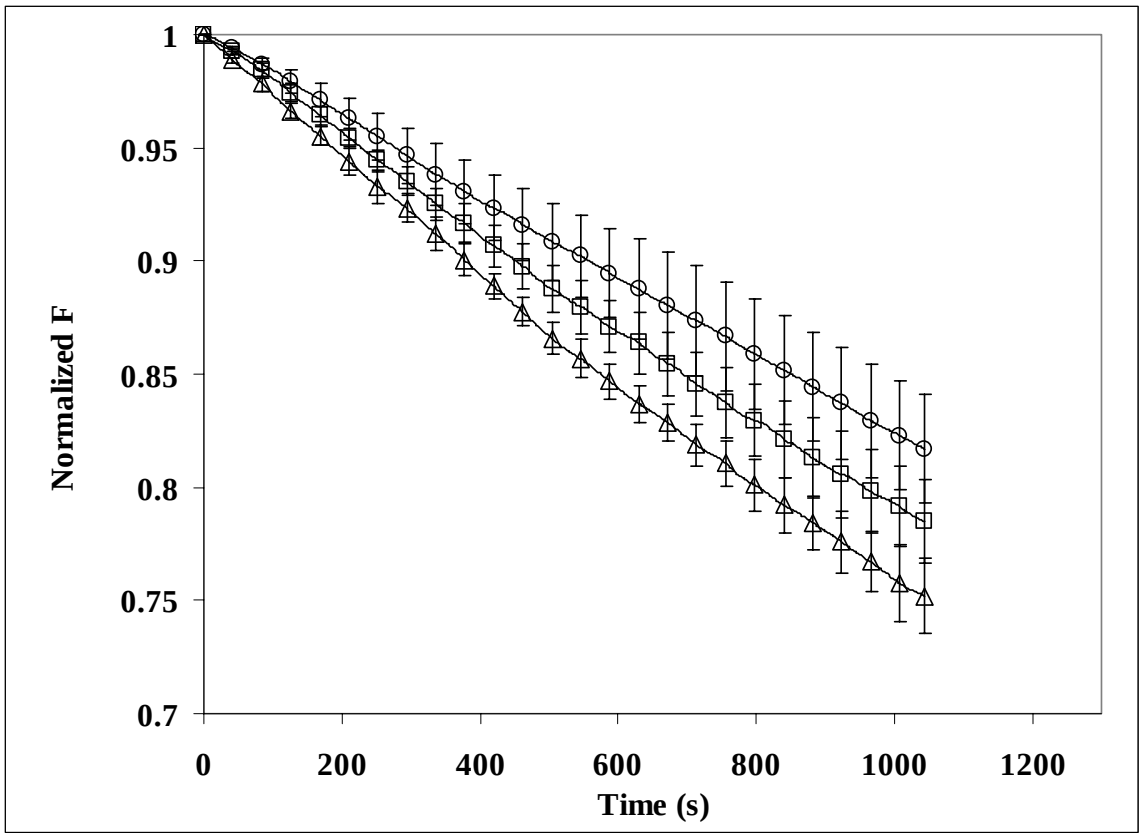

Figure 2.7a. 1% C6-PYR-PC Liposomes with no cholesterol and 0.3μM Fe^{+2}-EDTA and H_2O_2 addition at 0.8mL/hr with initial concentration at 3μM. Curves were normalized to 1 where Fenton degradation began. Each curve represents triplicate runs at each temperature. O= 15ºC, Δ= 23ºC, □=35ºC

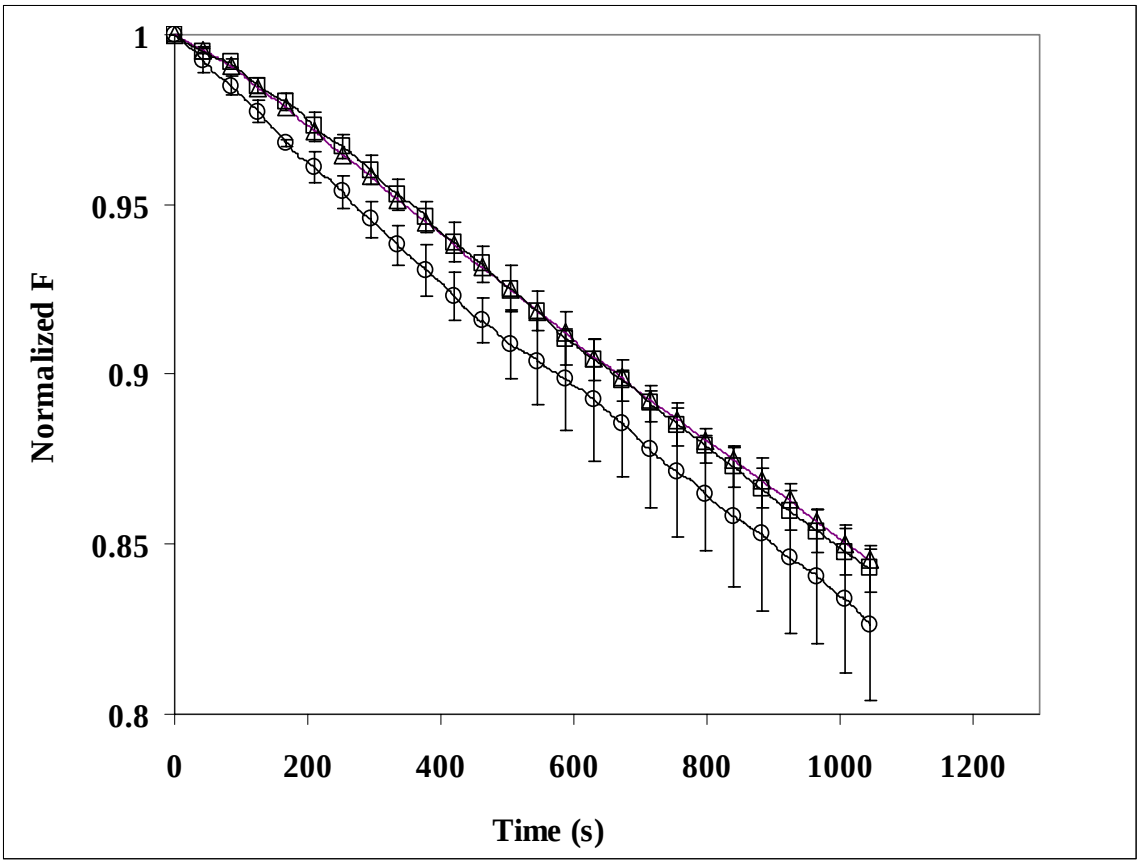

Figure 2.7b. 1% C6-PYR-PC liposomes with cholesterol and 0.3μM Fe^{+2}-EDTA and H_2O_2 addition at 0.8mL/hr with initial concentration at 3μM. Curves were normalized to 1 where Fenton degradation began. Each curve represents triplicate runs at each temperature. O= 15ºC, Δ= 23ºC, □=35ºC

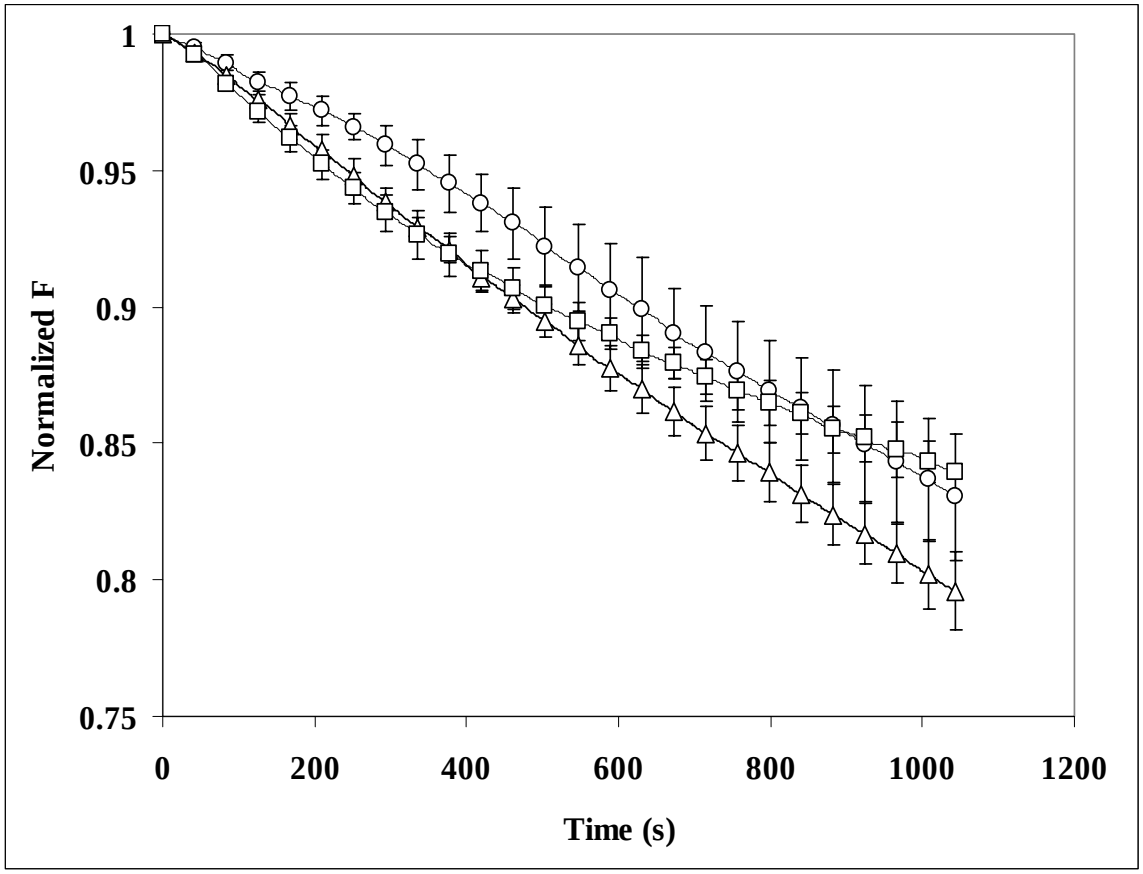

Figure 2.8a. 1% C10-PYR-PC Liposomes with no Cholesterol and 0.3μM Fe^{+2}-EDTA and H_2O_2 addition at 0.8mL/hr with initial concentration at 3μM. Curves were normalized to 1, where Fenton degradation began. Each curve represents triplicate runs at each temperature. O= 15ºC, Δ= 23ºC, □=35ºC

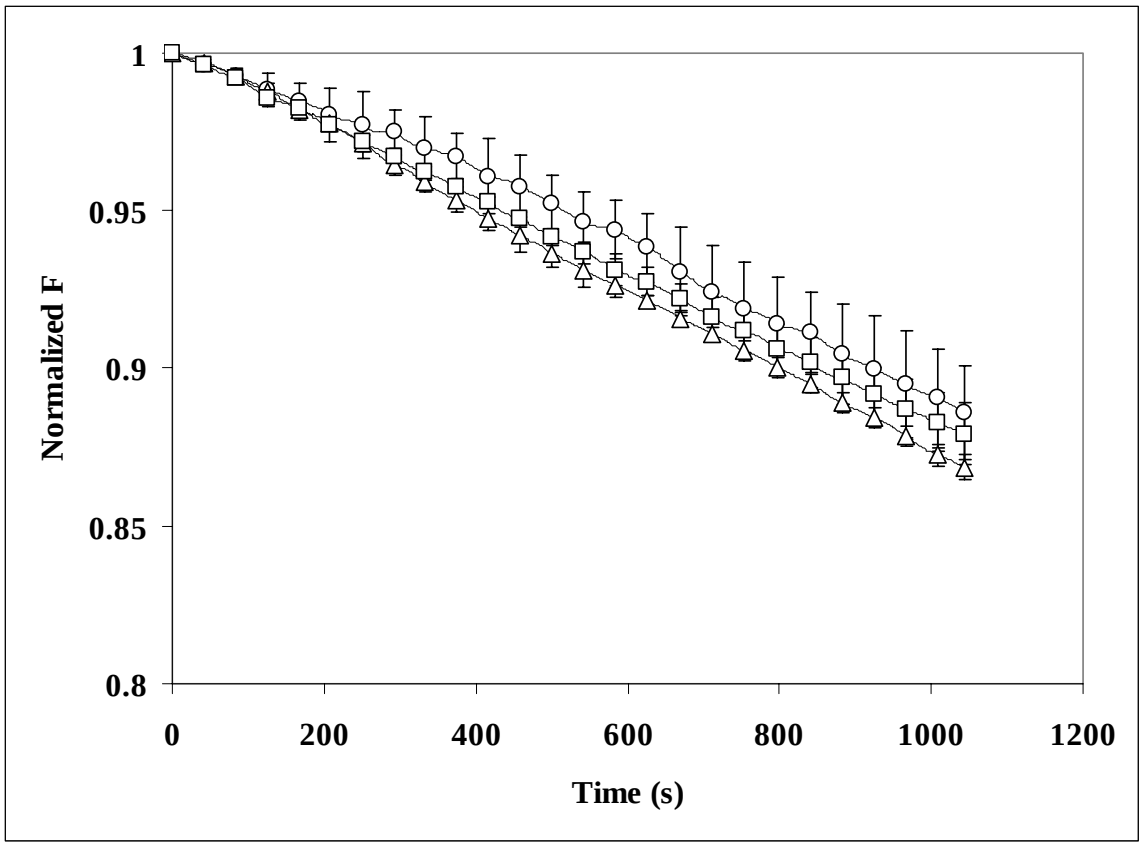

Figure 2.8b. 1% C10-PYR-PC Liposomes with Cholesterol and 0.3μM Fe^{+2}-EDTA and 2.4nM/hr H2O2 addition. Curves were normalized to 1 where Fenton degradation began. Each curve represents triplicate runs at each temperature. O= 15ºC, Δ= 23ºC, □=35ºC

Table 2.3. Observed rates of fluorescence loss for fluorescent membrane probes degraded with low dose of hydroxyl radical generated with 0.3 μM Fe^{+2}-EDTA and 3 μM H_2O_2 (aq) added at 0.8 mL/hr. The unit is arbitrary fluorescence units per second. Reported error is one standard deviation for replicate experiments (N = 3).

	15°C	23°C	35°C
C6 probe with Cholesterol	$(1.1 \pm 0.2) \times 10^{-4}$	$(1.52 \pm 0.04) \times 10^{-4}$	$(1.56 \pm 0.05) \times 10^{-4}$
C6 probe without Cholesterol	$(1.8 \pm 0.3) \times 10^{-4}$	$(2.4 \pm 0.1) \times 10^{-4}$	$(2.1 \pm 0.2) \times 10^{-4}$
C10 probe with Cholesterol	$(1.1 \pm 0.1) \times 10^{-4}$	$(1.29 \pm 0.01) \times 10^{-4}$	$(1.18 \pm 0.10) \times 10^{-4}$
C10 probe without Cholesterol	$(1.7 \pm 0.2) \times 10^{-4}$	$(2.0 \pm 0.1) \times 10^{-4}$	$(1.50 \pm 0.09) \times 10^{-4}$

For the C6-PYR-PC probe in membranes prepared with 1:1 DMPC:cholesterol, increasing the temperature from 15 to 23 °C resulted in a 38% increase in probe degradation rate. Further increasing the temperature to 35 °C resulted in no further increase in degradation rate. For the C10-PYR-PC probe in membranes prepared with 1:1 DMPC:cholesterol, increasing the temperature from 15 to 23 °C resulted in a 17% increase in probe degradation rate. Further temperature increase to 35 °C resulted in a slightly lower reaction rate than for 23 °C. Unlike the higher iron/peroxide experiments described above, the C6 and the C10 probes showed the same rate of reaction at 15 °C, but the C6 probe had a substantially faster rate of reaction at the two higher temperatures studied.

Liposomes with no cholesterol were also prepared in order to assess the effects of cholesterol. Reaction of the probes with hydroxyl radical was substantially higher in the absence of cholesterol. Overall, when present, cholesterol assumes the role of a hydroxyl radical scavenger at all the temperatures studied with both probes. This conclusion is based on the observation of lower probe degradation rates in the presence of cholesterol. This change in reaction rate is likely due to the absence of the scavenging effect exerted by cholesterol. In the presence of cholesterol, radical species entering the membrane can react with cholesterol, reducing the available concentration of hydroxyl radical. Because cholesterol exerted a protective effect for both in-membrane probes, it is clear that cholesterol radicals did not play an important role in the rate of probe degradation under the conditions used here.

Such radicals may be important over longer time scales, but in these studies, no evidence of cholesterol radical reaction with the probes was found (see mass spectral results discussed below). The behavior of the C6 and C10 probes as a function of temperature was similar with and without cholesterol.

It is important to note that these experiments were conducted with low oxidant levels. In contrast to many other studies, depletion of natural scavengers, in this case cholesterol did not occur under the low dosing conditions used in these experiments. The low dose experiments more closely mimic the conditions likely to be found in real cellular systems[25].

To gather more evidence regarding the involvement of hydroxyl radicals in the degradation of the membrane bound C6-PYR-PC probe, a lipophilic hydroxyl radical scavenger (biphenyl) was incorporated into DMPC/cholesterol liposomes. As shown in Figure 6a, addition of biphenyl inhibited the observed degradation rate of C6-PYR-PC liposomes. Increasing the biphenyl content increased this inhibitory effect. These results indicate that a radical species was in fact present in the lipid region of the membrane. Taken together with other evidence presented in this paper, this result supports the theory that hydroxyl radical was able to penetrate into the lipid layer of the membrane. For the deeper C10-PYR-PC probe, addition of biphenyl did not result in a significant change in probe degradation rate as shown in Figure 6b. The lack of scavenging effect for the C10 probe is unexpected, and may indicate that the biphenyl probe aggregates near the C6 pyrene probe but not near the C10 pyrene probe. Such positioning of molecules within different regions of the membrane has been previously reported.[19]

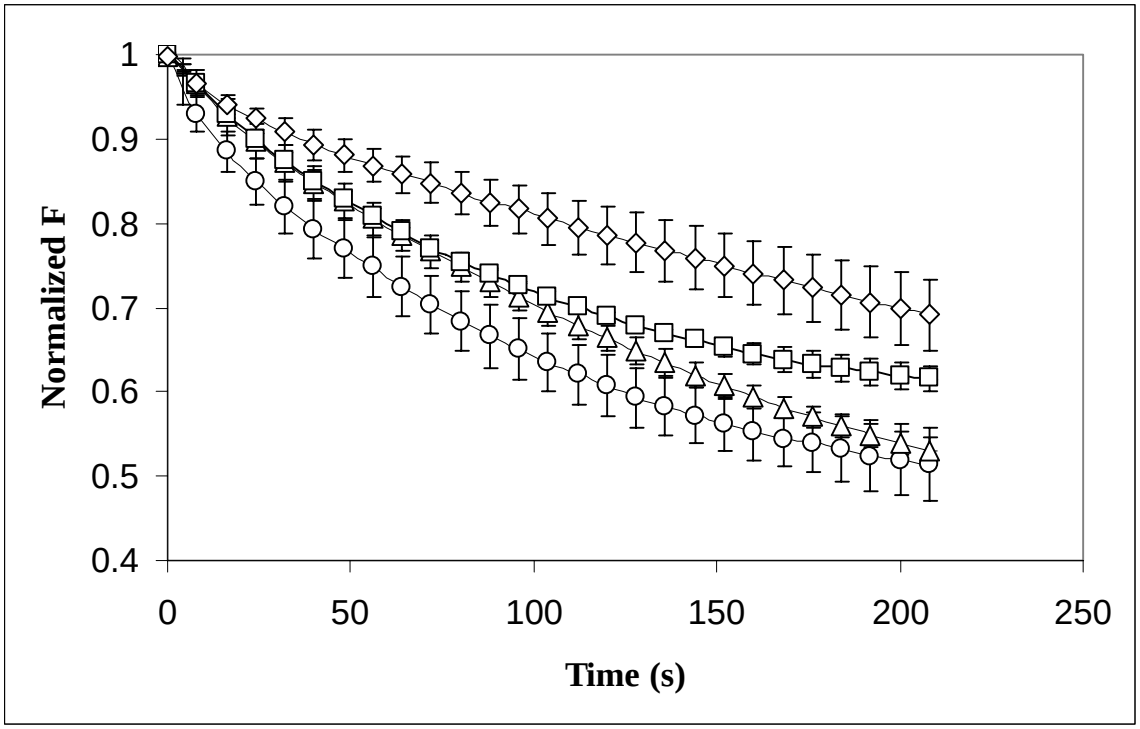

Figure 2.9a. Effect of varying biphenyl concentration with C6-PYR-PC liposomes at 35ºC with bolus addition of 0.2mM Fe^{+2}-EDTA with H_2O_2 addition at 0.8mL/hr with initial concentration at 1.5M. Curves were normalized to 1 where liposomes were added. Each curve represents triplicate runs at each temperature.
O=0% Biphenyl, Δ= 0.5% Biphenyl, □=1.5% Biphenyl, ◊=3% Biphenyl

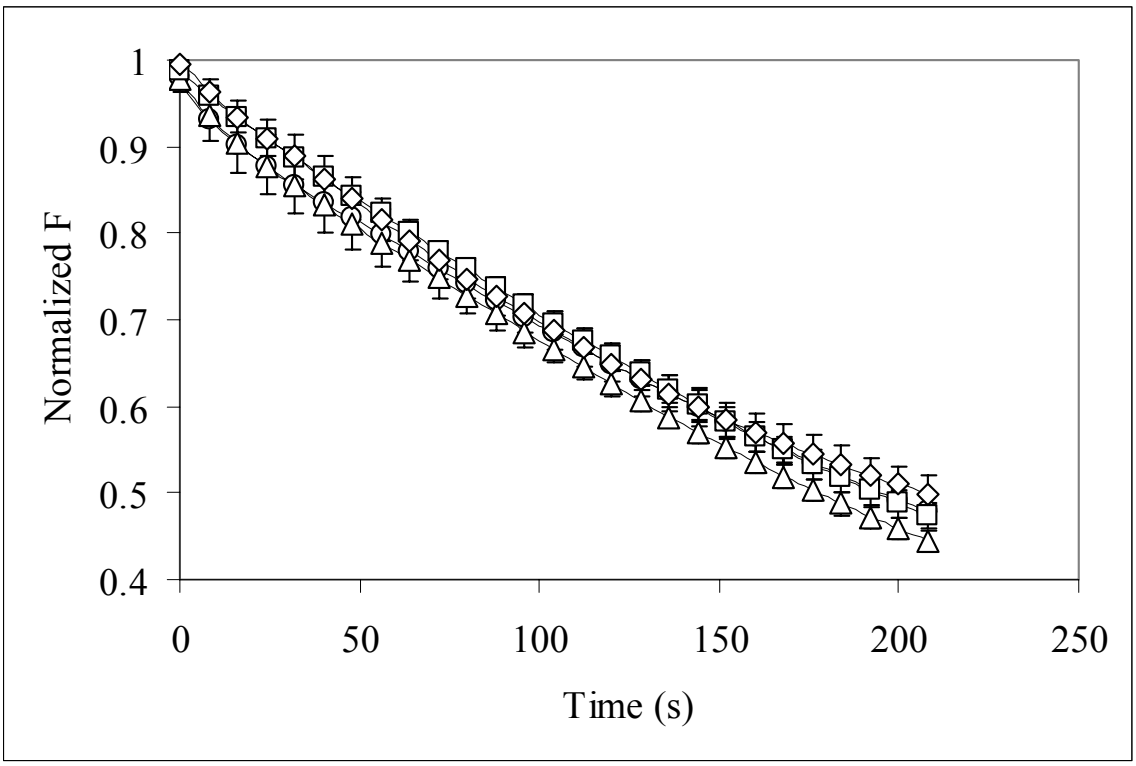

Figure 2.9b. Effect of varying biphenyl concentration with C10-PYR-PC liposomes at 35ºC with bolus addition of 0.2mM Fe^{+2}-EDTA with addition of H_2O_2 at 0.8mL/hr with initial concentration at 1.5M. Curves were normalized to 1 where liposomes were added. Each curve represents triplicate runs at each temperature.
O=0% Biphenyl, Δ= 0.5% Biphenyl, □=1.5% Biphenyl, ◊=3% Biphenyl

Despite the unexplained scavenging behavior for the C10 probe, the C6 data still support the model that hydroxyl radical penetrated inside the membrane.

MALDI-TOF MS

To further investigate the mechanistic involvement of hydroxyl radicals in lipid oxidation of the liposomes composed of a 1:1 molar ratio of DMPC to cholesterol, MALDI-TOF MS was employed.[46] Both oxidized and unoxidized liposomes were analyzed by MALDI-TOF MS in order to identify lipid oxidation products. Liposomes that were not treated with Fenton reagent showed only peaks corresponding to intact cholesterol. (Figure 10). In the presence of the Fenton reagent, the only cholesterol oxidation product observed was the protonated ketone of cholesterol at m/z 401 (Figure 11), indicating that cholesterol was oxidized in the presence of hydroxyl radical. However, reaction of the pyrene probe was slower in the presence of cholesterol indicating that cholesterol acted as a scavenger rather than an important intermediate in probe degradation in these experiments.

In mass spectra for DMPC that was not exposed to oxidants, strong signals were observed for the protonated, sodiated and potassiated adducts of DMPC as expected at m/z 678, 700, and 716, respectively (Figure 12).

However, both under high and low iron/peroxide loadings, no peaks associated with oxidized DMPC were found (Figure 13). The lack of lipid oxidation products is not surprising since a fully saturated phospholipid was used. Compared to unsaturated hydrocarbons, fully saturated hydrocarbons are slower to react with hydroxyl radical.[7]

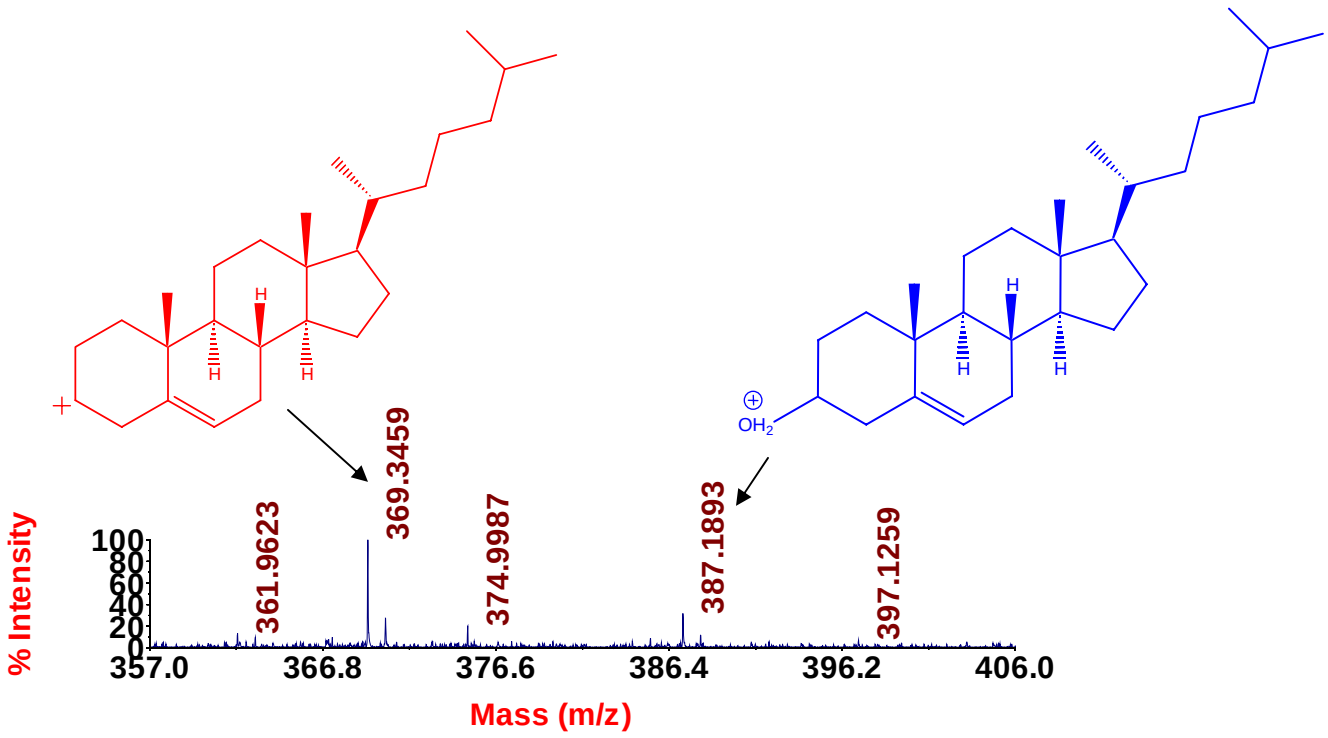

Figure 2.10. Blank cholesterol with no Fenton Reagent: m/z 369 is cholesterol water loss product and m/z is protonated cholesterol product

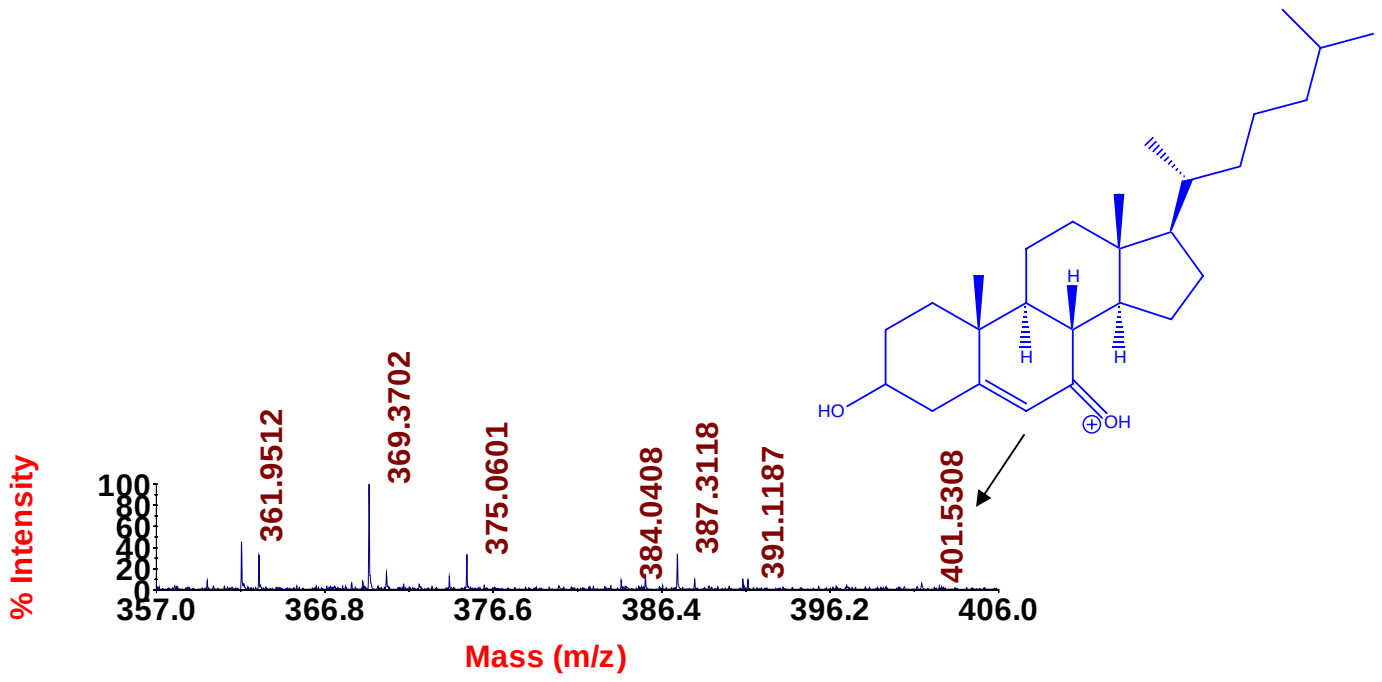

Figure 2.11. Cholesterol with Fenton reagent and protonated ketone

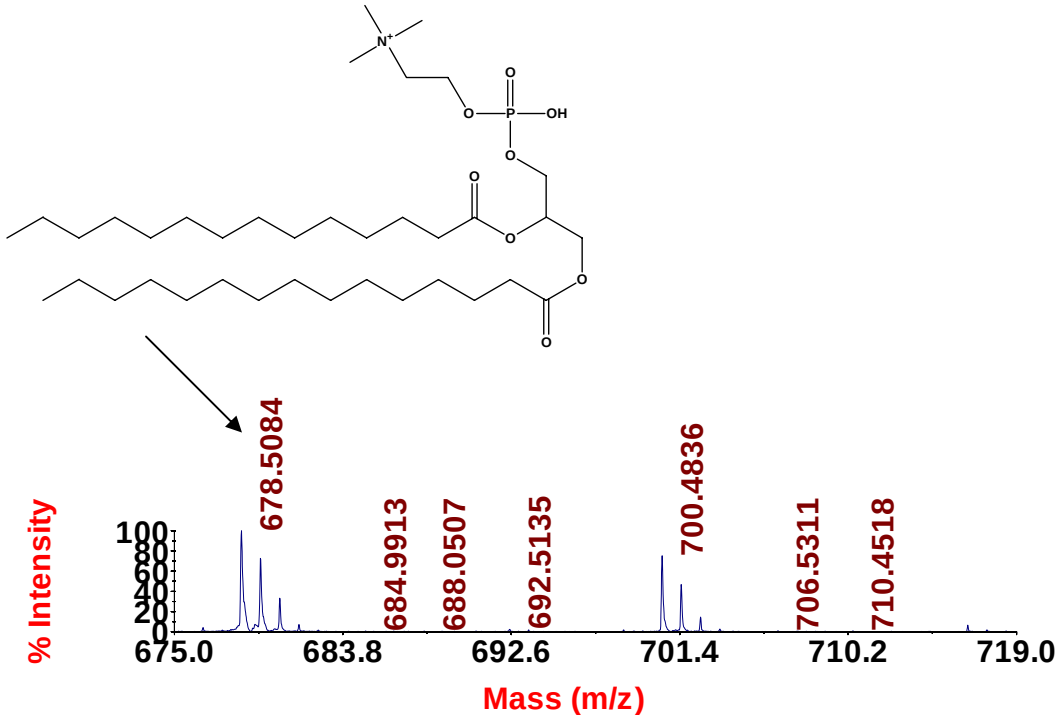

Figure 2.12. Blank DMPC with no Fenton Reagent; protonated DMPC at m/z 678

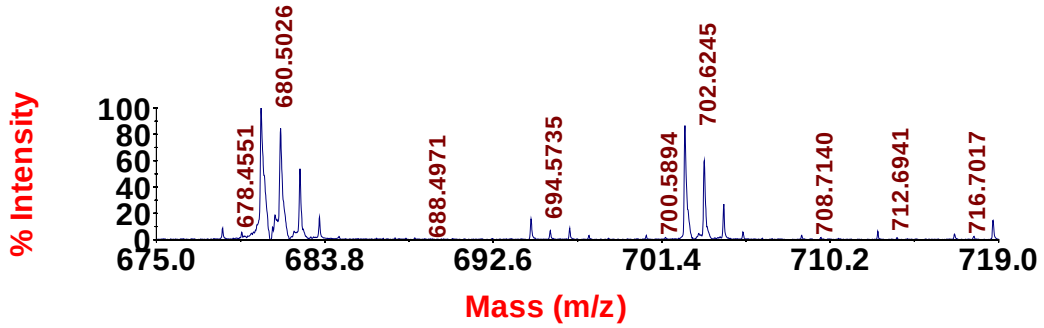

Figure 2.13. DMPC with Fenton reagent

Effects of Cholesterol

Oxidation of the pyrene fluorescent label became slower in the presence of cholesterol. This result indicates that cholesterol scavenged hydroxyl radical and served as an antioxidant. If cholesterol radicals were an important intermediate in these studies, increasing the cholesterol content would have resulted in enhancement of the probe degradation rate rather than the observed protection of the probe. Consequently, it is highly unlikely that cholesterol radical intermediates made a major contribution to the probe degradation under the conditions used in these studies.

The observed kinetics for in membrane probe oxidation are not consistent with a secondary radical mechanism. In numerous studies involving lipid peroxidation, an initial lag phase is observed followed by a propagation phase involving lipid peroxyl intermediates.[47] The lag phase involves slow probe oxidation due to protective scavenging by membrane components, while the rate of oxidation increases dramatically during the propagation phase[47] when intermediate radical concentrations are substantial and natural scavengers are depleted. In our systems, no lag phase was observed. We can therefore conclude that either lipid peroxides or other relevant intermediates are not important in the systems we used or the lag time was not exceeded. In either case, the predominant pathway for pyrene probe oxidation was direct attack of hydroxyl radical on the in-membrane probe.

This conclusion is supported by the lack of observed lipid peroxide products and by the observed protective mechanism of cholesterol, which did show evidence of hydroxyl radical attack.

All of these data indicate that hydroxyl radical directly oxidized the fluorescent probes within the membranes used in these studies. While these system are simple compared to real membranes, our data provide evidence that hydroxyl radical formed in aqueous environments can penetrate into lipid bilayers. For real membranes over longer time frames than studied here, secondary radical reactions, as observed in some studies [10, 47], are likely to play an important role in membrane oxidation reactions. However, it is clear from this study that initial attack by hydroxyl radical inside the lipid layer of membranes is possible.

Conclusions

The data reported here demonstrate that hydroxyl radicals formed in the aqueous phase surrounding unilamellar DMPC liposomes can penetrate into the hydrophobic lipid bilayer. Four results strongly support the theory that the hydroxyl radicals reacted directly with the fluorescent probes: 1) the use of a fully saturated lipid resulted in minimal formation of lipid peroxides which were undetectable by MALDI-TOF MS; 2) minimal formation of cholesterol oxidation products were observed at low iron/peroxide dosing; 3) addition of cholesterol resulted in decreased probe oxidation rates, indicating that cholesterol radicals could not have been a major pathway for probe oxidation; and 4) the observed kinetics of probe oxidation were not consistent with a system that proceeds via secondary radical formation.

The effect of temperature on the system was also studied by observing the rate of fluorescence degradation of three probes of varying lipophilicity while bracketing the phase transition temperature of DMPC.

The results revealed an increase in the rate of degradation with increasing temperature in the presence of a 1:1 molar ration of DMPC to cholesterol. However, under physiologically relevant conditions without cholesterol, the degradation of the pyrenyl probes mirrored the results of Kraske and co-workers [22] where the highest rate of degradation occurred at T_m = 23ºC. Interestingly enough, in the presence of cholesterol under physiologically relevant conditions, cholesterol behaved as an inhibitor of degradation of the pyrenyl probes at temperatures above, below and at T_m. These results are corroborated by the results of previous findings using azo-initiators where cholesterol reduced the rate of propagation and termination of the reaction and 'tightened' the packing of phospholipids bilayers.[47, 48] The results of this study provide a method for monitoring direct reaction of hydroxyl radical across a water-membrane interface. Furthermore, the results illustrate the effects of both temperature and cholesterol on the extent of radical penetration into the hydrophobic membrane. Additional studies focusing on other membrane constituents and different reactive transients can be easily achieved using the methods described in this work, ultimately leading to an improved understanding of membrane oxidation.

Acknowledgements

The authors acknowledge Drs. Zeev Rosenzweig, Thuvan Piehler, and Gabriela Blagoi for technical assistance with liposome preparation and characterization and Dr. Kevin Stokes for access to the dynamic light scattering equipment.

This project was supported by the Louisiana Board of Regents (Health Excellence grant#HEF(2001-06)-08) and the National Science Foundation (NSF-0611902). Chanel Fortier was supported by a Louisiana Board of Regents fellowship Grant #LEQSF(2001-2006)-GF-32.

References

(1) Jenner, P. *Annals of Neurology* **2003**, *53*, S26-S38.
(2) Passi, S. G., G.; Cocchi, M. *Progress in Nutrition* **2006**, *8*, 241-256.
(3) Lee, K. J. J., Hye Gwang *Toxicology Letters* **2007**, *173*, 80-87.
(4) Laggner, H. H., Marcela; Sturm, Brigitte; Gmeiner, Bernhard M. K; Kapiotis, Stylianos *FEBS Letters* **2005**, *579*, 6486-6492.
(5) Cheng, F.-C. J., Jen-Fon; Tsai, Tung-Hu *Journal of Chromatography, B* **2002a**, *781*, 481-496.
(6) Terman, A. B., Ulf T. *Antioxidants & Redox Signaling* **2006**, *8*, 197-204.
(7) Pignatello, J. J. O., Esther; MacKay, Allison *Critical Reviews in Environmental Science and Technology* **2006**, *36*, 1-84.
(8) Burkitt, M. J. *Progress in Reaction Kinetics and Mechanisms* **2003**, *28*, 75-103.
(9) Borg, D. C. S., Karen M. *Oxy-Radicals in Molecular Biology and Pathology* **1988**, 427-441.
(10) Aikens, J. D., Thomas A. *Archives of Biochemistry and Biophysics* **1993**, *305*, 516-525.
(11) Minotti, G. A., Steven D. *The Journal of Biological Chemistry* **1987**, *262*, 1098-1104.
(12) Tien, M. S., Bruce A.; and Aust, Steven D. *Archives of Biochemistry and Biophysics* **1982**, *216*, 142-151.
(13) Schaich, K. M. B., D.C. *Lipids* **1988**, *23*, 570-579.
(14) Gutteridge, J. M. C. *FEBS Letters* **1984**, *172*, 245-249.
(15) Li, Q.-T. Y., Mui Huang; Tan, Boon Kheng *Biochemical and Biophysical Research Communications* **2000**, *273*, 72-76.
(16) Barber, D. J. W. T., J.K. *Radiation Research* **1978**, *74*, 51-65.
(17) Barenholz, Y. C., Tina; Korenstein, Rafi; Ottolenghi, Michael *Biophysics Journal* **1991**, *60*, 110-124.
(18) Viani, P. C., Giovanna; Cestaro, Benvenuto *Biochemica et biophysica acta, Biomembranes* **1991**, *1064*, 24-30.
(19) Viani, P. C., Roberta; Cervato, Giovanna; Gatti, Patrizia; Cestaro, Benvenuto *Biochemica et biophysica acta* **1996**, *1315*, 78-86.
(20) Chattopadhyay, A. *Chemistry and Physics of Lipids* **1990a**, *53*, 1-15.
(21) Chattopadhyay, A. L., E. *Biochemica et biophysica acta* **1988b**, *938*, 24-34.
(22) Kraske, W. M., Donald B. *Biochemica et biophysica acta* **2001**, *1514*, 159-164.
(23) Chatterjee, S. N. A., Sanjiv *Free radical biology & medicine* **1988**, *4*, 51-72.
(24) Stohs, S. J. B., D. *Free radical biology & medicine* **1995**, *18*, 321-336.
(25) Antunes, F. C., Enrique *Free radical biology & medicine* **2001**, *30*, 1008-1018.
(26) Lindsey, M. E. T., Matthew, A. *Environmental Science and Technology* **2000a**, *34*, 444-449.
(27) Lindsey, M. E. T., Matthew, A. *Science of the Total Environment* **2003b**, *307*, 215-229.

(28) Anzai, K. A., Tetsuya; Furukawa, Yoshiko; Matsushima, Yoshikazu; Urano, Shiro; Ozawa, Toshihiko *Archives of Biochemistry and Biophysics* **2003**, *415*, 251-256.
(29) Cheng, S.-A. F., Wai-Kit; Chan, Kwong-Yu; Shen, P.K. *Chemosphere* **2003b**, *52*, 1797-1805.
(30) Karas, M. H., Franz *Analytical Chemistry* **1988**, *60*, 2299-2301.
(31) Tanaka, K. W., Hiroaki; Ido, Yutaka; Akita, Satoshi, Yoshida, Yoshikazu; Yohida, Tamio *Rapid Communications in Mass Spectrometry* **1988**, *2*, 151-153.
(32) Atkinson, R. A., Janet *Environmental Health Perspectives Supplements* **1994**, *102*, 117-126.
(33) Christian, G. G., Ed. *Anal. Chem.*, 5th ed.; John Wiley and Sons: New York, 1994.
(34) Tsukanova, V. G., David W.; Salesse, Christian *Langmuir* **2002**, *18*, 5539-5550.
(35) McNamara, K. P. R., Z. *Analytical Chemistry* **1998**, *70*, 4853-4859.
(36) Schiller, J. A., J.; Benard, S.; Muller, M.; Reichl, S.; Arnold, K. *Analytical Biochemistry* **1999**, *267*, 46-56.
(37) Bligh, E. G. D., W.J. *Canadian Journal of Biochemistry and Physiology* **1959**, *37*, 911-917.
(38) Zschornig, O. B., Christian; Sub, Rosmarie; Arnold, Klaus; Schiller, Jurgen *Letters in Organic Chemistry* **2004**, *1*, 381-390.
(39) Shen, X. T., Jingdong; Li, Jun; Li, Xinyuan; Chen, Yuling *Free radical biology & medicine* **1992**, *13*, 585-592.
(40) Kalyanasundaram, K. T., J.K.
JACS **1977**, *99*, 2039-2044.
(41) L'Heureux, G. P. F., M. *Biophysical Chemistry* **1988a**, *30*, 293-301.
(42) Binks, J. B., Ed. *Photophysics of Aromatic Molecules*; Wiley-Interscience: New York, 1975.
(43) L'Heureux, G. P. F., M. *Biophysical Chemistry* **1989b**, *34*, 163-168.
(44) L'Heureux, G. P. F., M. *Journal of Photochemistry and Photobiology, B* **1989c**, *3*, 53-63.
(45) Turro, N. J. K., Ping-Lin *Langmuir* **1986**, *2*, 438-442.
(46) Schiller, J. S., R.; Arnhold, J.; Fuchs, B.; Lessig, J.; Mueller, M.; Petkovic, M.; Spalteholz, H.; Zschoernig, O.; Arnold, K. *Progress in Lipid Research* **2004**, *43*, 449-488.
(47) Frankel, E. N., Ed. *Lipid Oxidation*; The Oily Press: Dundee, 1998.
(48) Halliwell, B. G., J.M.C., Ed. *Free Radicals in Biology and Medicine*; Oxford University Press, Inc.: New York, 1999.

Evaluation of Hydroxyl Radical Penetration into Unsaturated Lipid Membranes Using Fluorescently Labeled Membrane Probes

Abstract

Hydroxyl radicals formed using modified-Fenton chemistry were monitored as they penetrated into liposomal membranes. The hydroxyl radicals were formed in the aqueous exterior media of fluorescently-labeled liposomes. The effect of cholesterol on the penetration depth of hydroxyl radicals was determined. Fluorescent probes of varying lipophilicity were used along with different unsaturated phospholipids constituting the liposomes. Modified-Fenton chemistry was observed at physiologically relevant conditions. The results support fluorescent probe reaction with hydroxyl radicals by degradation of probe fluorescence. Rates of reaction between the probes and the oxidant are reported. Fluorescently-tagged liposomes in the presence of alpha and gamma tocopherol were studied. At the concentrations studied, the alpha tocopherol exhibited pro-oxidant behavior and gamma tocopherol exhibited neither pro-oxidant nor antioxidant behavior.

Introduction

Hydroxyl radicals are a form of reactive oxygen species (ROS) which have been labeled as toxic because of their ability to react with and degrade biologically important molecules.[1] Hydroxyl radicals are important physiologically because of their involvement in the onset of some diseases[2, 3] and aging.

Because of their short lifetimes, it is very difficult to measure the concentration of hydroxyl radicals, especially in systems with more than one phase. Thus, a variety of techniques have been used previously to track their reactivity including EPR ,[4-6] pulse radiolyis,[7-10] [11] and oxygen consumption.[12]

Pyrenyl-phospholipids have been used in previous studies to study membrane biophysics, lipid biochemistry, and cell biology.[13] These compounds have advantageous properties including being hydrophobic, having a long excited lifetime, and forming excimers at high concentrations. Also, because the flourophore is covalently attached to a phospholipid molecule, the depth and orientation of the fluorophore in the bilayer is often better defined compared to free pyrene or other probes. However, a limitation to using pyrenyl-phospholipids is that the fluorophore is bulky compared to the underivatized lipid chain. The width of the pyrene fluorophore is about twice that of an aliphatic chain, adding more rigidity compared to a saturated alky chain [13]. However, assessing the extent of disruption caused by the pyrenyl-phospholipids is not straightforward. A larger headgroup like phosphatidylcholine compared to phosphatidylethanolamine can potentially mask the the effect of changes in acyl chain dimensions. Also, studies have shown that C10-PYR-PC is only slightly larger than the egg-yolk phosphatidylcholine or dipalmitoyl-phosphatidylcholine in the liquid-crystalline state.[14]

Cholesterol has been found to be indispensable in mammalian membranes having numerous roles to play including cell signaling, directing the permeability of cell membranes, and acting as an antioxidant.[15, 16]

Cholesterol can also segregate itself into lipid rafts having cholesterol-rich and cholesterol-poor domains.[17] It has been reported that cholesterol, rather than polyunsaturated fatty acids, is the target for reaction with ROS.[18] In addition, for lipid peroxidation of model membranes, cholesterol significantly inhibited the reactivity of hydroxyl radicals generated with ultrasonic radiation.[19] Thus, the effect of cholesterol on the current system was studied.

Recent reports have shown that the most powerful lipid-soluble antioxidant is vitamin E (tocopherols).[20] However, it has also been shown to be a pro-oxidant under micromolar conditions.[21] The oxidation of alpha-tocopherol in micelles and liposomes by reactive oxygen species including the hydroxyl radical has been studied.[22] It was determined that hydroxyl radicals were effective oxidants of alpha-tocopherol in both micelle and phospholipid media, and the efficacy of their attack was sensitive to the charge on the micelle or model membrane. Vitamin E represents 8 types of analogues including alpha, beta, gamma, and delta tocopherols and the tocotrienols. While alpha tocopherol has been widely studied, contributions of the other tocopherol analogues as antioxidants have been less studied. Consequently, the effect of alpha and gamma tocopherols were individually assessed.

A fluorescence technique has been previously used to study the penetration depth of hydroxyl radicals into saturated liposomes. (Fortier and Tarr unpublished results) It is the goal of this research study to expand on this data by using liposomes formed from unsaturated phospholipids, including variation in the placement of the double bond.

This study revealed information on the site-specific reactivity of the hydroxyl radical with the fluorescent probes embedded in the lipid bilayer of the liposomes.

Materials

Three fluorescent phospholipids probes were used in this study. Two probes, 1-hexadecanoyl-2-(1-pyrenehexanoyl)-sn-glycero-3-phosphocholine (C6-PYR-PC), and 1-hexadecanoyl-2-(1-pyrenedecanoyl)-sn-glycero-3-phosphocholine (C10-PYR-PC) were obtained from Invitrogen (Carlsbad, CA). In addition, another probe 1-hexadeconyl-2(-1-pyrenedodecanoyl)-sn-glycero-3-phosphocholine (C12-PYR-PC) was obtained as a gift from Pentii Somerharju (Helsinki, Finland). Three unsaturated phospholipids were used as obtained from Avanti Polar Lipids, egg yolk phosphatidylcholine (EYPC), and two synthetic phospholipids 1,2-dipetroselinoyl-*sn*-glycero-3-phosphocholine (Cis6PC) and 1,2-dioleoyl-*sn*-glycero-3-phosphocholine (Cis9PC), where the latter two phospholipids differ in the placement of the double bond within the tail groups. The structures of the phospholipids and fluorescent probes are depicted in Figures 3.1 and 3.2, respectively. Ferrous sulfate heptahydrate and phosphate-buffered saline (PBS, 0.9% NaCl) were obtained from Sigma (Milwaukee, WI). Hydrogen peroxide (30% aqueous) was purchased from Fisher (Waltham, MA) and its concentration was measured iodometrically.[23] Cholesterol was purchased from Aldrich (St. Louis, Missouri). Chloroform and EDTA were purchased from EM Science (Gibbstown, NJ).

All aqueous solutions were prepared using Nanopure UV (Barnstead/Thermolyne, Dubuque, IA) deionized water with a distilled water feed to the water purifier. All reagents were used as received without further purification.

Experimental Methods

Preparation of Liposomes

The pyrenyl-labeled liposomes were prepared using a modified approach by McNamara and Rosenzweig.[24] Briefly, stock solutions of 20 mg/mL egg yolk phosphatidylcholine, 25 mg/mL of Cis6PC or 25 mg/mL Cis9PC were made in chloroform. An 80 µL aliquot of one of these stock solutions was added to the fluorescent probes which were present at 0.25 mol% of the total lipid content. The probes, C_6-PYR-PC, C_{10}-PYR-PC or C_{12}-PYR-PC were added individually. The lipids were dried overnight under a gentle stream of nitrogen. The following day the fluorescently lipid films were hydrated with 1 mL of 1 mM PBS buffer while vortexing to generate multilammelar liposomes. The final lipid concentration was 2 mM.

The liposomes were extruded 13 times using an Avanti mini extruder fitted with a 100 nm polycarbonate membrane filter to generate unilamellar liposomes. Extruded lipids were stored at 4 ºC and diluted further prior to use.

Dynamic Light Scattering

All dynamic light scattering experiments were carried out with a Protein Solution dynamic light scattering instrument and analyzed using Dynamics Software.

Settings on the instrument were for aqueous buffer conditions. For each liposome sample, 40 measurements were taken at a total lipid concentration of 0.2 mM.

Fluorescence Studies

The fluorescence experiments were carried out using a Perkin Elmer LS 55 Luminescence Spectrometer equipped with a magnetic stirrer set on low. The quartz cuvette path length was 10 mm (Starna Cells, Atascadero, CA). Degradation of the fluorescent probes was followed by monitoring fluorescence emission at fixed excitation and emission wavelengths as a function of time. For the pyrenyl probes, the excitation and emission wavelengths were set at 345 and 377 nm, respectively.

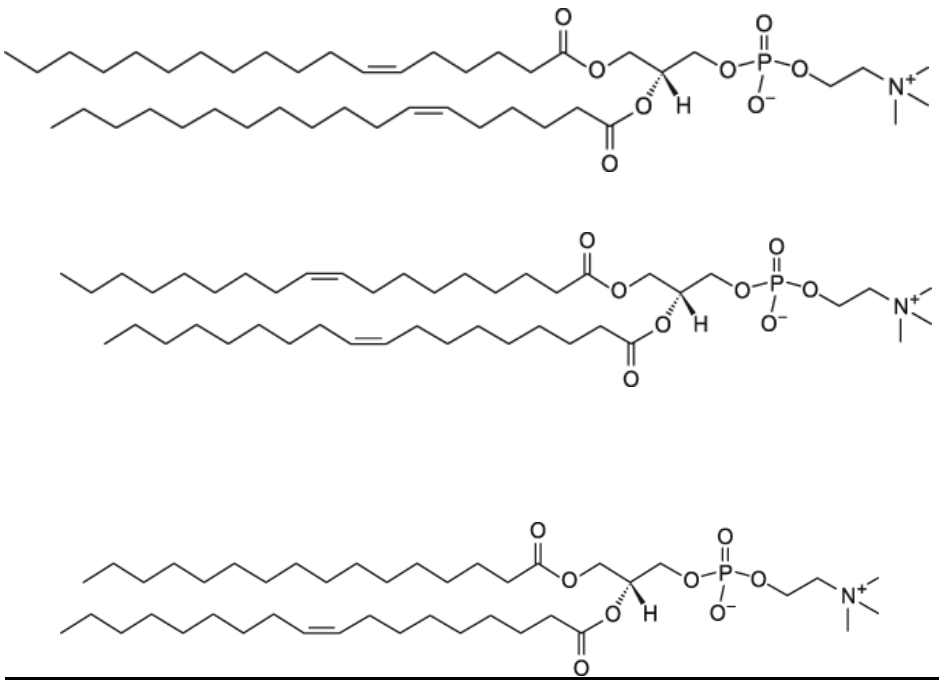

Figure 3.1.Unsaturated Phospholipid Structures. For EYPC, a single representative structure is presented, but this material is a mixture of several phospholipids.

C_6-PYR-PC

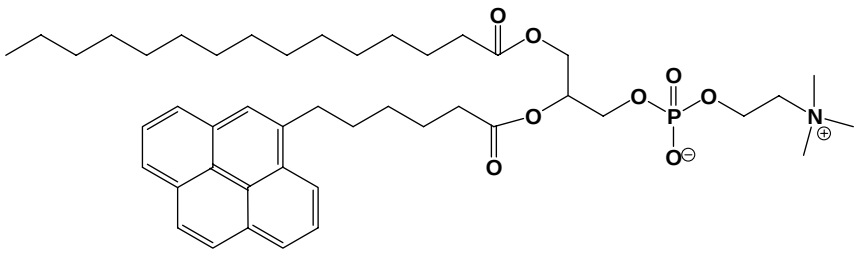

C_{10}-PYR-PC

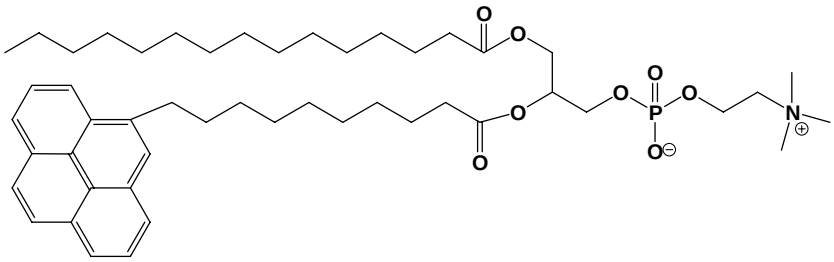

C_{12}-PYR-PC

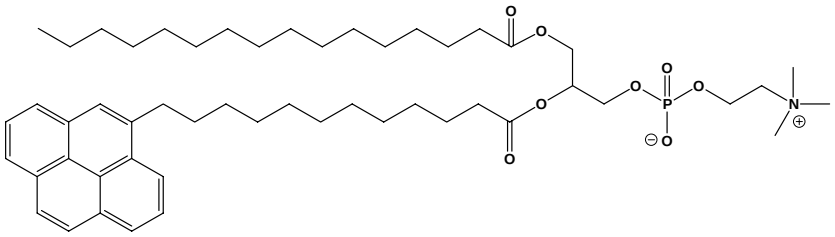

Figure 3.2. Fluorescently labeled phospholipid probes

Fenton Experiments

Experiments were conducted with iron and peroxide concentrations near physiological conditions. For these studies, 3 mL of a 1 mM PBS buffered solution of liposomes (3.3 μM lipid) was added to the cuvette. To this cuvette were then added Fe^{+2} and EDTA to achieve a concentration of 0.3 μM for each.
The solution was stirred for 600 s, then a 3 μM solution of H_2O_2 (aq) was continuously added at 0.8 mL/hr until a final volume of 0.23 mL was delivered. For these experiments, all figures are labeled time zero when H_2O_2 addition began.

For all experiments, the temperature of the cuvette and its contents were controlled by a thermostated cuvette holder. All experiments were carried out at 37ºC, a physiologically relevant temperature. The rates of probe degradation were determined using linear regression. Two controls were carried out. The first consisted of the liposome sample with no iron (II)-EDTA added to the hydrogen peroxide. In the second control, in place of hydrogen peroxide, pure water was added to the iron(II)-EDTA liposomal sample.

Results and Discussion

Egg yolk PC experiments

For the egg yolk PC experiments degradation of the C6-PYR-PC probe was inhibited in the presence of cholesterol as shown in Figure 3.1a. In contrast, the C10- and C12-PYR-PC probes showed no difference in degradation in the presence and absence of cholesterol.

The difference in the behavior of the C6 probe compared to the C10 and C12 probes with respect to cholesterol is likely due to the different positions of the probes within the lipid bilayer. Cholesterol is not uniformly distributed within the bilayer, and the different positions of the probes may result in different interactions with cholesterol. Furthermore, the different displacement of the large pyrene probe from the membrane interface may cause some changes in permeability of the membrane surface. Due to the dynamic nature of these systems, it is difficult to draw definitive conclusions based on the available data. Moreover, the C6-PYR-PC may have closer lipid packing tail to tail and higher curvature at the headgroup that may make these liposomes more susceptible to hydroxyl radicals and Fe-EDTA.[25]

Comparing the C6, C10, and C12 probes without cholesterol, the degradation rates decrease as the length of the probe increases (Table 1). This result is in agreement with previous observations (ref), and is most likely caused by the greater distance of the probe from the membrane interface. Since the radical is generated in the aqueous phase and the radical is very reactive, the concentration of the radical decreases as the distance from the water interface increases. In the presence of cholesterol, this trend is altered since cholesterol acted as a scavenger for the C6 probe, resulting in a lower rate of degradation of this probe.

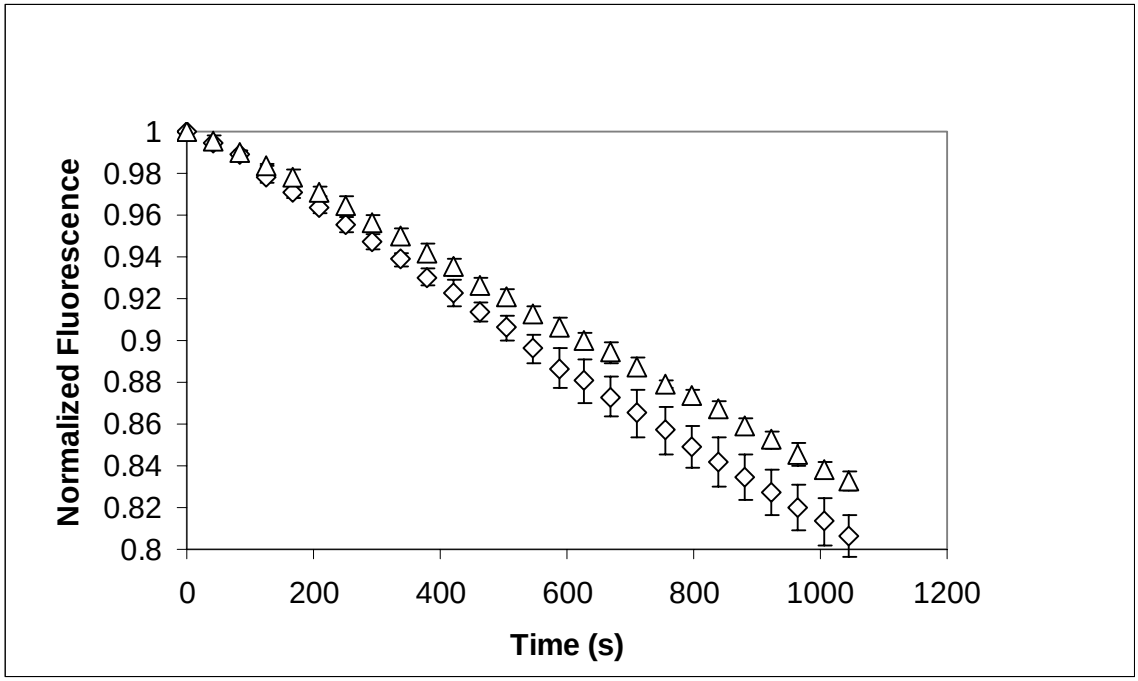

Figure 3.3a. Egg Yolk Phosphatidylcholine liposomes with C_6-PYR-PC with and without cholesterol

◇ = without cholesterol and Δ = with cholesterol

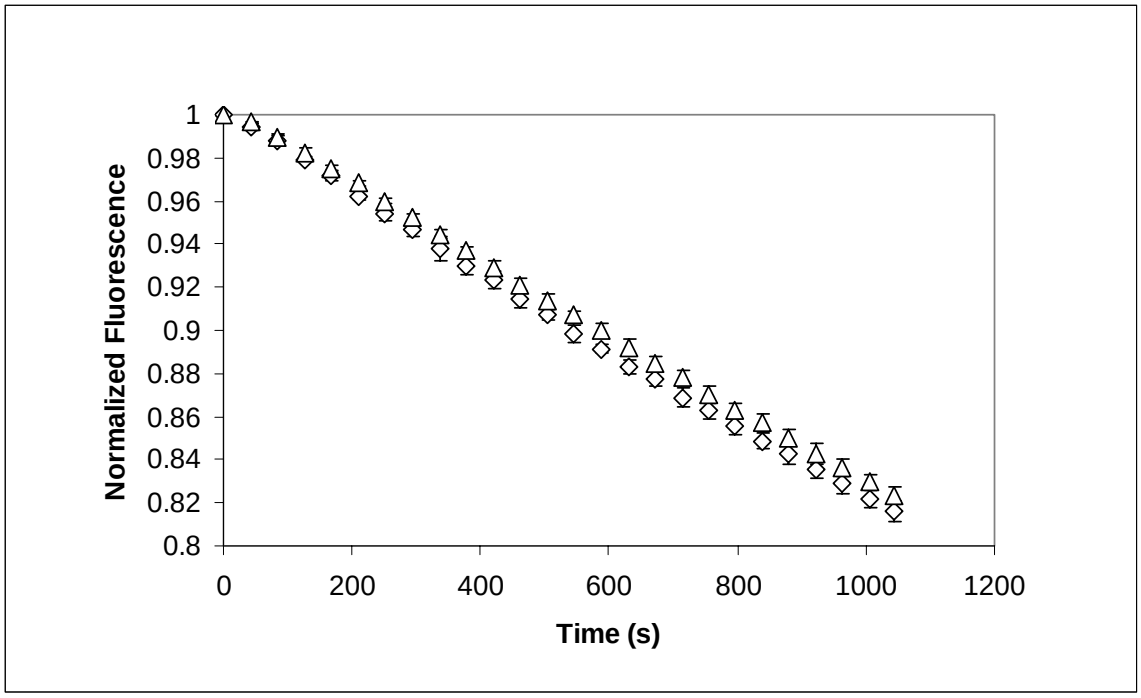

Figure 3.3b. Egg Yolk Phosphatidylcholine liposomes with C_{10}-PYR-PC with and without cholesterol

◇ = without cholesterol and Δ = with cholesterol

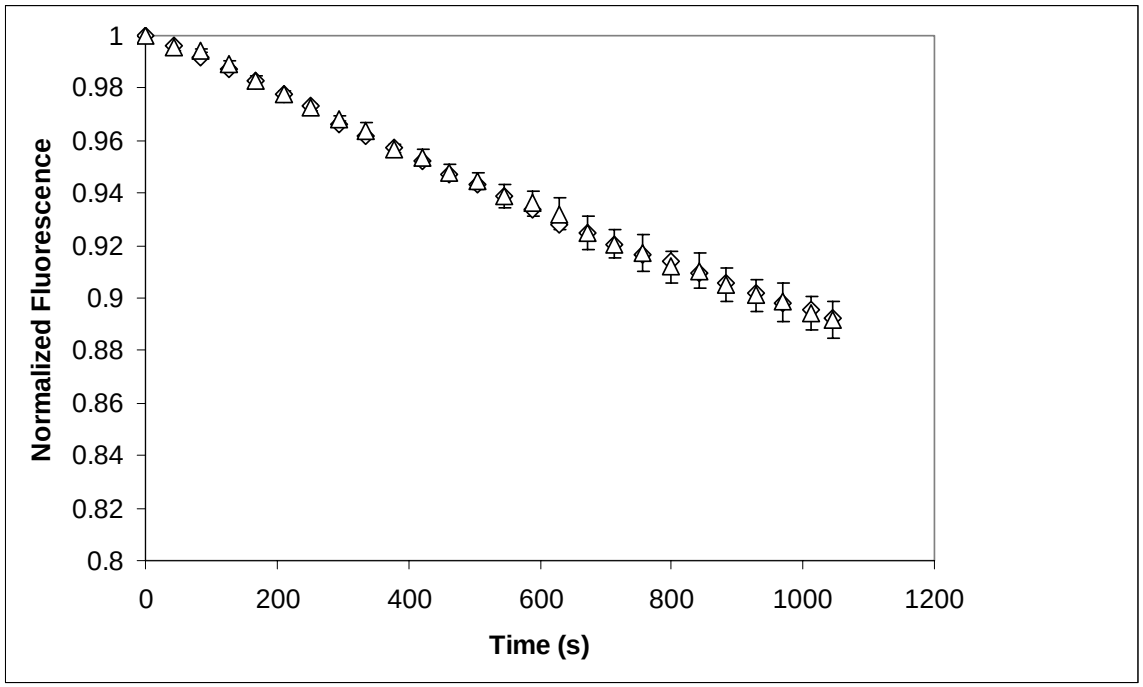

Figure 3.3c. Egg Yolk Phosphatidylcholine liposomes with C_{12}-PYR-PC with and without cholesterol

◇ = without cholesterol and Δ = with cholesterol

However, the degradation rate of the C12 probe is still lower than that of the C10 probe, which on average is closer to the membrane interface.

For both the Cis6PC liposomes with no cholesterol, the C6-PYR-PC probe gave the fastest rates of degradation when exposed to aqueous hydroxyl radical. Unlike the EPC liposomes, the C12 probe in the Cis6PC liposomes reacted faster then the C10 probe. For the Cis9PC liposomes, the behavior was also different than that seen for EPC liposomes. Cis9PC liposomes without cholesterol showed equivalent degradation rates for C6 and C10 probes and showed the highest degradation rate for the C12 probe.

Cis6PC liposomes prepared with 1:1 cholesterol showed the highest degradation rate for the C10 probe, while the C6 and C12 probes exhibited similar rates of degradation. The Cis9PC liposomes with 1:1 cholesterol also exhibited the highest degradation rate for the C10 probe, but the C12 probe had a very low rate of probe degradation.

The effect of cholesterol on probe degradation for the Cis6PC and Cis9PC liposomes did not show any clear trends. In some cases, addition of cholesterol resulted in increased degradation rates, while in other cases cholesterol addition resulted in decreased probe degradation rates. These results are difficult to interpret, suggesting that the role of cholesterol is complex. Cholesterol can act as a free radical scavenger and can change the permeability and rigidity of the membrane. Furthermore, cholesterol can aggregate into certain regions of the membrane.

If different probes are located closer or farther from such regions, the effect of cholesterol on probe oxidation could vary dramatically.

Vitamin E experiments

The results of the vitamin E experiments are shown in Figures 3.4a, 3.4b, and 3.4c and 3.5. Over the concentration range studied for the vitamin E, it was observed that the alpha-tocopherol behaved as a pro-oxidant rather than a radical scavenger as it has been reported earlier. [26] Other authors have previously reported on this pro-oxidant activity of alpha-tocopherol.[27-29] This behavior may be due to the ability of alpha-tocopherol to reduce the catalytic iron present. [30] For the gamma-tocopherol experiments there was no observable effect on the degradation rates. There have been conflicting results regarding the effect of gamma-tocopherol. Some reports suggest that the antioxidant activity of gamma-tocopherol is less than that of the alpha- and beta-tocopherol. [30]

Other reports suggest that gamma-tocopherol had a higher antioxidant activity than alpha-tocopherol.[31] It has been shown that at micromolar concentrations, tocopherols can behave as pro-oxidants in a synergistic way with catalytic metal ions, lipid peroxides, and other oxidizing agents.[29] In addition, based on the concentrations of vitamin E and polyunsaturated lipids *in vivo* that being, $1/10^2$,lipid to antioxidant ratio, it is clear that alpha-tocopherol can act as an efficient scavenger of hydroxyl or alkoxyl radicals. In addition, vitamin E reacts very quickly with peroxyl radicals and may scavenge more than 90% of peroxyl radicals before peroxyl radicals can attack lipids.[30]

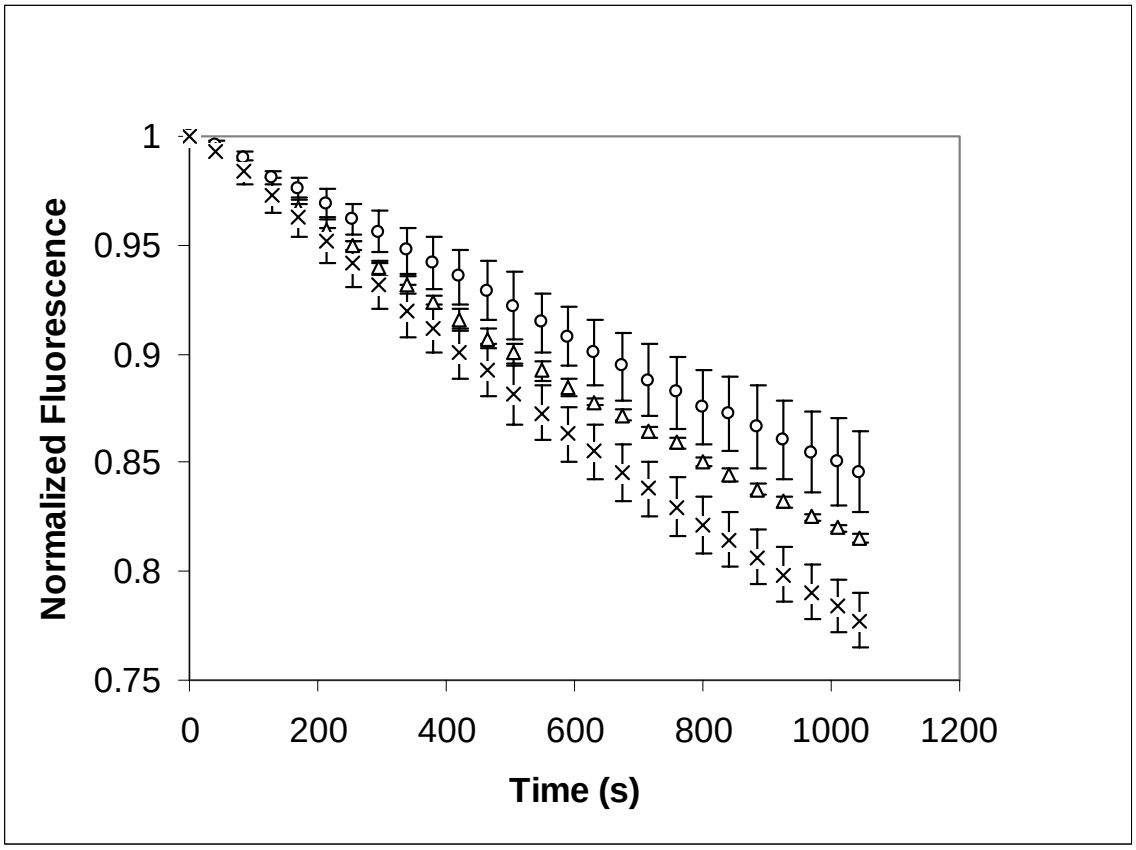

Figure 3.4a. The effect of alpha-tocopherol on the degradation of C_6-PYR-PC in Cis6PC liposomes without cholesterol.

o = 0μM alpha tocopherol, Δ = 0.11% alpha-tocopherol, x = 0.20% alpha-tocopherol

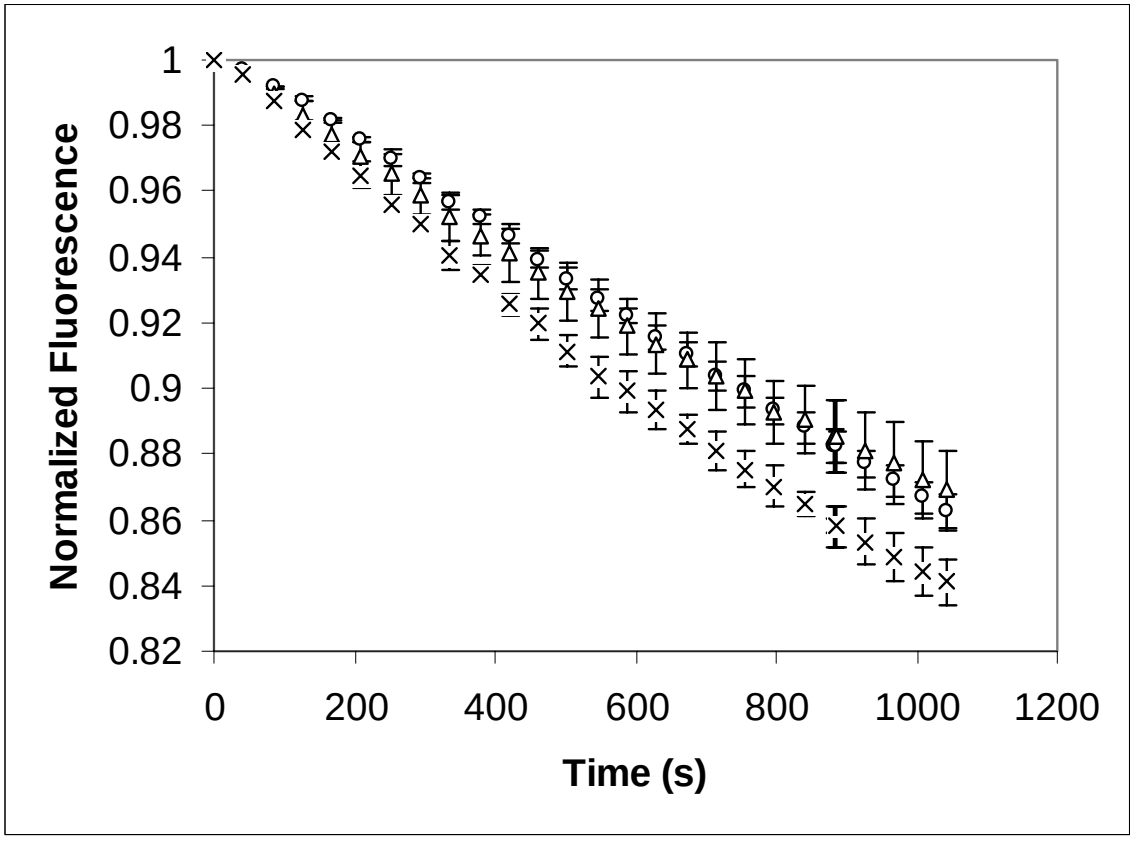

Figure 3.4b. The effect of alpha-tocopherol on the degradation of C_{10}-PYR-PC in Cis6PC liposomes without cholesterol.

o = 0μM alpha tocopherol, Δ = 0.11% alpha-tocopherol, x = 0.20% alpha-tocopherol

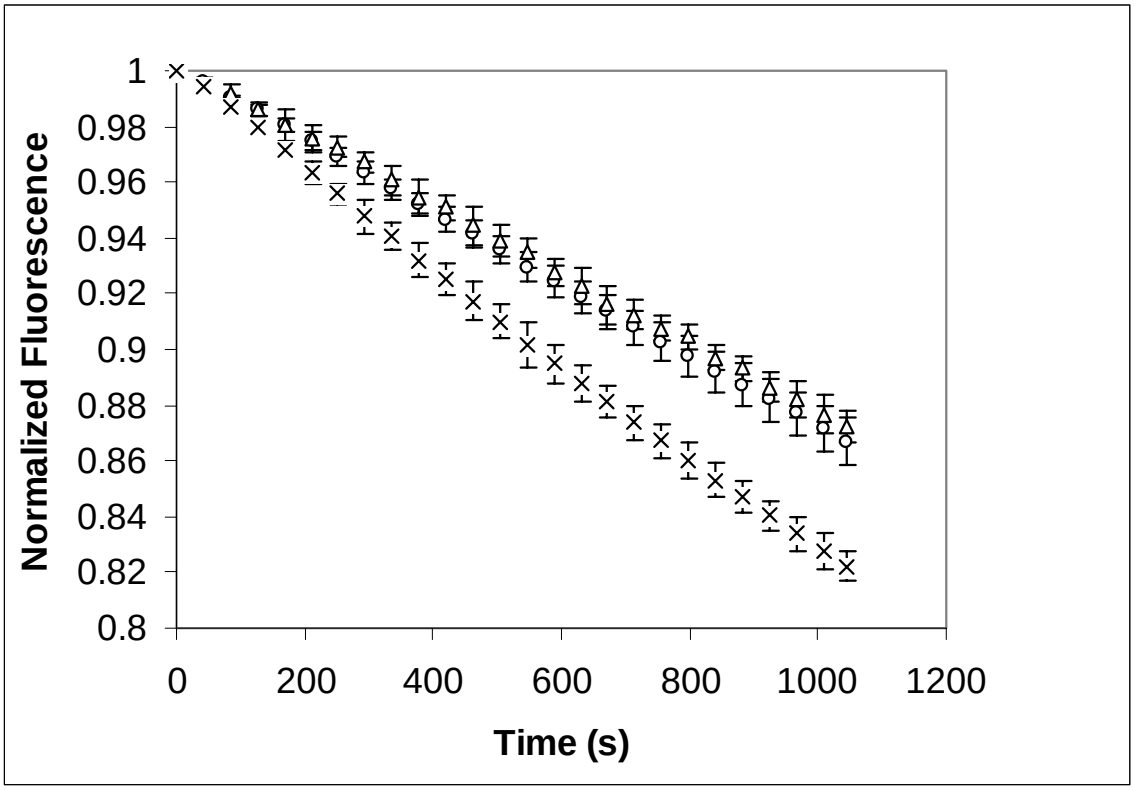

Figure 3.4c. The effect of alpha-tocopherol on the degradation of C_{12}-PYR-PC in Cis6PC liposomes without cholesterol.

o = 0μM alpha tocopherol, Δ = 0.11% alpha-tocopherol, x= 0.20% alpha-tocopherol

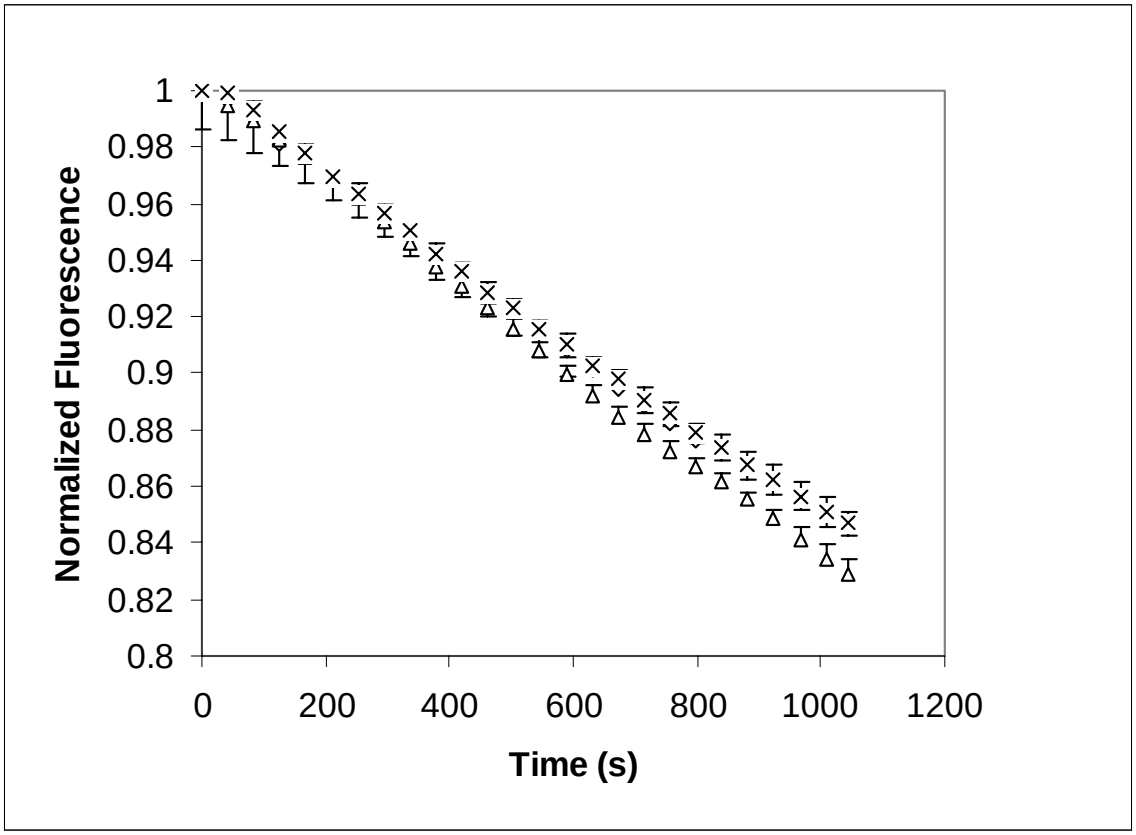

Figure 3.5. Effect of gamma tocopherol on C6-PYR-PC cis6PC liposomes with no cholesterol

o = 0μM gamma-tocopherol, Δ = 0.11% gamma-tocopherol, x = 0.20% gamma-tocopherol

Given this observation, it can be deduced that hydroxyl radicals are being generated because in this report, alpha-tocopherol appears to be a pro-oxidant. Rates of fluorescence loss as a function of exposure time were determined for each individual probe under varying conditions. These data are presented in Table 1 as the change in fluorescence with respect to time (ΔF/s).

Size of the liposomes and effect of additives

The unsaturated phospholipids Cis6PC and Cis9PC were found to be 17.6 angstroms while the probe lengths for C_6-PYR-PC, C_{10}-PYR-PC and C_{12}-PYR-PC were determined to be 20.4, 23.9, and 24.9 angstroms, respectively using Spartan modeling software. This effect of the rigidity and increased size of the pyrenyl phospholipids may change the microenvironment surrounding the double bonds in the unsaturated phospholipids.

In the case of the fluorescent probes with and without cholesterol, the cholesterol may have been present in lipid rafts with high and low amounts of cholesterol segregated out.[32] This may lead to pro-oxidant or antioxidant behavior observed with the fluorescent probes. Secondly, the results may be due to the positioning of the cholesterol.[33] For a doubly unsaturated phospholipid the cholesterol effect may be governed by its placement of its hydroxyl near the center of the bilayer.[33] Consequently, it may be hard to expect the cholesterol to be pro-oxidant but its behavior determined by its placement and orientation. The orientation of the cholesterol is probably upright with the hydroxyl radical facing the water-lipid interface in these singly unsaturated lipids.[33]

Due to the deeply embedded position of the C_{12}-PYR-PC had the lowest fluorescence degradation rates. Also, the differences in reactivity of the C6- and C10-PYR-PC may have been due to the placement of vitamin E in the liposomes with regard to the fluorescent probes. Thus, degradation of C10-PYR-PC would be less favored by scavenging of the radical at lesser penetration depths.

Table 1. Observed probe degradation rates for several probes and membranes with and without cholesterol, and with alpha- and gamma-tocopherol. Rates represent decrease in arbitrary fluorescent units per sec.

Probe	Phospho-lipid	No additives	With cholesterol (1:1)	With 0.3% α-tocopherol	With 0.5% α-tocopherol	With 0.004%γ-tocopherol	With .01% γ-tocopherol
C6-PYR-PC	EYPC	$(1.9111 \pm 2.36) \times 10^{-7}$	$(1.646 \pm 1.56) \times 10^{-7}$				
C10-PYR-PC	EYPC	$(1.800 \pm 3.02) \times 10^{-7}$	$(1.747 \pm 1.67) \times 10^{-7}$				
C12-PYR-PC	EYPC	$(1.064 \pm 3.04) \times 10^{-7}$	$(1.076 \pm 2.73) \times 10^{-7}$				
C6-PYR-PC	Cis6PC	$(1.5324 \pm 3.01) \times 10^{-7}$	$(1.087 \pm 1.56) \times 10^{-7}$	$(1.795 \pm 0.513) \times 10^{-7}$	$(2.18224 \pm .5.72) \times 10^{-7}$	$(1.7 \pm 3.23) \times 10^{-7}$	$(1.536 \pm 3.11) \times 10^{-7}$
C10-PYR-PC	Cis6PC	$(1.30 \pm 9.25) \times 10^{-7}$	$(1.508 \pm 2.58) \times 10^{-7}$	$(1.25 \pm 1.35) \times 10^{-7}$	$(1.74 \pm 2.66) \times 10^{-7}$		
C12-PYR-PC	Cis6PC	$(1.37 \pm 1.59) \times 10^{-7}$	$(0.982 \pm 1.25) \times 10^{-7}$	$(1.28 \pm 3.65) \times 10^{-7}$	$(1.57 \pm 5.58) \times 10^{-7}$		
C6-PYR-PC	Cis9PC	$(1.000 \pm 2.05) \times 10^{-7}$	$(1.147 \pm 2.17) \times 10^{-7}$				
C10-PYR-PC	Cis9PC	$(0.009 \pm 1.25) \times 10^{-7}$	$(1.206 \pm 1.09) \times 10^{-7}$				
C12-PYR-PC	Cis9PC	$(1.357 \pm 2.27) \times 10^{-7}$	$(0.0507 \pm 0.728) \times 10^{-7}$				

Conclusions

It has been demonstrated that the reactivity of three fluorescent probes in liposomes can be affected by the degree and placement of unsaturation in liposomal phospholipids. Antioxidant behavior of alpha- and gamma-tocopherol were not observed in the current study. In addition, pro-oxidant behavior has been previously observed at % concentrations of alpha-tocopherol.[29] The high variability of the effects of cholesterol on the current study may be due to the placement of cholesterol in the liposomal membrane and whether or not it is segregated into domains where it is cholesterol-rich and cholesterol-poor.[34] This segregation may lead to high or low permeability of the hydroxyl radical depending on the rigidity of the membrane. The reactivity of alpha-tocopherol as a pro-oxidant may be due to the tocopherol radical being protected in the liposomal membrane due to its low water solubility where it can generate more propagative species that are longer-lived. In addition, the effects of placement of the double bond on the unsaturated liposomes may affect the degree to which the hydroxyl radicals can penetrate the membrane. In addition, the higher degradation rate of C6-PYR-PC may be due to the higher curvature of the liposomes at the headgroup compared to C10-PYR-PC and C12-PYR-PC.

References

1. Pignatello, J. J. O. E., MacKay, Allison;, Critical Reviews in Environmental Science and Technology. **2006,** 36, 1-84.
2. Passi, S. G. G. C., M., *Progress in Nutrition* **2006,** 8, 241-256.
3. Jenner, P., *Annals of Neurology* **2003,** 53, S26-S38.
4. Matuszak, Z. R., Krzsztof J; Chignell, Colin F, Reaction of melatonin and related indoles with hydroxyl radicals: EPR and spin trapping investigations. *Free Radical Biology and Medicine* **1997,** 23, (3), 367-372.
5. Misik, V. M., I. Tong; Stafford , Richard E.; Weglicki, William B., Reactions of captopril and epicaptopril with transition metal ions and hydroxyl radicals: an epr spectroscopy study. *Free Radical Biology and Medicine* **1993,** 15, (6), 611-619.
6. Kochany, J. B., James R., Mechanism of photodegradation of aqueous organic pollutants. 1. EPR spin-trapping technique for the determination of hydroxyl radical rate constants in the photooxidation of chlorophenols following the photolysis of hydrogen peroxide. *Journal of Physical Chemistry* **1991,** 95, (13), 5116-5120.
7. Getoff, N. S., Sonja; Lubec, Gert., Reactivity of homocysteine-thiolactone and alpha-methylhomocysteine with eaq- and OH-radical; a pulse radiolysis study. *Life Sciences* **1998,** 63, (16), 1469-1484.
8. Fox, M. A., The role of hydroxyl radicals in the photocatalyzed detoxification of organic pollutants: pulse radiolysis and time-resolved diffuse reflectance measurements. *Trace metals in the environment* **1993,** 3, 163-167.
9. Lawless, D. S., N.; Meisel, D., Role of hydroxyl radicals and trapped holes in photocatalysis. A pulse radiolysis study. *Journal of Physical Chemistry* **1991,** 95, (13), 5166-5170.
10. Shetty, N. P. J., Hans J. Lyngs; Jensen, Jens Due; Colling, David B; Shetty, H. Shekar, Roles of reactive oxygen in interactions between plants and pathogens. *Journal of Plant Pathology* **2008,** 121, (3), 267-280.
11. Sridhar, R. B., P. C.; Powers, E. L.:. , A pulse radiolysis study of the addition of hydroxyl free radicals to nitrone spin trap. *Oxygen Radicals Chemical and Biological Proceedings* **1984**, 101-107.
12. Zini, R. B., Alain; Morin, Didier, The differential effects of superoxide anion, hydrogen peroxide and hydroxyl radical on cardiac mitochondrial oxidative phosphorylation. *Free Radical Research* **2007,** 41, (10), 1159-1166.
13. Somerharju, P., Pyrene-labeled lipidsd as tools in membrane biophysics and cell biology. *Chemistry and Physics of Lipids* **2002,** 116, 57-74.
14. Somerharju, P. J., Virtanen, J.A., Eklund, K.K., Vainio,P., Kinnunen, P.K., 1-Palmitoyl-2-pyrenedecanonoyl glycerophospholipids as membrane probes: evidence for regular distribution in liquid-crystalline phosphatidylcholine bilayers. *Biochemistry* **1985,** 24, 2773-2781.
15. Yeagle, P. L., *Cholesterol in Membrane Models* CRC Press: Boca Raton 1993; p 1-12.
16. Smith, L. L., Another Cholesterol Hypothesis: Cholesterol as Antioxidant. *Free Radical Biology and Medicine* **1991,** 11, 47-61.

17. Papanikolaou, A. P., A.; Murphy, C., Papamarcaki, T., Tsolas, O., Drab, M., Kurzchalia, T. V. Kasper, M.; Christoforidis, S., Cholesterol-dependent Lipid Assemblies Regulate the Activity of the Ecto-nucleotidase CD39. *Journal of Biological Chemistry* **2005,** 28, 26406-26414.
18. Liu, Z.-Q. S., Hong-Yan, Cholesterol, not polyunsaturated fatty acids, is target molecule in oxidation induced by reactive oxygen species in membrane of human erythrocytes. *Cell Biochemistry and Biophysics* **2006,** 45, (2), 185-193.
19. Jana, A. K., Agarwal, S., Chatterjee, S.N,, Ultrasonic radiation induced lipid peroxidation in liposomal membrane. *Radiation and Environmental Biophysics* **1986,** 25, (4), 309-314.
20. Alessi, M., Paul, T., Scaiano, J.C., Ingold, K.U., The Contrasting Kinetics of Peroxidation of Vitamin-E Containing Phospholipid Unilamellar Vesicles and Human Low-Density Lipoprotein. *JACS* **2002,** 124, 6957-6965.
21. Neuzil, J. T., Shane R.; Stocker, Roland, Requirement for, promotion, or inhibtion by alpha-tocopherol of radical-induced initiation of plasma lipoprotein lipid peroxidation. *Free Radical Biology and Medicine* **1996,** 22, (1/2), 57-71.
22. Fukuzawa, K., Gebicki, J. M., Oxidation of alpha-tocopherol in Micelles and Liposomes by the Hydroxyl, Perhydroxyl, and Superoxide Free Radicals. *Archives of Biochemistry and Biophysics* **1983,** 226, (1), 242-251.
23. Christian, G. G., *Anal. Chem.* John Wiley and Sons: New York, 1994.
24. McNamara, K. P., Rosenzweig, Z., Dye-Encapsulating Liposomes as Fluorescence-Based Oxygen Nanosensors. *Analytical Chemistry* **1998,** 70, (22), 4853-4859.
25. Li, Q.-T., Yeo, Mui Huang, Tan, Boon Kheng, Lipid Peroxidation in Small and Large Phospholipid Unilamellar Vesicles Induced by Water-Soluble Free Radical Sources. *Biochemical and Biophysical Research Communications* **2000,** 273, 72-76.
26. Galli, C., Simopoulos, A.P., Tremoli, E., Physiological Requirements of Vitamin E as a Function of the Amount and Type of Polyunsaturated Fatty Acid. *Fatty Acids and Lipids: Biological Aspects* **1994,** 75, 166-168.
27. Dad, S., Bisby, R.H., Clark, I.P., Parker, A.W., Formation of singlet oxygen from solutions of Vitamin E. *Free Radical Research* **2006,** 40, (3), 333-338.
28. Pearson, P., Lewis, S.A., Britton, J., Young, I.S., Fogarty, A., The Pro-Oxidant Activity of High-Dose Vitamin E Supplements in Vivo. *Biodrugs* **2006,** 20, (5).
29. Hajiani, M., Golestani, A., Shariftabrizi, A., Rastegar, R., Payabvash, S., Salmasi, A.H., Dehpour, A.R., Pasalar, P., Dose-dependent modulation of systemic lipid peroxidation and activity of anti-oxidant enzymes by Vitamin E in the rat. *Redox report* **2008,** 13, (2), 60-66.
30. Niki, E., Noguchi, N., Dynamics of Antioxidant Action of Vitamin E. *Accounts of Chemical Research* **2004,** 37, (1), 45-51.
31. Jiang, Q., Chisten, S., Shigenaga, M.K., Ames, B.N., Gamma-tocopherol, the major form of Vitamin E in the US diet, deserves more attention. *American Journal of Clinical Nutrition* **2001,** 74, 714-722.

32. Sugahara, M., Uragami, M., Regen, S.L., Selective Association of Cholesterol with Long Chain Phospholipids in Liquid-Ordered Bilayers: Support for the existence of lipid rafts. *JACS* **2003,** 125, (43), 13040-13041.
33. Harroun, T. A., Cholesterol is Found to Reside in the Center of a Polyunsaturated Lipid Membrane. *Biochemistry* **2008**.
34. Jacob, R. F., Mason, R. P., Lipid Peroxidation Induces Cholesterol Domain Formation in Model Membranes. *Journal of Biological Chemistry* **2005,** 280, (47), 39380-39387.

Chapter 4. Conclusions and Future Directions

The overall goal of this project was to determine the penetration depth of hydroxyls radical into liposomal membranes and to determine if hydroxyl radicals were in fact initiators of lipid oxidation. The experimental design was to fluorescently-tag liposomes at varying lipophilic depths in order to track their reaction with hydroxyl radicals. Hydroxyl radicals were shown to be initiators of lipid oxidation by varying the Fe(II) and hydrogen peroxide concentrations. In addition, the biphenyl hydroxyl radical scavenger studies revealed that one of the fluorescent probes were scavenged by the hydroxyl radicals.the hydroxyl radicals were scavenged by the biphenyl scavenger.

These experiments were not the first experiments to determine the penetration depth of reactive oxygen species (ROS) into liposomal membranes[1, 2]. Also, fluorescence has been previously used to detect other ROS[3], like superoxide. [4] However, our experiments were novel since they employed the fluorescent probes covalently attached to the liposome and used a multi-faceted approach to study both the liposomes and the phospholipids constituting the liposomes. In addition, our experiments generated a constant steady-state concentration of hydroxyl radical by introducing the hydrogen peroxide using a syringe pump. This was a new way to follow hydroxyl radicals instead of putting bolus additions of catalytic chelated iron in the presence of hydrogen peroxide. There have been some accounts of Fenton chemistry in liposomes or micelles with the bolus additions of iron and hydrogen peroxide[5, 6]. However, this approach was not conducted under physiological conditions.

Under physiological conditions there is a steady state production of hydrogen peroxide and hydroxyl radicals. In addition under physiological conditons, the iron (II) and hydrogen peroxide concentration were in the micromolar range.

There have also been some accounts of Fenton chemistry taking place using Eelectron Spin Rresonance (ESR)[7, 8]. In fact, there was a study to determine hydroxyl radicals penetration at predetermined depths using EPR (Electron Paramagnetic Resonance) and newly designed spin traps[9]. Although this method has been touted as being the most informative of radical transient species, this technique requires expensive equipment, extensive training to operate the instrument, and there is no guarantee that DMPO, a popular spin trap, only reacts exclusively with hydroxyl radicals[10]. In contrast, our fluorescence-based method was very sensitive, easy to use and had equipment costs much lower than EPR.

Chapter 5. Future Directions

One possible future experiment would be to generate fluorescently-tagged lipobeads and follow their reaction of the hydroxyl radicals with the fluorescent probe. This experiment would be the opposite of complementary to those currently being carried out in our lab because the probe would be chemically attached to the a polymeric support at the inside of the lipid layer instead of the bering anchored as a phospholipid within the bilayer. If these experiments show a similar kinetic profile with those of the liposome experiments this would corroborate our assertion that the probe indeed reacts with the hydroxyl radicals generated in the surrounding aqueous media. This experiment is important since movement of the phospholipid based probe could

allow the fluorophore to move closer to the water-lipid interface. A probe anchored on a lipid coated beed would not have the ability to move close to the water-lipid interface.

Figure 4.1 Lipobead and Unilammelar Liposome, A = anchor, FP = fluorescent probe (2-aminoanthracence)

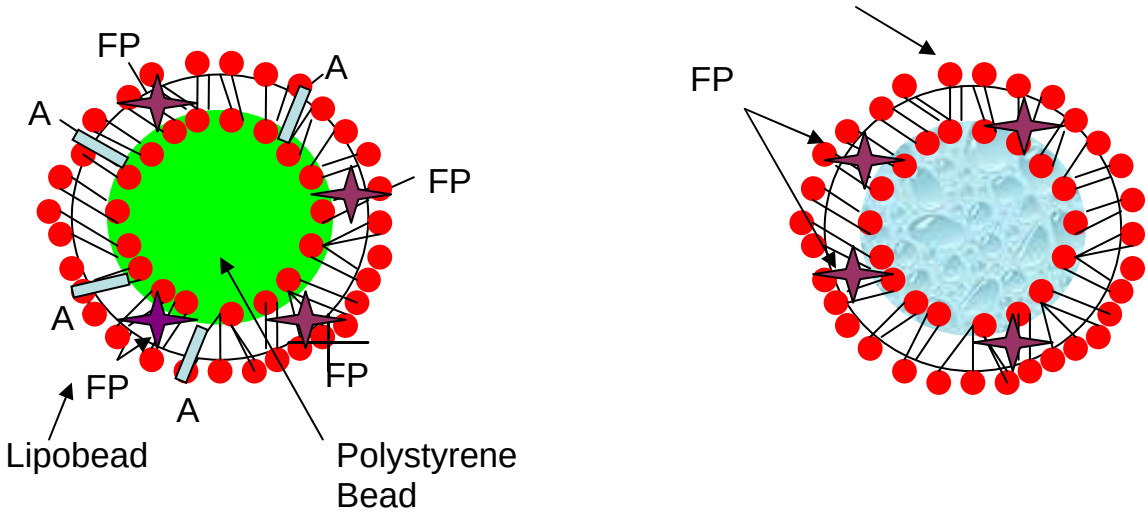

Previously, liposomes or polymeric beads have been used in drug delivery systems, drug targeting, protein separation, enzyme immobilization, blood cell substitution, and biosensors.[11-18]Polymeric bead systems have an advantage over liposome systems as being more mechanically stable and having a higher loading capacity than liposomes under various experimental conditions.[19] However, the liposomal system was a better model for cellular membranes due to its composition and behavior. Consequently, the hybrid system called "lipobeads" or "lipid microspheres" allow for the benefits of both systems to be realized where the polymeric beads is encased by a lipid bilayer.

Lipid bilayers have been previously used to encapsulate various solid surfaces including glass[20], plastic[16], metal[21], and modified polymers[22] which have been used for various biological applications. Gao and Huang[23] introduced the first encapsulated hydrogel liposome system. However this system was flawed because it lacked anchors to provide mechanical stability to the lipid bilayer.[24] Consequently, Lee and co-workers[2424] introduced a system having a hydrogel polymeric core encapsulated by a lipid bilayer with fatty acid lipid anchors. In this case, the lipid bilayer was formed spontaneously when the hydrogel core came in contact with a liposome suspension due to the fatty acid anchors on the hydrogel. This hydrogel model would be fitting to use in our lab where the lipid bilayer would spontaneously self-assemble on our carboxy-modified polystyrene beads.

In our experiments, we would first chemically bind the fluorescent probe, 2-aminoanthracene, to the carboxy-modified beads using an (1-Ethyl-3-(3-dimethylaminopropyl)carbodiimide Hydrochloride)/ N-hydroxysuccinimide (EDC/NHS) as

a conjugation step. Subsequent Then chemically binding of "anchors" to the bead as using an EDC/NHS conjugation step again which would lead to the self-assembly of a lipid bilayer upon exposure to phospholipids. This experiment can be easily modified to perform intracellular measurements of hydroxyl radicals because similar biosensors composed of lipobeads have been taken up in cells using phagocytosis.[17]

In addition, liposomes or lipobeads incorporating membrane proteins[25] would also be an interesting take on the following experiments. The membrane proteins could be chemically bound to the liposomes using conjugation chemistry to give site-specific reaction with the hydroxyl radicals surrounding the system in the aqueous media. The membrane protein can be incorporated into the liposomal bilayer and its effect on the degradation of fluorescently-labelled phospholipids can be assessed by introducing the Fenton reagent into the system in the surrounding aqueous environment. In addition,this experiment would give information about the behavioral properties of membrane protein in a liposomal bilayer environment.

1. Kwon, O. B., Kang, J. H., Lipid peroxidation induced by the Cu,Zn-superoxide dismutase and hydrogen peroxide system. *Biochemistry and Molecular Biology International* **1999,** 47, (4), 645-653.

2. Frimer, A. A., Strul, G., Buch, J. Gottlieb, H.E., Can superoxide organic chemistry be observed within the liposomal bilayer? *Free Radical Biology and Medicine* **1996,** 20, (6), 843-852.

3. Afri, M., Frimer, A A., Cohen, Y., Active oxygen chemistry within the liposomal bilayer Part IV: Locating 2'7'-dichlorodihydrofluorescein (DCFH) and 2',7'-dichlorodihydrofluorescein diacetate (DCFH-DA) in the lipid bilayer. *Chemistry and Physics of Lipids* **2004,** 131, 123-133.

4. Ohyashiki, T., Nunomura, M. Katoh, T., Detection of superoxide anion radical in phospholipid liposomal membrane by fluorescence quenching method using 1,3-diphenylisobenzofuran. *Biochimica et Biophysica Acta, Biomembranes* **1999,** 1421, (1), 131-139.

5. Braughler, J. M., Chase, R.L., Pregenzer, J.F., Oxidation of ferrous iron during peroxidation of lipid substrates. *Biochimica et Biophysica Acta* **1987,** 921, 457-464.

6. Li, Q.-T., Yeo, M.H., Tan, B.K., Lipid Peroxidation in Small and Large Phospholipid Unilamellar Vesicles Induced by Water-Soluble Free Radical Sources. *Biochemical and Biophysical Communications* **2000,** 273, 72-76.

7. Anzai, K., Aikawa, T., Furukawa, Y., Matsushima, Y., Urano, S. Ozawa, T., ESR measurement of rapid penetration of DMPO and DEPMPO spin traps through lipid bilayer membranes. *Archives of Biochemistry and Biophysics* **2003,** 415, 251-256.

8. Cheng, S.-A., Fung, W-K., Chan K-Y., Shen P.K., Optimizing electron spin resonance detection of hydroxyl radical in water. *Chemosphere* **2003,** 52, 1797-1805.

9. Hay, A., Burkitt, M.J., Jones, C.M., Hartley, R.C., Development of a new EPR spin trap, DOD-8C (N-[4-dodecyloxy-2-(7'-carboxyhept-1'-yloxy)benzylidene]-N-tertbutlyamine N-oxide) for the trapping of lipid radicals at a predetermined depth with biological membranes. *Archives of Biochemistry and Biophysics* **2005,** 435, 336-346.

10. Halliwell, B., Gutteridge, J.M.C., Biologically relevant metal-ion dependent hydroxyl radical generation. *FEBS Letters* **1992,** 307, (1), 108-112.

11. Cai, S. J., McAndrew, C.S. Leonard, B.P., Chapman, K.D., Pidgeon, C., *Journal of Chromatography A* **1995,** 696, 49-62.

12. Chang, T. M. S., *Biomaterial Artificial Cells Immobilized Biotechnology* **1992,** 20, 159-179.

13. Ong, S., Liu, H., Qiu, X., Bhat, G., Pidgeon, C., *Analytical Chemistry* **1995,** 67, 755-762.

14. Rogers, J. A., Choi, Y.W., *Pharmaceutical Research* **1993,** 10, 913-917.

15. Rolland, A., *Pharmaceutical Particulate Carriers: Therapeutic Applications*. Dekker: New York, 1993.

16. Rothe, U., Aurich, H., Engelhard, H., Oesterhelt, D., *FEBS Letters* **1990,** 263, 308-312.

17. McNamara, K. P., Nguyen, T., Dumitrascu, G., Ji, J., Rosenzweig, N. and Rosenzweig, Z., Synthesis, Characterization, and Application of Fluorescence Sensing

Lipobeads for Intracellular pH Measurements. *Analytical Chemistry* **2001,** 73, 3240-3246.

18. Ma, A., Rosenzweig, Z., Synthesis and analytical properties of micrometric biosensing lipobeads. *Analytical and Bioanalytical Chemistry* **2005,** 382, 28-36.

19. Gregoriadis, G., *Liposome Technology*. 2 ed.; CRC Press: Boca Raton, 1994; Vol. 3.

20. Bayer, T. M., Bloom, M., *Biophysical Journal* **1990,** 58, 357-362.

21. Plant, A. L., *Langmuir* **1993,** 9, 2764-2767.

22. Ma, A., Rosenzweig, Z., Submicrometric Lipobead-Based Fluorescence Sensors for Chloride Ion Measurements in Aqueous Solution. *Analytical Chemistry* **2004,** 76, 569-575.

23. Gao, K., Huang, L., *Biochimica et Biophysica Acta* **1987,** 897, 377-383.

24. Jin, T., Pennefather, P., Lee, P.I., Lipobeads: a hydrogel anchored lipid vesicle system. *FEBS Letters* **1996,** 397, 70-74.

25. Daghastanli, K. R. P., Ferreira, R. B., Thedei, G., Maggio, B., Ciancaglini, P., Lipid composition-dependent incorporation of multiple membrane proteins into liposomes. *Colloids and Surfaces, B: Biointerfaces* **2004,** 36, (3-4), 127-137.

VITA

Chanel Fortier was born in New Orleans, Louisiana and attended Xavier University Preparatory High School. She attended Louisiana State University where she received her Bachelor's degree in chemistry. She then received her Ph.D. under the direction of Dr. Matthew Tarr in December of 2008.